ABSTRACT

BOYETTE, WESLEY RYAN. Thrust and Specific Impulse Optimization of Eight-Centimeter Valveless Pulsejets at Low Subsonic Flight Speeds. (Under the direction of Dr. William L. Roberts).

The purpose of this research was to develop a method of accurately measuring the thrust and specific impulse of valveless pulsejets that are approximately eight centimeters in length. Previous methods of doing such were largely unsuccessful. A vertically arranged thrust stand and electronic balance were ultimately able to produce reliable results. Seven inlets were then tested on a forward facing arrangement. The maximum thrust achieved was 24.4 mN and specific impulse peaked at 295 seconds. Comparison revealed that increasing inlet length has a positive effect on pulsejet performance. Each inlet was tested at simulated forward flight speeds as well, showing that shorter inlets perform optimally at lower speeds than longer inlets. Additionally, a relationship between pulsejet performance, frequency and exhaust temperature was identified. Similar tests were performed on hybrid configurations as well, which combine forward-facing and rearward-facing inlets. Of the five hybrid configurations tested, maximum thrust was 31.2 mN and maximum specific impulse was 232 seconds. This series of tests revealed that these configurations also showed improvement in performance at higher forward flight speeds and at smaller inlet areas. In all cases, hydrogen was used as the fuel, due to its very short chemical time. Pulsejets at this scale are also shown to be capable of operating on acetylene, although with reduced performance.

Thrust and Specific Impulse Optimization of Eight-Centimeter Valveless Pulsejets at Low Subsonic Flight Speeds

by
Wesley Ryan Boyette

A thesis submitted to the Graduate Faculty of
North Carolina State University
in partial fulfillment of the
requirements for the Degree of
Master of Science

Aerospace Engineering

Raleigh, North Carolina

2008

APPROVED BY:

Dr. Andrey V. Kuznetsov

Dr. Terry Scharton

Dr. William L. Roberts
Chair of Advisory Committee

Biography

The author was born Wesley Ryan Boyette on June 27,1980 in Hudson, North Carolina to Warren and Ruby Boyette. He was the youngest of three with two older sisters; Lara and Katie. At the age of nine, his family moved to Wendell, North Carolina where he stayed until graduating from East Wake High in 1998. He then attended the University of North Carolina at Chapel Hill for four years, obtaining a B.S. in Biology and a B.A. in Geography. In 2003, he enrolled full-time at North Carolina State University studying Aerospace Engineering and received his B.S. in 2006, graduating Magna Cum Laude. Immediately following graduation, he began his Master's work under the direction of Dr. William Roberts.

"Chance favors only the prepared mind." – Louis Pasteur

Acknowledgements

Firstly, I would like to thank Dr. Roberts for offering his wealth of knowledge and assistance during my studies and research at NCSU. I would also like to thank Dr. Scharton and Dr. Kuznetsov for their help. Tim Turner has been a tremendous help and a large part of my research was made possible by the financial contribution of his company, Permafuels. I also appreciate Mike Breedlove and Skip Richardson for their professional and expeditious help with getting my hardware machined. Of course, none of this would have been possible without the support of my loving family. Finally, I would like to thank my friends for keeping me level-headed throughout this process.

Table of Contents

List of Figures ..... **vi**

List of Tables ..... **viii**

1 Introduction **1**
1.1 Theory of Operation **1**
1.2 History **5**
1.3 Related Work **6**
1.4 Previous Research at AERL **8**
1.5 Objectives **13**

2 Experimental Apparatus **15**
2.1 Pulsejet Designs **15**
2.1.1 Forward Facing 15
2.1.2 Rearward 18
2.1.3 Modified Rearward 19
2.1.4 Optimized 22
2.1.5 Four Centimeter 23
2.1.6 Pertinent Design Dimensions and Ratios 24
2.2 Air Delivery System **24**
2.2.1 Cautionary Considerations 27
2.2.2 Velometer 27
2.3 Fuel Delivery System **29**
2.3.1 Flowmeters and Valves 29
2.3.2 Fuel Injectors 29
2.4 Spark Ignition **32**
2.4.1 Transformer and Switch 32
2.4.2 Igniter 33
2.5 Electronic Balance **35**
2.6 Load cell **36**
2.7 Thrust stand **38**
2.7.1 For Load Cell 38
2.7.2 For Mass Balance 41
2.8 Heating apparatus **42**
2.9 Sound Level Meter **44**
2.10 Startup procedure **44**

3 Forward Facing Configuration **49**
3.1 Evolution of a Methodology **49**
3.1.1 Load Cell 49
3.1.2 Electronic Balance 53
3.1.3 Final Apparatus 56
3.1.4 Difficulties and Considerations 58
3.2 Thrust and Specific Impulse Results **61**

3.3 Performance as a Function of Inlet Diameter 80
3.4 Performance as a Function of Inlet Length 82
3.5 Performance as a Function of Fuel Flow Rate 87
3.6 Performance as a Function of Simulated Forward Velocity 90

4 Frequency and Temperature 97
4.1 Measured Frequency 97
4.2 Exit Temperature 102
4.3 Analytical Frequency 103
4.4 Frequency, Temperature and Performance 107

5 Hybrid Configurations 110
5.1 Thrust and Specific Impulse Results 111
5.2 Hybrid Configuration Trends 124
5.3 Case Study: Inlet 700-081 127

6 Other Results 131
6.1 Operation on Hydrocarbon Fuels 131
6.2 Sound Pressure Level 134
6.3 Comparisons with Computational Results 134
6.4 "Optimized" Geometry 136
6.5 Experiments on 4 Centimeter Valveless Pulsejet 138

7 Conclusions 139

8 Future Work 141

9 References 142

List of Figures

Figure 1-1: Humphrey cycle in p-V space 2
Figure 1-2: Example of a valved pulsejet (Foa, 1960) 3
Figure 1-3: Example of a valveless pulsejet (Foa, 1960) 4
Figure 2-1: Side view of 8 cm pulsejet 16
Figure 2-2: 8 cm pulsejet and inlets 18
Figure 2-3: Modified 8 cm pulsejet with 125 deg inlets and rearward injection 21
Figure 2-4: 8 cm modified hybrid running on acetylene 21
Figure 2-5: Typical 8 cm pulsejet and "optimized" pulsejet 22
Figure 2-6: 4 cm model along with 8 cm pulsejet and penny 23
Figure 2-7: Control panel. (A) Power supply, (B) Ignition switch, (C) Air rotometer, (D) Hydrogen regulator valve, (E) Hydrogen stop valve 26
Figure 2-8: Fuel injector with propane flames 31
Figure 2-9: Fuel injector arrangement within combustion chamber 31
Figure 2-10: Igniter while sparking 35
Figure 2-11: Electronic balance with 1.00 gram weight 36
Figure 2-12: Omega DLC101-10 dynamic force sensor 37
Figure 2-13: Drawing of vertical thrust stand designed for load cell 40
Figure 2-14: Final modified thrust stand with labeled components 42
Figure 3-1: Load cell voltage output during fuel cutoff 52
Figure 3-2: Mass versus time profile for typical run in early mass balance testing 54
Figure 3-3: Effects of obstruction location in pulsejet flowfield for inlet 700-125. (A) No obstruction, (B) Obstruction in inlet farfield, (C) Obstruction in inlet nearfield, (D) Obstruction in exhaust nearfield 58
Figure 3-4: Evidence of effects of clamping location. (A) Clamped behind combustion chamber, (B) Clamped at inlet 59
Figure 3-5: Thrust data for inlet 300-125 63
Figure 3-6: Specific impulse data for inlet 300-125 64
Figure 3-7: Thrust data for inlet 415-125 65
Figure 3-8: Specific impulse data for inlet 415-125 66
Figure 3-9: Thrust data for inlet 550-125 67
Figure 3-10: Specific impulse data for inlet 550-125 68
Figure 3-11: Thrust data for inlet 700-125 70
Figure 3-12: Specific impulse data for inlet 700-125 71
Figure 3-13: Thrust data for inlet 700-100 73
Figure 3-14: Specific impulse data for inlet 700-100 74
Figure 3-15: Thrust data for inlet 700-081 76
Figure 3-16: Specific impulse data for inlet 700-081 77
Figure 3-17: Thrust data for inlet 700-150 79
Figure 3-18: Specific impulse data for inlet 700-150 80

Figure 3-19: Thrust data for inlets of same area at 50 m/s 83
Figure 3-20: Thrust data for inlets of same area at 0 m/s 84
Figure 3-21: Maximum thrust and Isp for inlets of varying length 86
Figure 3-22: Peak thrust for each fuel flow rate 88
Figure 3-23: Peak specific impulse for each fuel flow rate 89
Figure 3-24: Forward flight speed at which peak thrust occurs by fuel flow rate 93
Figure 3-25: Airspeed for which maximum Isp occurs as a function of inlet length 94
Figure 4-1: Frequency measurements for inlet 300-125 98
Figure 4-2: Frequency measurements for inlet 415-125 99
Figure 4-3: Frequency measurements for inlet 550-125 100
Figure 4-4: Frequency measurements for inlet 700-125 101
Figure 4-5: Temperature as a function of frequency 103
Figure 4-6: Percent error in frequency 106
Figure 5-1: Thrust data for inlet 500-088 + 180 deg hybrid 112
Figure 5-2: Specific impulse data for inlet 500-088 + 180 deg hybrid 113
Figure 5-3: Thrust data for inlet 700-081 + 180 deg hybrid 114
Figure 5-4: Specific impulse data for inlet 700-081 + 180 deg hybrid 115
Figure 5-5: Hybrid configuration in "torch" mode 116
Figure 5-6: Thrust data for inlet 700-081 + 125 deg hybrid 117
Figure 5-7: Specific impulse data for inlet 700-081 + 125 deg hybrid 118
Figure 5-8: Thrust data for inlet 700-100 + 125 deg hybrid 120
Figure 5-9: Specific impulse data for inlet 700-100 + 125 deg hybrid 121
Figure 5-10: Thrust data for inlet 700-125 + 125 deg hybrid 123
Figure 5-11: Specific impulse data for inlet 700-125 + 125 deg hybrid 124
Figure 5-12: Thrust for all cases with inlet 700-081 at 50 m/s 129
Figure 5-13: Specific impulse for all cases with inlet 700-081 at 50 m/s 130
Figure 6-1: Thrust results for "Optimized" 8 cm pulsejet 137

List of Tables

Table 2-1: Critical dimensions and ratios for pulsejet configurations 24
Table 2-2: Required rotometer settings for simulated velocity 28
Table 3-1: Dimensions of inlets tested 61
Table 4-1: Averaged analytical and measured frequencies 105
Table 4-2: Average performance characteristics for 4 inlets 107
Table 5-1: Peak results for hybrid configurations 125
Table 6-1: Comparison of computational and experimental results 135

1 Introduction

The pulsejet is a member of a small group of thrust generators that are unsteady. The mechanical simplicity of the pulsejet makes it relatively easy to construct and operate. On the other hand, its unsteady nature and the competing governing principles of fluid mechanics, acoustics, and chemical kinetics make analysis and prediction of pulsejet behavior a very formidable task.

1.1 Theory of Operation

The pulsejet operates on the Humphrey cycle. A diagram of the Humphrey cycle is given below in Figure 1-1. The cycle begins with 1-2, isentropic compression. This is followed by 2-3, isochoric heat addition provided by combustion. The path 3-4 is the isentropic expansion following combustion. The cycle is completed by 4-1, isobaric heat rejection. The pulsejet is generally separated into three components: inlet, combustion chamber, and exhaust. The inlet brings fresh air into the combustion chamber, which initially contains hot combustion products at sub-atmospheric pressure. Fuel, which is continually being released into the combustion chamber, then reacts with the fresh air and combustion of the gasses creates a large pressure rise at essentially constant volume. The pressure difference between the combustion chamber and the ambient pressure at the exhaust exit then causes the hot products to expand down the exhaust tube being released into the atmosphere. With the combustion chamber once again at sub-atmospheric pressure, the cycle restarts. Initially a spark is required to initiate combustion but after a number of cycles, the remaining hot gasses in the combustion chamber and the hot chamber walls are usually

sufficient for autoignition. In many cases, the post-expansion pressure in the combustion chamber is low enough for fresh reactants to be automatically pulled in through the inlet. As a result, pulsejets can often run statically with only an external fuel source necessary to maintain operation.

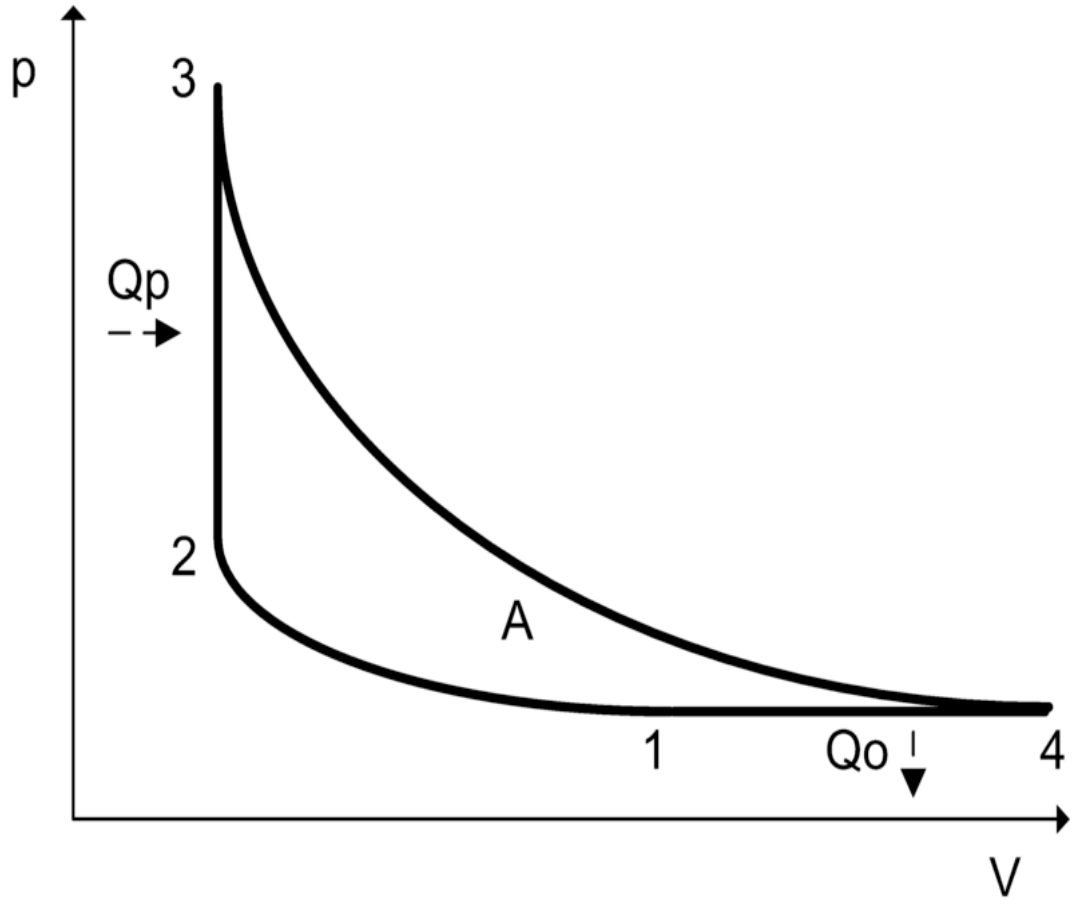

Figure 1-1: Humphrey cycle in p-V space

Pulsejets can be divided into two types: valved and valveless. Valved pulsejets contain a series of valves separating the inlet from the combustion chamber. An example diagram of one is given in Figure 1-2, with an enhanced view of the valves. These valves are situated in such a way that air is allowed to enter the combustion chamber but gasses in the

chamber cannot flow back into the inlet. Thus, the valves stay closed during the combustion phase and most of the expansion phase. The exhaust duct acts as a tube open at one end so once the pressure wave created by combustion reaches the exhaust plane, an expansion wave is reflected and travels back to the combustion chamber, creating low pressure and reopening the valves. Large pulsejets typically utilize valves for their superior performance but as the size of the pulsejet is reduced, valves may become a liability and one may wish to consider the valveless version.

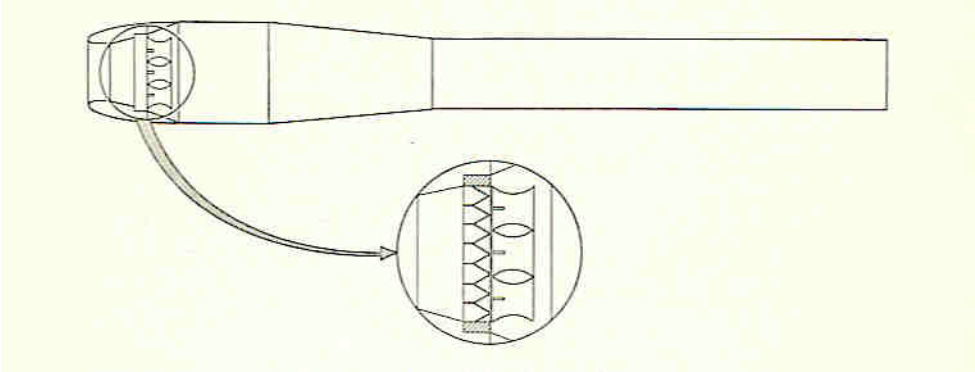

Figure 1-2: Example of a valved pulsejet (Foa, 1960)

The primary difference between the valveless and valved pulsejets is, of course, the absence of valves. In fact, the valveless pulsejet, shown in Figure 1-3, closely resembles a ramjet. One of the primary differences between it and a ramjet, as far as construction, is the abrupt increase in area from the inlet to combustion chamber. The absence of valves creates the drawback of lower combustion chamber peak pressures since the building pressure now has two escape routes. Furthermore, if gasses are allowed to exit through the inlet, they will contribute negatively to the thrust. However, at small scales, the valves become inefficient. One of the challenges of valveless pulsejets is designing the inlet in such a way that it is

difficult for combustion products to exit through the inlet. Some methods for doing so have included turning the inlets around and including immobile obstructions at the inlet-combustion chamber interface. Another challenge in valveless design is in scaling the dimensions appropriately so that the acoustic characteristics of the pulsejet allow operation. The valvless pulsejet essentially has two components with competing acoustics. The inlet and the exhaust have their own characteristic frequencies and both provide the expansion waves that are crucial to lowering combustion chamber pressure. If these frequencies are not matched sufficiently, operation may not be possible.

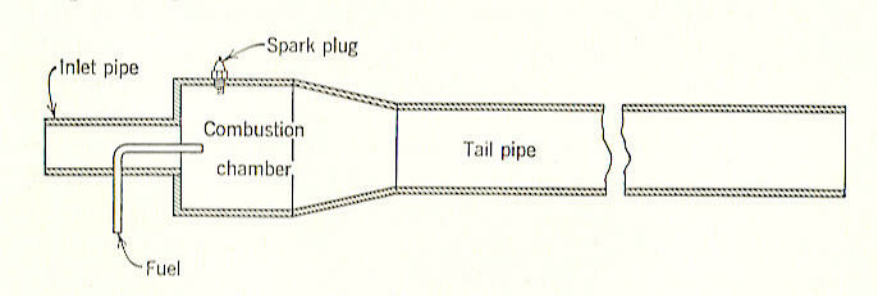

Figure 1-3: Example of a valveless pulsejet (Foa, 1960)

As with any propulsion system, pulsejets have their pros and cons. Probably the biggest advantage is the pulsejet's simplicity. This makes it cost effective, expendable, low maintenance, and easily scalable. For these reasons, it has been a popular choice for hobbyists. Also, there is evidence that unsteady modes of combustion are actually capable of higher cycle efficiency than any steady modes (Foa, 1960). And true constant volume combustion yields better performance than the more common constant pressure combustion (Brayton cycle). However, combustion in the pulsejet is not truly isochoric. Furthermore, other engines, particularly gas turbine engines, are able to build up much greater pressure

before combustion, which allows for much higher thermodynamic efficiencies. Also, the pulsejet is confined to subsonic operation. For these reasons, the pulsejet's practicality has been confined to a relative few and rather specific uses, and will probably never be seen as a good general-use propulsion system.

1.2 History

The concept of pulsating combustion is at least a couple of centuries old. By the turn of the 20th century, two French engineers, Esnault and Peltrie, had designed a cyclical engine that took advantage of pulsating combustion (Schoen, 2005). In 1909, Marconnet proposed the "reacteur-pulsateur", which according to Foa, was in every respect the precursor of the pulsejet (1960). By the 1930's, Paul Schmidt obtained a German patent for his Schmidt tube. In the following decade, he along with a team from the company Argus, developed the Argus-Schmidt tube which was responsible for propelling the German V-1 buzz-bomb, which had a limiting velocity of 500 km/hr (Putnam, 1986). This would be the first and last large-scale usage of pulsejets.

After WWII, the increasing efficiency of the turbojet made the pulsejet obsolete for most applications. Project Squid was a collaborative effort between the US Navy and the Air Force in the 1940s and 50s to further develop all types of jet propulsion, which led to some research in valveless pulsejets (Schoen, 2005). At the same time, SNECMA began developing versions of aerovalved pulse combustors (Putnam, 1986). Further research was undertaken on valveless pulsejets in the 1960s by Lockwood and Hiller (Ordon, 2006). Since then, little in the way of academic research has been done and pulsejets have largely been

relegated to the interests of hobbyists. This is an extremely brief overview of pulsejet history. For more information, one should consult Putnam's 1986 paper or the theses of Schoen, Ordon, or McCauley, all of which are cited in the References section.

1.3 Related Work

Recently, advances in technology have made small, unmanned aerial vehicles a hot research topic in the field of aeronautics. Smaller vehicles, of course, require smaller propulsion units as well. The question then becomes how best to utilize chemical energy through a micro-propulsive device. A few of the many options are rotary devices powered by batteries, chemical rockets, gas turbine engines, and pulsejets. One of the objectives of this research is to investigate the viability of pulsejets as a propulsion unit at very small scales.

The problem with using a system that relies on batteries is that the highest energy densities yet proven in batteries may still be an order of magnitude lower than energy densities presented by hydrocarbon fuels. Chemical rockets are fundamentally limited to low specific impulse relative to those of gas turbine engines and, at small scales, boundary layer effects will only make this situation worse. The more interesting and more relevant issue is how micro-gas turbine engines might compare to pulsejets at a similar scale.

The problems with microcombustion can essentially be grouped into three topics, as outlined by Waitz (1998). The first obstacle is the residence time in the combustion zone. Shorter length scales mean shorter residence times for similar mass flow rates. As the residence time of the reactants approaches the chemical kinetic time scale of the reaction, it

becomes a challenge to complete the combustion process to an appreciable degree while the reactants are still in the intended combustion chamber. The crucial parameter in this case is the Damköhler number, which is the ratio of the residence time to the characteristic chemical reaction time. The solution may to be increase residence time, which means increasing the combustor size. According to Waitz, if a full-size engine is scaled down by a factor of 500, then the volume of the combustor must grow relative to the engine by a factor of about 40 to provide sufficient residence time. On the other hand, one may want to increase the chemical kinetic time scale, which may be done by adding a catalytic surface. Unfortunately, this poses problems because a sufficient amount of surface area must be provided and sufficient time for diffusion of reactants to the catalytic surface becomes an equally important time factor (Spadaccini, 2007). Along with these factors, one must also consider the time necessary for sufficient reactant mixing.

The second obstacle is heat transfer losses. At low length scales, the surface area is much larger relative to the volume of the combustor. The additional surface area increases the convective heat loss from the hot combustion gases. At some critical size, the heat transfer from the flame front may be enough to quench the reaction. This will have the effect of reducing flammability limits and reducing the normally high combustor efficiencies of gas turbine engines (Waitz, 1998).

A third obstacle is material properties. Compressors and turbines are composed of a very large numbers of well-machined parts. These parts, in addition to being expensive to machine, have temperature and pressure limits. The use of ceramics can mediate the effects of high combustion temperatures on the turbine, however (Spadaccini, 2007). Ultimately, the

machining and use of such parts is possible but the complexities involved increase cost and decrease robustness.

The valveless pulsejet generally exhibits lower specific impulse than a valved pulsejet, which in turn has lower specific impulse than typical gas turbine engines. At the length scales studied in this research, adding valves to the pulsejet is not feasible, at least not in the petal valve configuration that is typically used. Certainly the valveless pulsejet is easier to machine than the micro-gas turbine engine because of its lack of moving parts, however, some of the same obstacles that exist with small gas turbine engines also exist with small valveless pulsejets. In particular, fuel choices are going to be limited by the residence time and heat transfer properties of the combustion chamber.

1.4 Previous Research at AERL

This research was conducted at the Applied Energy Research Laboratory at North Carolina State University in Raleigh, North Carolina. AERL has been conducting pulsejet research for several years now and I am only the most recent investigator. Much of this work has been made possible by the work that has preceded mine. Furthermore, the results and conclusions of the past have provided me with valuable guidance and knowledge not only about pulsejet operation but also laboratory methods. Each of these experimental investigators (all of whom were Master's students) made crucial contributions to the body of knowledge concerning pulsejets. I would be remiss if I did not report on their findings.

Michael Schoen was one of the first AERL pulsejet investigators and he received his M.S. in 2005. He performed his research on a 15 cm long valveless pulsejet. Although he

attempted operation using both hydrogen and propane, only hydrogen succeeded. It should be mentioned that "success" in this case, as with all AERL research preceding mine, meant continuous operation without forced air. The primary objective was to investigate the consequences of varying inlet length, inlet diameter, tail pipe length, and tail pipe exit geometry. His quantitative results include time-resolved chamber pressures and time-resolved thrust. However, no net thrust was measured for these cases, as the thrust stand was not sensitive enough for such low values. He found that one of the results of reducing inlet area was a decrease in the maximum allowable fuel flow rate. However, he found no trend associated with maximum fuel flow rate and inlet length suggesting boundary layer build up did not have significant effect on air intake volume. Schoen also suggested that higher operating frequencies allow higher fuel flow rates (Schoen, 2005). Ultimately, he laid the groundwork for much of the valveless pulsejet work that was completed later.

Adam Kiker, also a graduate student, finished his research in December of 2005. His work dealt with a valveless pulsejet that measured only 8 cm in length. The geometry of the smaller pulsejet was directly scaled down from the 15 cm pulsejet except that the combustion chamber was kept the same size. A version with forward facing inlet and a configuration using 2 rearward inlets were designed such that the total cross-sectional inlet area was equal for both. He attempted to use a Kistler load cell for thrust measurements but found it difficult to use in obtaining average thrust, and suggests using a linear load cell with a long rise time. Attempts to measure net thrust were largely unsuccessful. By measuring combustion chamber pressure, he found that with the forward facing inlet, the operating frequency shows little variance above 4 SLPM of hydrogen and that the jet runs most

efficiently around 5 or 6 SLPM where peak pressure is highest. In testing the rearward configuration, he actually found lower peak pressure in the combustion chamber and he indicates that the range of fuel flow rate is in the 4 to 6 SLPM range. He also notes that a reduction in exhaust diameter results in higher peak pressures. Kiker also attempted to construct and operate a 5 cm valveless pulsejet. The jet was coated with a catalyst (platinum) in order to speed up the chemical kinetics, but the author notes no apparent improvement after having done so. Eventually, he was able to operate the 5 cm model without air in a rearward configuration (Kiker, 2005). His work at the 8 cm scale is a direct predecessor to the work presented here.

The next graduate student working on pulsejets was Rob Ordon who graduated in 2006. He modified a BMS valved pulsejet into a 50 cm valveless version with different inlets. As with the previous students, he was unable to make net thrust measurements of the valveless model using his thrust stand. This was the first valveless model to run successfully on propane. It was found that as inlet diameter increased, more fuel was required to run the jet. Longer extensions allowed a greater variety of inlets and lower fuel flow rates. His results showed that frequency is a function of both exhaust length and inlet diameter in that increasing diameter increases the frequency. Perhaps his most important contribution was in showing that the inlet can be modeled as a Helmholtz resonator and the exhaust is similar to a quarter wave tube but more like a $1/6^{th}$ wave tube. For a Helmholtz resonator, one can determine the frequency using the speed of sound, c, the inlet area, S, the inlet length, L, and the combustion chamber volume, V.

$$f = \frac{c}{2\pi}\sqrt{\frac{S}{VL}}$$

Similarly for the exhaust tube, where L_b is the length of the exhaust;

$$f = \frac{c}{6L_b}$$

Ordon then shows that the measured frequency is well predicted by averaging the calculated frequencies of inlet and exhaust. He also did some testing of the valved hobby scale model, which showed significantly higher combustion chamber pressures than in valveless models, as expected (Ordon, 2006).

Finishing in 2006, Christian McCauley performed experiments on a wide range of pulsejets including the BMS hobby scale, a 1 meter long engine with 25 pounds of thrust, and a 25cm valveless model designed to work on heavy (liquid) fuels. His first achievement was in successfully running the 25 cm jet on propane which required adding a flare to the exit, adjusting the fuel injection system and including a warm-up period before cutting off air to provide adequate heating of the combustion chamber. Then to run on heavier liquid fuels, he discovered that the pulsejet must be started on propane then switched to the liquid fuel, which ran through preheating coils. Through his efforts, he was eventually able to run the 25 cm valveless model without air assistance on both gasoline and kerosene. Interestingly, no link was found between fuel choice and operating frequency; the frequency appears to be determined by geometry alone. Furthermore, his results agreed with Ordon's with respect to predicting the jet's frequency. One aspect of the jet's operation that he paid particular attention to was the type of fuel injector. He notes that the jet was highly sensitive to fuel

injector location and saw that it would not operate if fuel was injected oriented against the flow of air but operated most preferably oriented at 90 degress to the flow. Another observation was that fewer and smaller holes in the fuel injector were preferable due to improved mixing. McCauley was also able to investigate performance-enhancing methods such as forward flow deflectors and flow rectifiers (McCauley, 2006).

The most recent pulsejet experimentalist prior to myself was Ranjith Kumar who received his M.S. in 2007. Kumar did most of his work on the 50 cm valved pulsejet from BMS. He was able to use a thrust plate as a means of indirect thrust measurement. His thrust measurements were initially aimed at investigating the use of an augmenter. An augmenter is a device which is little more than a large tube located downstream of the pulsejet exit. It is able to enhance the thrust of the pulsejet by entraining extra air from outside of the pulsejet into the exhaust, effectively increasing the momentum flux that determines the thrust. By using an augmenter, he was able to achieve up to 1.5 times the unaugmented thrust. Kumar also attempted to validate some of the computational work performed by Tao Geng involving the effects of flares of varying area ratios on the exhaust of the pulsejet. His findings showed that the nominal flare with an area ratio of 1.4 and no curvature gave the best thrust performance. While these results did not agree with the computational results, the study was an important step for the group in that it was the first time experimental results were used to validate computational findings. He also did some experimental work with a 1 meter valved pulsejet and a large Helmholtz resonator (Kumar, 2007).

Alongside the experimental research at NCSU, Tao Geng helped with computational support and finished his PhD in 2007. Geng was able to investigate a number of different phenomena regarding pulsejets. His first task was to look at the 15 cm valveless pulsejet that Schoen was developing in the lab. He found that fresh air for the combustion cycle was introduced through the inlet only. Configurations with multiple opposed facing inlets had similar characteristics as the conventional forward facing versions. He also helped to explain how shorter pulsejet lengths require shorter combustion time scales and, thus, faster fuels. With the 8 cm model, his simulations matched the experimental results in operation frequency and peak pressure. He also did some modeling of the valved 50 cm pulsejet, with which he was able to investigate the importance of a flare at the exhaust exit that helps to augment thrust by inducing starting vortices (Geng, 2007). The ability to perform computational analysis side-by-side with experimental work has been tremendously advantageous.

1.5 Objectives

The following study explores a variety of issues concerning an 8 cm valveless pulsejet. The goal is to expand upon the extensive research that has already been performed at the AERL. This research has two primary objectives. While the effects of inlet geometry have been studied before, this is the first investigation to collect reliable net thrust measurements on a valveless model. Therefore, the first objective is to use net thrust and specific impulse to evaluate a number of different inlet geometries. Also, no previous researcher at this lab has looked at pulsejet operation at any condition other than static. Thus,

a second objective of this study is to study trends in thrust and specific impulse as a function of forward flight speed.

In addition to these primary goals, several other smaller phenomena are investigated. Frequency prediction based on a previously stated analytical model is performed with the forward facing inlets and links between frequency, temperature, and performance are confirmed. Alternative pulsejet configurations such as rearward facing and hybrid (rearward plus forward facing) inlets are considered. An "optimized" geometry that has been suggested through computational work is manufactured and tested briefly. Various fuels are tested and compared at the 8 cm level for the first time. Also, a 4 cm valveless model that is directly scaled down from the 8 cm model is tested on hydrogen and acetylene.

2 Experimental Apparatus

As mentioned, this research is a continuation of previous research at the AERL. For this reason, much of the hardware and many of the practices have been developed by others and handed down over the previous three years.

2.1 Pulsejet Designs

The vast majority of the work done on this project employed the use of an 8 cm valveless pulsejet using a forward facing inlet. Testing was done with slight variations on the base design. Each of these design permutations will be discussed in detail. All physical models were machined out of 1-inch diameter steel or stainless steel by the Mechanical and Aerospace Engineering Machine Shop.

2.1.1 Forward Facing

The dimensions for the forward facing inlet configuration were adopted from the work of Adam Kiker who initially designed the engine by scaling down the 15 cm version except keeping the combustion chamber the same size (Kiker, 2005). For this reason, the combustion chamber on the 8 cm pulsejet comprises considerably more of the volume fraction of the total engine than with other, larger designs. This gives it an odd "bulbous" look as opposed to the fairly slender shape of the 15 and 25 cm variations. Because the interior cannot be machined with an inlet, the main body includes only the combustion chamber and the exhaust tube, and the combustion chamber's interior is partially threaded to allow for inlet attachment. This arrangement allows for the fitting of any number of different inlets. Figure 2-1 is a side view of the 8 cm pulsejet with some of the length dimensions

given and the primary sections annotated. Table 2-1 lists the pertinent dimensions and ratios of this model. Note that although dimensions here are given in centimeters (except where threading is required) in order to keep consistent units throughout this document, the original drawings were prepared and submitted to the Machine Shop in inches.

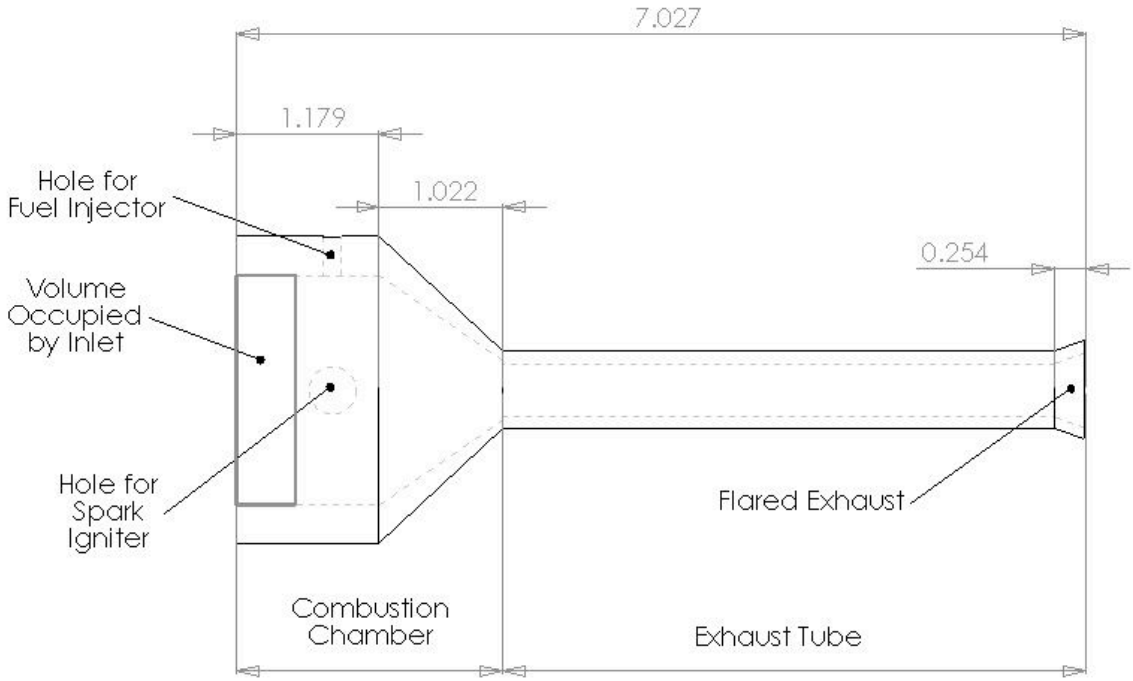

Figure 2-1: Side view of 8 cm pulsejet

The inlet base is designed to thread into the combustion chamber a length of 0.508 cm. Therefore, the combustion chamber is considered to occupy the volume beginning at the inlet base and ending at the point where the area tapers down to the size of the exhaust tube. There are two holes in this section of the pulsejet. The larger hole allows for the spark

igniter, which is a 10-32 screw (see section 2.4.2). The smaller hole is where the fuel injector is inserted (see section 2.3.2).

The exhaust tube begins where the tapered section ends and extends to the exit face. The version drawn here and tested is seen to have a flared exhaust. Many investigations of pulsejets, both valved and valveless, by the AERL researchers and others have indicated that a flared nozzle such as this is beneficial both for starting the pulsejet and for performance. In fact, a flared nozzle is standard issue for hobby pulsejets. The area ratio used in this design is around 2, which was taken roughly from computational results conducted by Tao Geng, indicating this was near the optimal value (Geng, 2007).

Several models using this design were manufactured while this research was ongoing. Some of the models had flared ends and others did not. Both types operated and no noticeable difference was observed. No quantitative comparison between flared and unflared designs was made as it was deemed outside of the scope of this project. All of the results using a forward facing inlet reported here were made with the same model. This is for several reasons. First, the initial set of models were made with slightly larger fuel injector holes than necessary. This caused unnecessary leakage of exhaust gasses from the combustion chamber, and was detrimental to the pulsejet's performance. Second, although these pulsejets are extremely simple devices, they too are subject to wear and tear with extended usage. It is not known how significantly this affects performance but erosion of the metal surface can be seen on both the interior and exterior and a slight curving of the exhaust tube is also apparent. For these reasons, a fresh model was manufactured and used solely for

the final set of measurements reported here. Figure 2-2 is a view of this model along with each of the inlets tested.

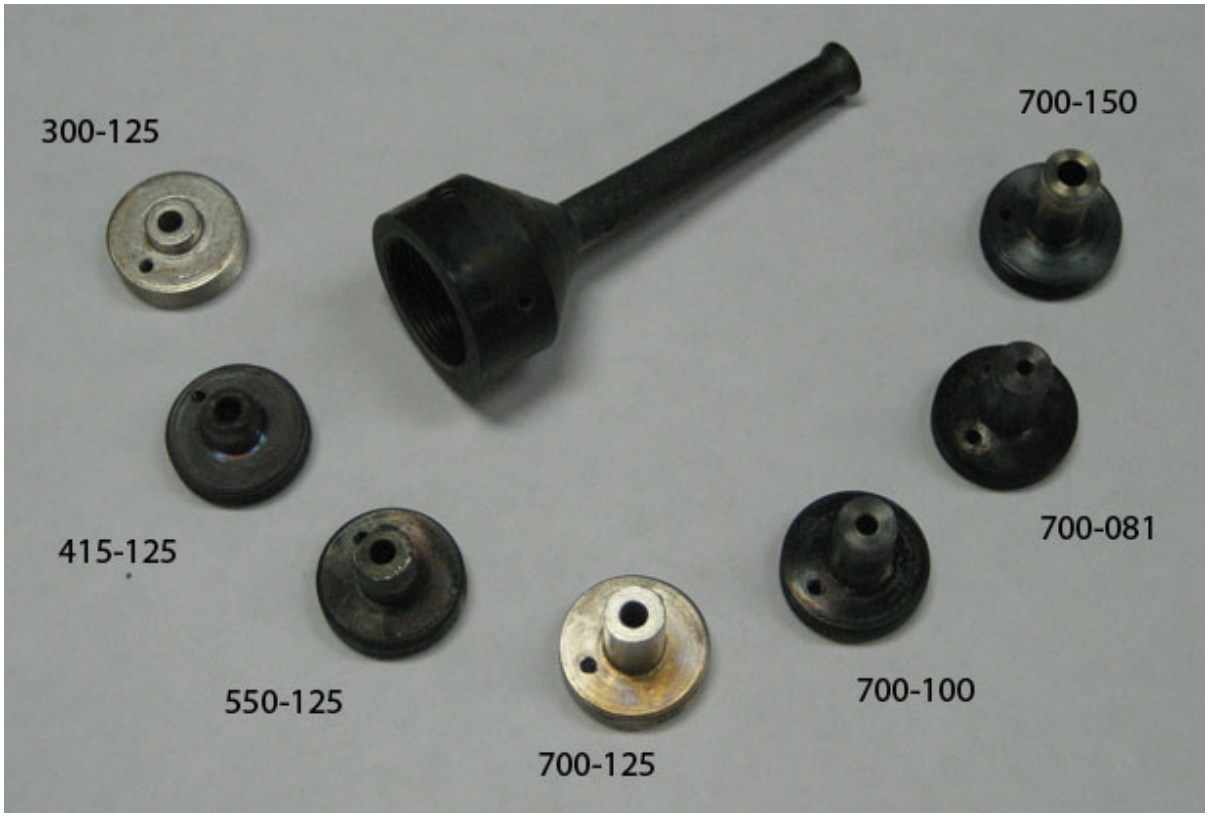

Figure 2-2: 8 cm pulsejet and inlets

2.1.2 Rearward

Most, if not all, of the jets from Kiker's research remained at the lab. A couple of 8 cm pulsejets ready for rearward facing inlets were available. These jets were geometrically similar to the forward facing configuration with only a few differences. Obviously, the big difference is that the combustion chamber now includes two holes that allow for screws oriented at 180 degrees with respect to the incoming airflow. The holes are on either side of the exhaust tube and threaded to accommodate 8-32 screws. The rearward facing inlets used

in all cases were 0.914 cm long with an individual area of 0.039 cm^2. The exhaust tube is 0.254 cm longer than in the geometry detailed above. Finally, there is no flared nozzle on this pulsejet. Rather, the exhaust tube is partially threaded to allow for extensions, although in this research, these extensions were never used. The inlet end of the combustion chamber may be plugged if one wishes to utilize the pulsejet in its rearward facing configuration. Alternatively, a forward facing inlet may also be used to create a hybrid configuration, utilizing both forward and rearward inlets, which has never been analyzed at AERL before.

2.1.3 Modified Rearward

The first original design constructed during this research is referred to as the modified rearward configuration. It has the same internal geometry as the configurations discussed so far and includes a flared nozzle. However, it differs from the previous discussions in two important ways.

First, this geometry has two holes in the combustion chamber that can accommodate slightly rearward facing inlets. The holes are threaded to fit 8-32 screws and are placed on either side of the exhaust tube. These holes are still located on the converging section of the combustion chamber but are located slightly closer to the chamber's straight section. Instead of being oriented at 180 degrees to the flow, they are oriented at 125 degrees.

The other difference is that the configuration is actually constructed of three parts. The combustion chamber is separate from the exhaust tube and is tapped beyond the tapered section to allow the exhaust tube to thread into it. The exhaust tube is then threaded at the end that meets with the combustion chamber and has an internal flared nozzle on the other

end but is straight along the exterior. Along the exterior, however, a groove has been machined that is just wide and deep enough to accommodate the fuel injector. The third component is a sleeve that fits over the fuel injector and exhaust tube and threads onto the exhaust tube's exterior at the combustion chamber end. The reasons for constructing this configuration are twofold. First, the exhaust is generally the hottest part of the pulsejet and is thus an ideal location for regenerative heating of the fuel. By running the fuel injector along the exhaust and having it in direct contact with this metal, this configuration offers the possibility of heating the fuel with no external heat addition source and no cumbersome tubing wrapped around the jet's exterior. Furthermore, it was already mentioned that having an inadequate seal between the fuel injector and combustion chamber may result in a loss of peak pressure, and thus overall performance. By getting rid of the hole in the wall of the chamber, any leakage along the fuel injector will now escape in the same direction as the exhaust gasses and should only contribute to the momentum in the desired direction.

As with the other configurations, the combustion chamber's straight section is threaded to allow for a plug or any number of forward facing inlets. A cross-sectional drawing of the separate components is shown in Figure 2-3. One version of the hybrid modified is shown in Figure 2-4 while running on acetylene, as proven by the characteristic white flames. This striking picture was taken in the dark for dramatic emphasis of the use of three inlets and one exhaust. It is also interesting to note the clear delineation between the combustion chamber piece (glowing red) and the outer sleeve between the chamber and the orange flame at the top of the view.

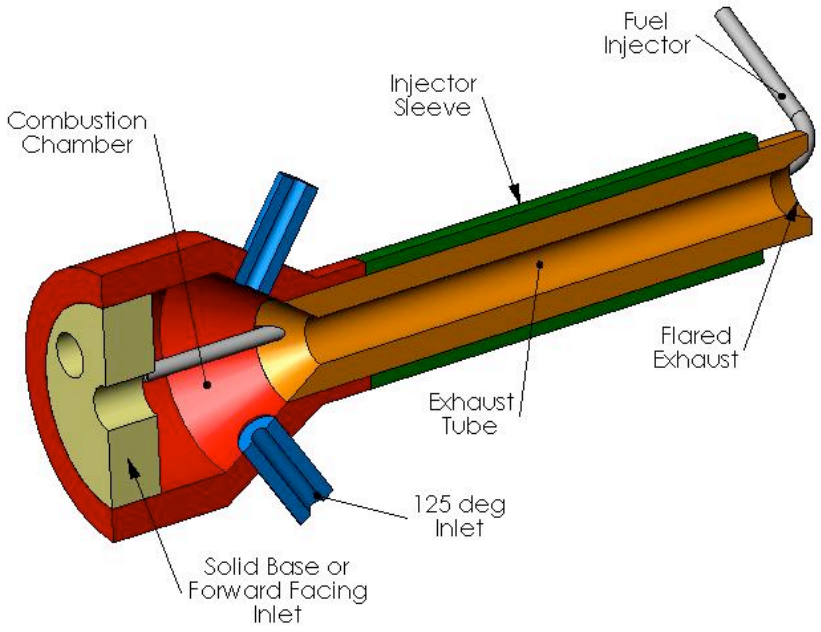

Figure 2-3: Modified 8 cm pulsejet with 125 deg inlets and rearward injection

Figure 2-4: 8 cm modified hybrid running on acetylene

2.1.4 Optimized

For the first time in the history of pulsejet research at AERL, computational results were used to assist in the development of an entirely new geometry. Fei Zhang developed a MATLAB code which, when given a total length and inlet length, will output an "optimized" geometry for the pulsejet. Based on the MATLAB results for a test case using an 8 cm long pulsejet at static conditions, a pulsejet was designed and manufactured in order to test the optimization code. The dimensions are given in Table 2-1. It is referred to as the "optimal" configuration. Two notable changes resulting from the optimization are the decrease in combustion chamber volume and the increase in exhaust tube area. This results in a reduction in chamber area to exhaust area ratio by a factor of almost 9. Other than a radically different internal geometry, one major difference between the "optimized" geometry and previous configurations is that the exterior required no extra machining, but, as a result, gave this model much thicker walls along the exhaust tube. Its shape gives it a very distinctive look. The machined model is shown in Figure 2-5 alongside a typical pulsejet for comparison.

Figure 2-5: Typical 8 cm pulsejet and "optimized" pulsejet

2.1.5 Four Centimeter

In addition to the extensive work conducted at the 8 cm level, some qualitative work was also done on a 4 cm model. This model was directly scaled down from the existing 8 cm models with all interior linear dimensions being cut in half. The walls were left relatively thicker due to the inherent difficulties in machining such small models. The initial design called for a fuel injector hole to be made on the converging section of the combustion chamber to allow for an injector with the same diameter as those used on the 8 cm models. This version can be seen in Figure 2-6 where an 8 cm pulsejet and a penny are shown for size comparison. However, a later design used a smaller fuel injector hole to be placed on the straight section of the combustion chamber, as was done with the 8 cm model. Likewise, this model included a flared exhaust and allowed for different inlets.

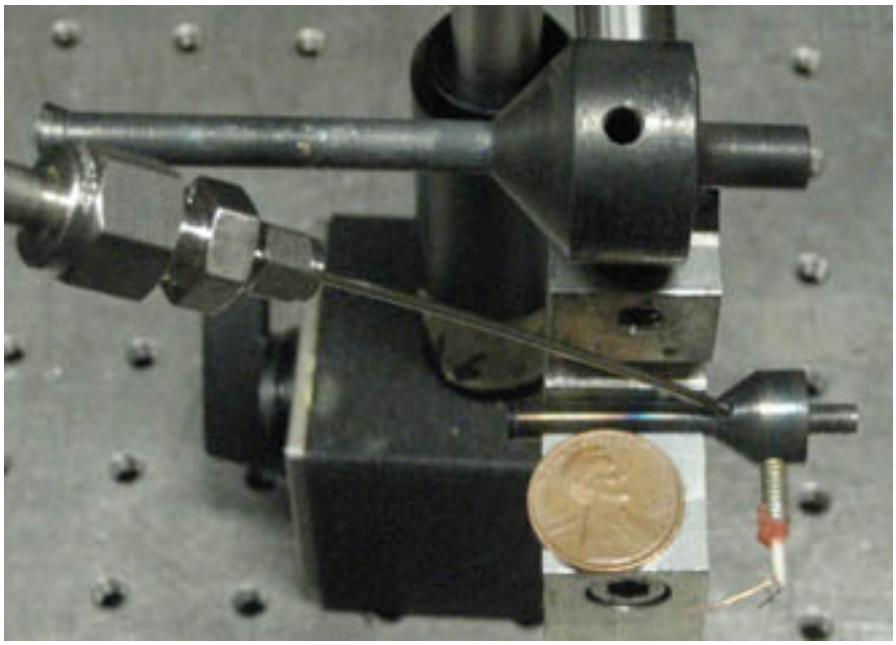

Figure 2-6: 4 cm model along with 8 cm pulsejet and penny

2.1.6 Pertinent Design Dimensions and Ratios

Table 2-1 gives all of the crucial dimensions and ratios for each design. It is important to realize that these dimensions play a critical role in determining the pulsejet's operating characteristics. Even seemingly slight changes in such design parameters can have dramatic effects on performance, including rendering the pulsejet inoperable.

Table 2-1: Critical dimensions and ratios for pulsejet configurations

Parameter	8 cm Forward Facing	8 cm 180deg Rearward	8 cm 125deg Modified Rearward	8 cm "Optimized"	4 cm Forward Facing
CC diameter (cm)	1.905	1.905	1.905	0.750	0.953
CC area (cm^2)	2.850	2.850	2.850	0.442	0.713
CC length (cm)	1.694	1.694	1.694	1.600	0.843
CC volume (cm^3)	3.164	3.164	3.164	0.601	0.395
Exhaust diameter (cm)	0.445	0.445	0.445	0.500	0.224
Exhaust area (cm^2)	0.156	0.156	0.156	0.196	0.039
Exhaust length (cm)	4.826	5.080	5.080	5.000	2.540
Flare area (cm^2)	0.304	0.156	0.317	0.392	0.073
Flare area/Exhaust area	1.95	1.00	2.04	2.00	1.85
CC area/Exhaust area	18.33	18.33	18.33	2.25	18.10

2.2 Air Delivery System

All of the pulsejets that have been used at this facility require a forced injection of air in order to begin operation. Prior to this investigation, however, the air was only used in starting the pulsejet and, if at all possible, was removed from the pulsejet's inlet as soon as independent operation was possible. For the present research, the air was not only necessary for starting the pulsejet, but it was also used to simulate forward flight speeds in lieu of a wind tunnel. For this reason, the air delivery system was a crucial component of my testing apparatus.

At the AERL, there is an Ingersoll-Rand UP6-15CTAS-150 air compressor unit. This unit has a small tank, which can be pumped up to about 900 kPa (9 atm). This unit is then connected to a much larger tank which, when connected through a valve, is allowed to store air at the same pressure. This tank is then connected through a series of hoses to a regulator valve. By manipulating this valve, the user is able to control the amount of airflow passing through the line. The line is connected to an Omega variable-area rotometer capable of measuring up to 39 SLPM of air. In reality, however, one can go as high as 41 SLPM by allowing the center of the ball to rest between the "AIR" mark and the Omega symbol at the top of the glass portion. This rotometer was positioned on a control panel that was thankfully constructed before this research began and located next to the optical table where the majority of the experiments were conducted. Shown in Figure 2-7, it contains components of the air delivery system, fuel delivery system, and spark ignition system.

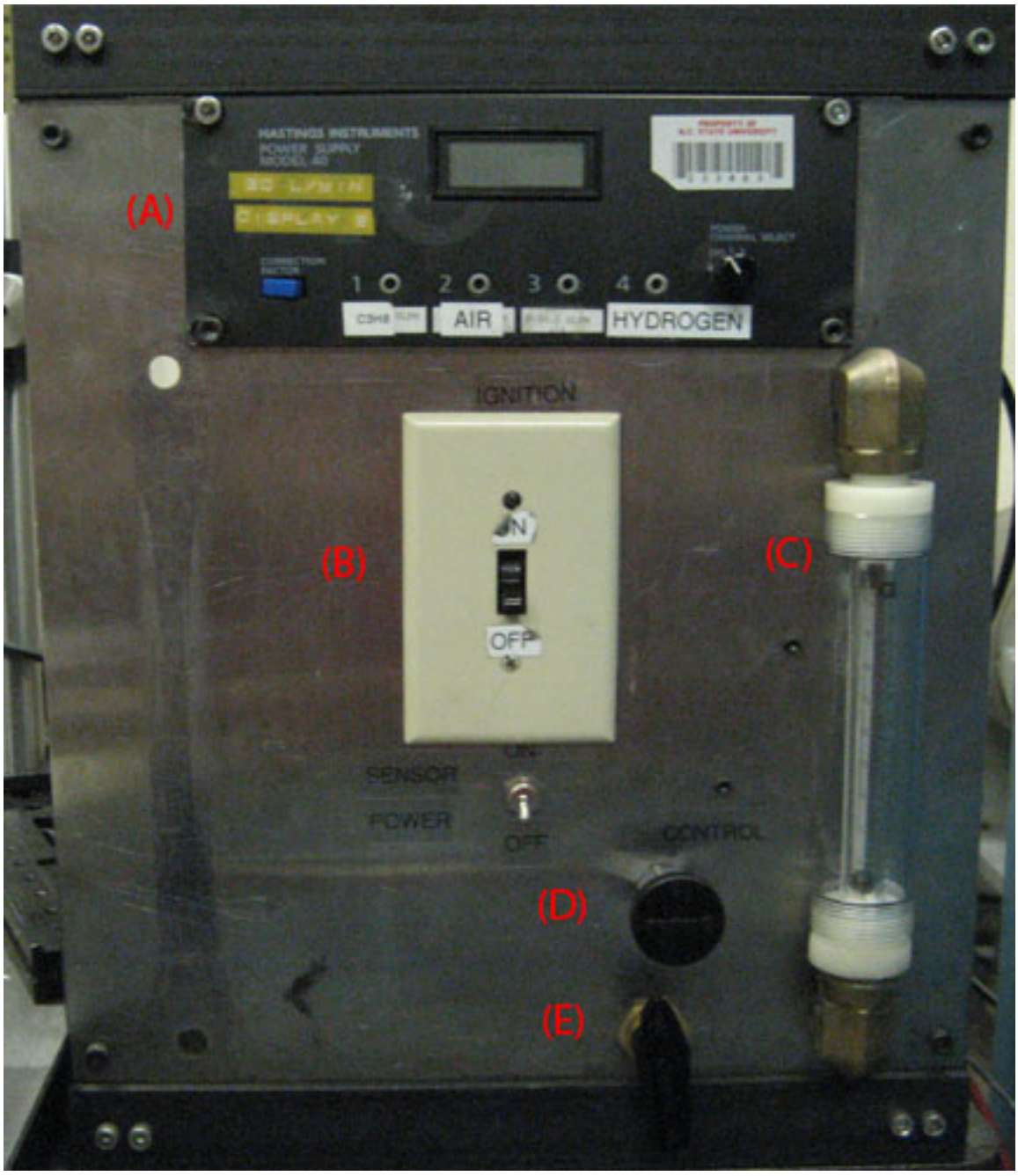

Figure 2-7: Control panel. (A) Power supply, (B) Ignition switch, (C) Air rotometer, (D) Hydrogen regulator valve, (E) Hydrogen stop valve

Having passed through the rotometer, the air is then allowed to travel through a line of quarter-inch plastic tubing which can be connected to quarter-inch stainless steel tubing.

The exit of this stainless steel section forms the nozzle that is directed at the inlet face of the pulsejet during operation. This nozzle blasting air at the inlet can then be used as a simulated wind tunnel if the air speed is known at the inlet face.

2.2.1 Cautionary Considerations

It is very likely that the air exiting the nozzle exhibits pressures above atmospheric in the near field. Some distance may be required in order for this air to expand to ambient pressure. If the nozzle is too close to the inlet, the increased pressure may artificially enhance the pulsejet's performance, yielding unrealistic results. In order to prevent this as much as possible, the nozzle exit should be placed as far as possible from the inlet face. Furthermore, the air exits the nozzle with a parabolic velocity profile and quickly transitions to turbulence. On the other hand, the inner diameter of the air nozzle is about 0.444 cm, which is sufficiently larger than most of the inlet diameters, indicating that the entire inlet face should see the same incoming velocity.

For these reasons, this method can only be considered a rough approximation to wind tunnel conditions, which in turn is an approximation to actual flight conditions. This should be kept in mind when considering the results presented herein. Of course, this discussion does not apply to any results for static cases as the air nozzle plays no role in the experiment once the pulsejet has started and is running independent of forced air.

2.2.2 Velometer

In order to measure the air speed at any location away from the air nozzle exit, an Alnor Instrument Co. Series 6000P Velometer was purchased. Though traditionally used for

HVAC systems, this equipment was useful in estimating airflow rates for this purpose. It used one of two pitot probes (each with a different sensitivity) to measure up to 10000 feet per minute, which corresponds to about 50 meters per second. As it turned out, 50 m/s was the target velocity, and by placing the probe directly in the path of the air exiting from the nozzle, it was possible to match a velocity with a volume flow rate for a given distance between the probe and nozzle exit.

As mentioned above, it was deemed advantageous to have the nozzle as far from the inlet face as possible. Thus, the goal was to find the maximum distance that the nozzle could be placed away from the inlet face while still achieving 50 m/s airspeed at the inlet. Since the air rotometer could not exceed 41 SLPM, the distance was found that corresponded to 41 SLPM and 50 m/s. This distance was measured as 2.95 cm. Using the velometer, Table 2-2 was then constructed, finding the corresponding volume flow rate for a given airspeed for a distance of 2.95 cm. These airflow settings were used in all of the experiments and great care was taken to ensure that the distance between the air nozzle and inlet face was kept at this distance for all cases.

Table 2-2: Required rotometer settings for simulated velocity

Airspeed (m/s)	Rotometer reading (SLPM)
0	0
10	12.5
20	21.0
30	28.5
40	35.0
50	41.0

2.3 Fuel Delivery System

All of the fuels used in the experiments discussed here were delivered to the pulsejet in gaseous form. These fuels (with one minor exception) were all stored in large containers provided by National Welders Supply. The fuel of choice, as in past research on small pulsejets, was hydrogen, and to a lesser extent, acetylene and propane.

2.3.1 Flowmeters and Valves

Fuel flow rates were regulated using two flowmeters. Each flowmeter was a Hastings Mass Flowmeter Model 200H. A Hastings Instruments Power Supply Model 40 was connected to both flowmeters and provided a digital readout of the volumetric fuel flow rates. The user interface of the power supply can be seen on the control panel in Figure 2-7 as well as the regulator valves for the hydrogen supply line. Hydrogen was monitored on Channel 4 while acetylene and propane were monitored on Channel 1. The regulator valves for acetylene and propane were not part of the control panel but were instead attached to the nearby optical table. The hydrogen was controlled through a Swagelok SS-31RS4 metering valve that allows up to 12.7 SLPM with a pressure drop of 10 atm. However, expecting lower fuel flow rates than with hydrogen, the acetylene and propane were controlled by way of a SS-SS4 metering valve that only allows 1.1 SLPM at 10 atm.

2.3.2 Fuel Injectors

Once the fuel leaves the flowmeter, it is transported through quarter-inch plastic tubing to a section of quarter-inch stainless steel tubing which leads to a fuel injector. The system of using a fuel injector connected to quarter-inch steel tubing was also adopted from

Kiker's work. The injector itself is made from hypodermic tubing available from SmallParts, Inc. The tubing has 0.058-inch outer diameter and 0.042-inch inner diameter. The outer diameter is large enough to fit snuggly in 1/16 inch tubing, so a 1/4 inch to 1/16 inch adapter is all that is needed to fashion a fuel injector with a size appropriate for the 8 cm pulsejet. Twelve-inch sections of the tubing were purchased and then each section could be split into four 3-inch pieces.

The next step was drilling holes into the tubing. Once again, the Machine Shop was helpful doing so. Two holes measuring 0.020 inches in diameter were drilled through both sides of the tubing. The holes can be oriented in any number of ways and a few different orientations were tried. McCauley found that fuel injectors with the holes oriented perpendicular to the incoming airflow seemed to work best (McCauley, 2006). This arrangement also seemed to work best for the 8 cm pulsejet although no quantitative data was taken to support this claim. With a couple of exceptions, all of the data presented here was taken with the injector shown in Figure 2-8 which features two holes, both oriented at 90 degrees to the flow, with diameters of 0.020 inches and with a distance of 0.080 inches separating them. This injector is shown with propane flames emanating from its holes to easily illustrate how they are oriented. The wide base of the flame gives an idea of how far apart the holes are. Furthermore, the holes were placed along the tube such that they would be in the center of the combustion chamber once the closed end of the tube reached the far side of the chamber wall. This arrangement is diagrammed in Figure 2-9. As for closing one end of the tube, the open end was crimped with a pair of pliers. The resulting flat end could

then be grinded down slightly in order to fit through the pulsejet's hole. This resulted in some leakage through the closed end but not any significant amount.

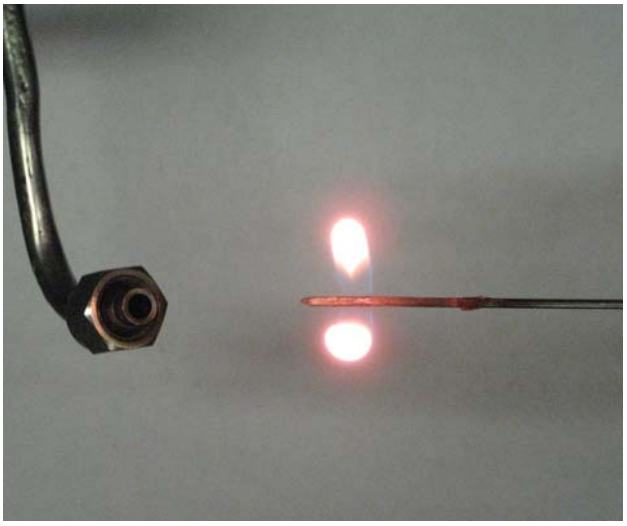

Figure 2-8: Fuel injector with propane flames

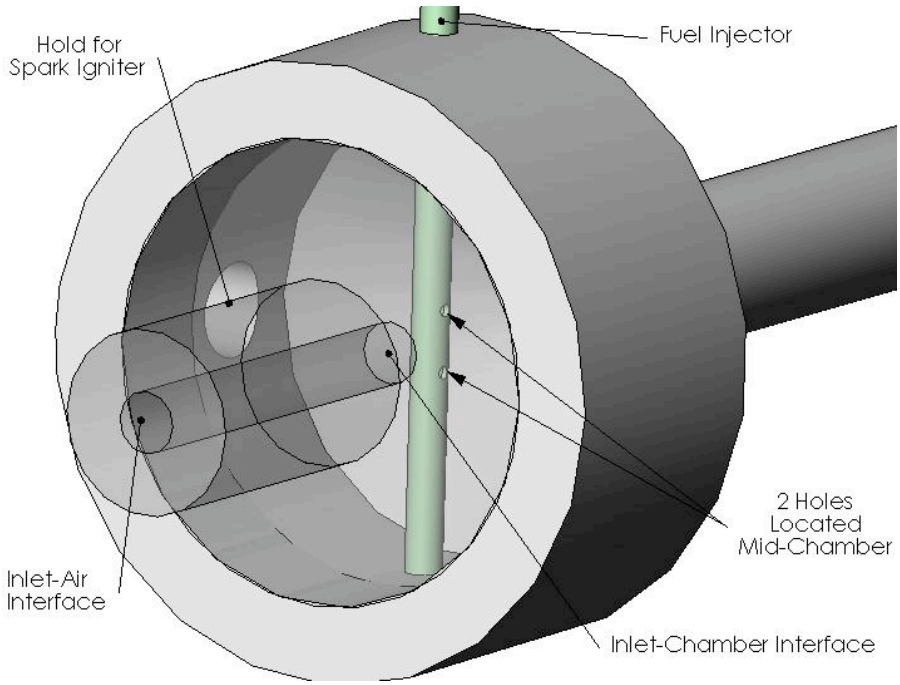

Figure 2-9: Fuel injector arrangement within combustion chamber

The exceptions to this rule are the modified rearward configuration and the injector used for the 4 cm model. The modified rearward configuration calls for the same size tube, but in this case the tube must curve slightly once it is in the combustion chamber in order to reach the center. As a consequence of this orientation, two sets of orthogonal holes were placed near the closed end of this injector. For the 4 cm model, a similar orientation as above was used but the injector itself was fashioned from tubing with an outside diameter of 0.036 inches and was placed inside the tubing used on the 8 cm models. An exposed portion of this tubing was then inserted into the 4 cm pulsejet.

2.4 Spark Ignition

In addition to a fuel source and an air source, a pulsejet needs an ignition source in order to start. It may be possible to preheat the pulsejet body to autoignition temperatures and start the engine that way, but a spark most easily provides the ignition source. Once the pulsejet has warmed up sufficiently, the spark is no longer needed. For the small and thin-walled 8 cm pulsejets running on energetic fuels such as hydrogen, the spark was usually only needed for a couple seconds if the air and fuel settings were appropriate.

2.4.1 Transformer and Switch

Because spark plugs generally require very high voltages to be fired properly, a simple connection to a traditional outlet at 120 V is not sufficient. For this reason, a transformer is necessary to step-up the voltage by stepping-down the current. Originally, a Franceformer interchangeable ignition transformer was used for this purpose. This transformer was able to output 10 kV, which was sufficient for sparking. It was later

replaced by a Pan-Tech Enterprises, Inc. model number HX-001 transformer that was capable of 12 kV. Power from the transformer to the "hot" wire was controlled with an ignition switch, which can be seen on the control panel in Figure 2-7. Once the pulsejet was running well, the switch was turned off.

2.4.2 Igniter

Unfortunately with the 8 cm pulsejets, the option of using an off-the-shelf spark plug is not available due to size constraints. For this reason, an ignition source must be fashioned by the experimenter. Adam Kiker had, of course, tackled this problem before and his solution was to use a copper wire inserted into a ceramic tube. The ceramic tube could then be inserted into a metal screw that could then thread into the pulsejet's combustion chamber. With the "hot" wire attached to the copper wire and energized, a spark would form between the end of the wire inside the pulsejet and the walls of the pulsejet, which was grounded. The spark inside the combustion chamber would then be responsible for igniting the gaseous mixture.

This method was essentially adopted for this research with some modifications. The problem with sparking off of the combustion chamber wall was that the position of the igniter had to be just right. Many times, this required constant readjustment of the igniter itself and required a great deal of patience for what was seemingly one of the most trivial aspects of the pulsejet. Furthermore, it was not uncommon for the ceramic insert itself to be pushed out by the building pressure while running which would immediately terminate the pulsejet's operation.

The solution was to use two separate copper wires; one to connect to the "hot" lead and one to be grounded. With this set-up, the spark would form between the two wires instead of between a wire and the wall. Ceramic tubes that are designed for thermocouples can be purchased from Omega. The ideal tubes are 1/8-inch thick with two holes running lengthwise through them. These holes are just large enough to fit 22 guage copper wire through them and the fit is tight enough so that the wires do not slip easily out of position. The wires were positioned so that a short portion (no more than 0.1 inches) of each wire slipped out the end that would be placed in the combustion chamber. The spark would then form at this location. Out the other end, enough wire was left for easy attachment of alligator clips. The trick was to crack the ceramic piece such that one wire would exit the top at a different location than the other and then the two wires were bent away from each other. This was done to prevent the spark from occurring at the exposed end of the igniter as opposed to the end inside the pulsejet. The ceramic piece could then be fitted into a 10-32 screw, which would then be screwed into the hole tapped in the chamber. This arrangement is shown in Figure 2-10 with the ground wire on the left, the "hot" wire on the right, and a spark forming between the two wires. It was also important that the ceramic piece just barely fit inside the screw. There may be an adhesive that works even under the extreme temperatures encountered with pulsejet operation but high temperature silicon was ineffective. Nonetheless, if the ceramic could stay put in the screw, this arrangement formed a very sturdy and reliable igniter. A similar but smaller arrangement was eventually used to ignite the 4 cm models as well.

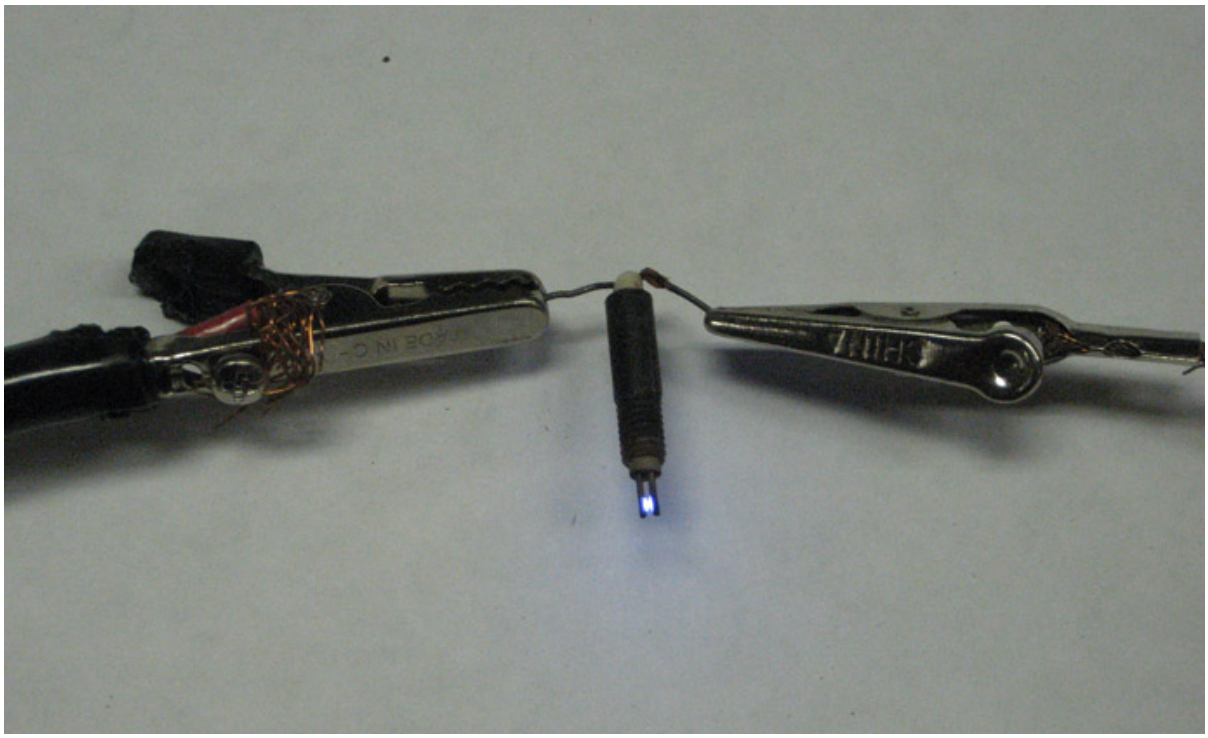

Figure 2-10: Igniter while sparking

2.5 Electronic Balance

For making measurements of mass, an Ohaus GT2100 electronic balance was utilized. This balance has an easily readable digital display that reports mass to the hundredth of a gram. To determine if the balance was accurate, a series of standard masses were tested. Masses of 5 g, 1 g, 0.5 g, 0.1 g, 0.05 g, and 0.01g were all tested. The results for the tests were remarkable. In all cases, the balance was accurate to within 0.01 g. For the lighter masses especially, the balance often underreported the actual mass by 0.01 g. What was interesting was that in almost every case where the mass was underreported while the balance was loaded, the display returned to -0.01 g after unloading instead of returning to

0.00 g. The balance can be seen in Figure 2-11 with the 1 g brass weight placed on the center of the balance's plate.

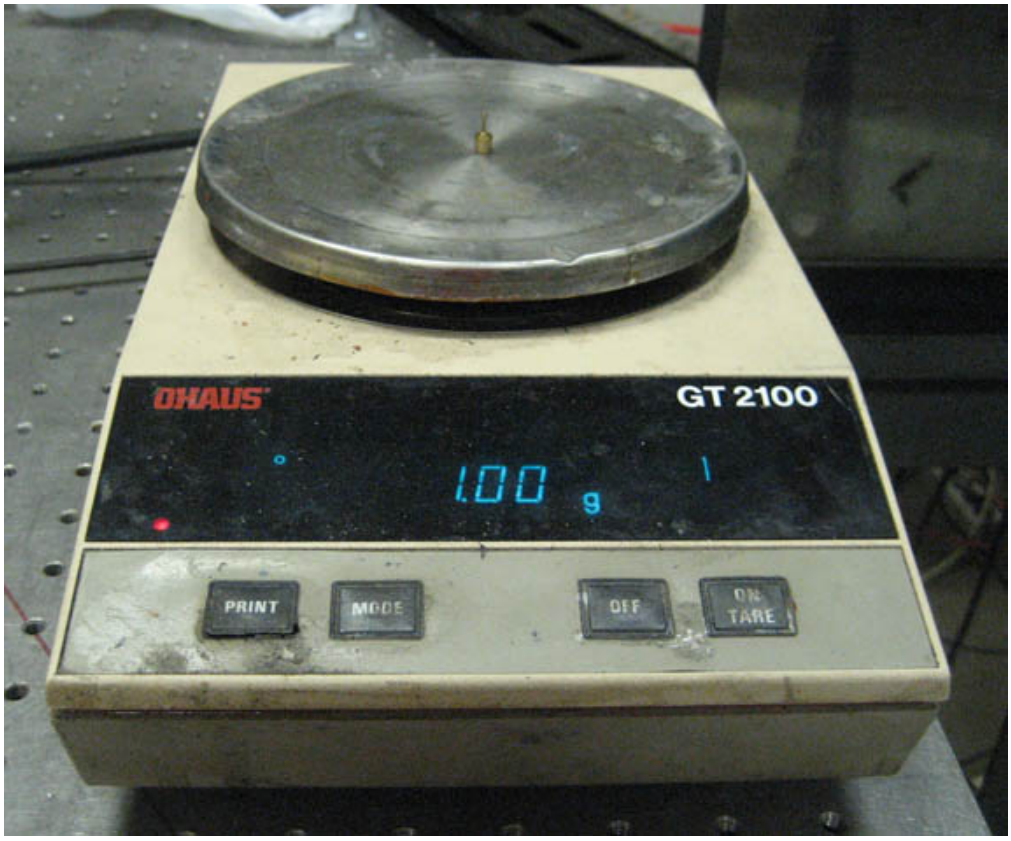

Figure 2-11: Electronic balance with 1.00 gram weight

2.6 Load cell

As with many of the previous investigations, an attempt to obtain time-resolved thrust data in addition to net thrust data was made. To this end, it was decided to purchase a new dynamic load cell. The Omega DLC101-10 dynamic force sensor, pictured in Figure 2-12, was chosen for the job. For this particular force sensor, a force applied to the upper plate distributes the force evenly across very thin quartz crystals. The stress in the crystals then

produces an electrostatic charge that is converted instantly to voltage. This voltage output is what indicates the dynamic force on the sensor.

Figure 2-12: Omega DLC101-10 dynamic force sensor

It is important to realize that the sensor is setup to operate at a zero bias condition meaning that the time-averaged voltage will always tend to zero volts. Once a load is applied and the force sensor is powered, the discharge time constant determines the amount of time it takes for the voltage to settle to zero. For this particular sensor, the time constant was reported as 50 seconds. This presents a problem if one is trying to measure the net force on the sensor. Nevertheless, measuring time-resolved thrust is relatively straight forward if one knows the sensitivity, which for this sensor was given as 511.7 mV/lbf or 115 mV/N. For

instance, if one sees a voltage output of 5.75 mV, this would correspond to a force of about 50 mN. The other important parameters to keep in mind are that the sensor had a high frequency of 25kHz and a maximum load of 10 lbf, which are both far beyond the expected range of the 8 cm pulsejets.

In addition to the load cell, a few other components were necessary to produce results. An Omega ACC-PSI Power Supply supplied power to the sensor. The output could be sent to an oscilloscope if the user simply wanted to monitor the data visually. Alternatively, the output could be sent to a LabView program on a nearby computer. This program was set up to record the signal and produce an FFT instantaneously. Previous researchers had used the same program to record instantaneous thrust and pressure data.

2.7 Thrust stand

Equally as important as the method of measurement is the structural apparatus in thrust measurements. Previous AERL researchers had tried a couple of different thrust stand configurations but none had been able to get credible net thrust measurements. Producing reliable thrust data was the most important objective of the research presented here and knowledge of past attempts was helpful.

2.7.1 For Load Cell

The Omega dynamic force sensor's design naturally suggests a vertical arrangement. Previous tests of valveless pulsejets, as described, revealed just how small the thrust could be so any horizontal design would need to be virtually frictionless. Ball bearings were considered briefly, but even they create too much friction. Air bearings might have been a

good option but the setup becomes complicated and probably expensive. Instead, the idea of setting up the apparatus vertically seemed much more practical. There is no apparent reason why a valveless pulsejet would behave differently depending on its orientation with respect to Earth. Furthermore, there are no friction considerations if the thrust stand simply sits atop the load cell.

Other considerations were necessary though. The load cell is sensitive to temperature changes so the pulsejet could not be arranged with the exhaust facing down and blowing onto the load cell. But if the exhaust points upward, the inlet of course faces downward and room must be left between the inlet and the bottom of the thrust stand in order for the pulsejet to breathe. Finally, the thrust stand also needed to be lightweight and rigid to give it a very high natural frequency; one that would not interfere with the signal produced by the pulsejet cycle.

With the help of Dr. Roberts and an undergraduate student, the final design of a thrust stand emerged and the designs were sent to the Machine Shop to be manufactured out of aluminum. The design can be seen in Figure 2-13. The pulsejet connects to the upper plate and the lower plate connects directly to the force sensor via a 1/4-28 set screw. The two plates are then separated by three aluminum rods, which are tapped for 10-24 screws at each end in order to attach them securely to the plates. The rods were cut at 3 inches each which fortunately left just enough room to include the air nozzle at a distance of 2.95 cm from the inlet face as noted above. The initial design required the upper plate to have a center hole that was threaded to allow the inlet (which would also be threaded) to screw into the plate. A second version allowed the inlet to slide through the center hole while another hole offset from the center allowed a 2-56 screw to attach the inlet to the plate.

Figure 2-13: Drawing of vertical thrust stand designed for load cell

The main difficulty with this setup is figuring out how to deliver fuel to the pulsejet. As described above, the pulsejet is manufactured to have a fuel injector inserted into the combustion chamber. This external force on the pulsejet could have a profound artificial effect on any force measurements if one did not correctly account for it. One option was to let the injector hang loosely onto the pulsejet so that the injector itself would hopefully move with the pulsejet as it operated. Another option was to eliminate the external force of the injector by widening the inlet slightly and bringing the injector up through the inlet. Both options were tested.

2.7.2 For Mass Balance

Attempts were also made to use the mass balance to measure thrust. Once the idea of running the pulsejet vertically was accepted, using the balance seemed like an obvious solution. The electronic balance had at least two advantages. First, it was very accurate. Second, the pulsejet frequency is so high that the balance would only be able to read net thrust. As with the load cell setup, the question again is how to account for the fuel injector and the fuel line leading from it to the flowmeter. Two attempts were made at measuring the thrust in this way. In the first attempt, the fuel injector was positioned parallel to the hole in the pulsejet with the hope that there was enough room for movement built into the setup to allow for any movement associated with thrust.

In the second attempt, a modified thrust stand was assembled that attempted to fix the position of the fuel injector so that any forces between the injector and the pulsejet would only create internal forces, in that they would have no effect on the force measured by the electronic balance. Figure 2-14 is a labeled picture of this modified thrust stand. Here, the original thrust stand has been attached to a large aluminum base plate. Also attached to this plate is a vertical bar that uses an aluminum-clamping device to hold the fuel injector in place. The only external force, other than the forced air and the thrust of the pulsejet, is the force created by the fuel line. There is no way to eliminate all external forces. Rather, the working theory behind this attempt is that the force created by the fuel line on the fuel injector would be easier to control and account for than the force created by the fuel injector

on the pulsejet. As shown, a 90 degree elbow is used to allow the fuel line hang straight down without touching the base plate or the table on which the balance is sitting.

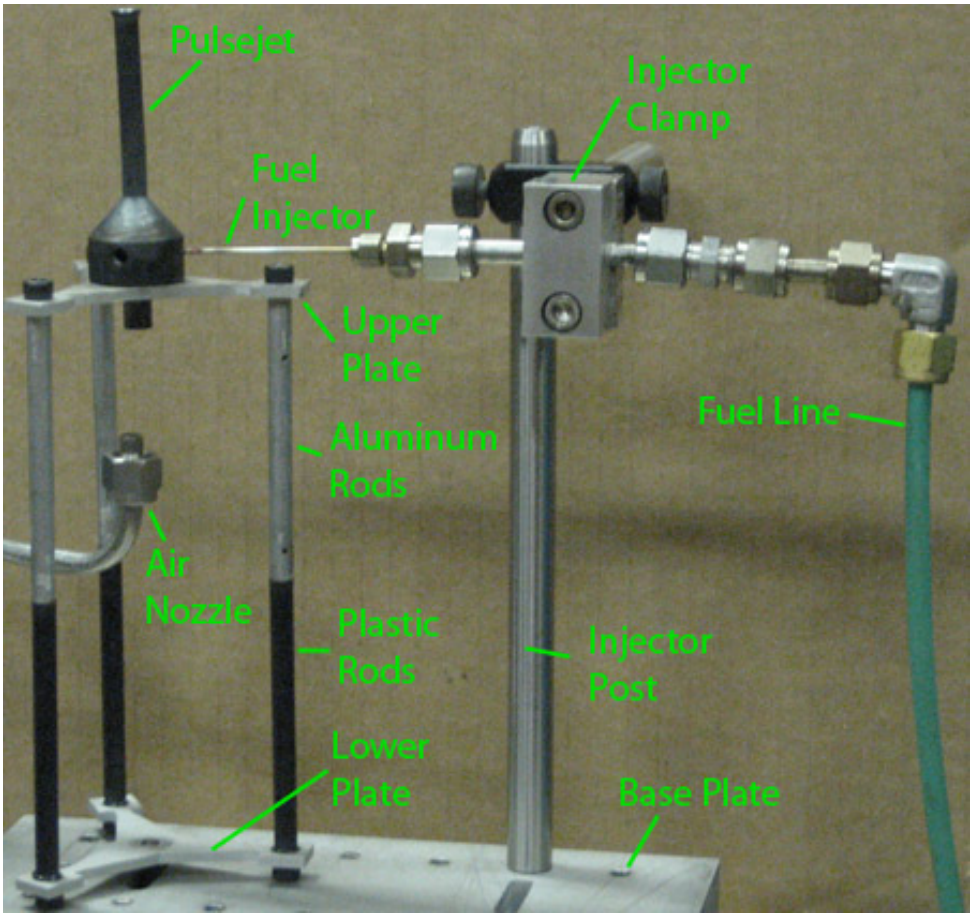

Figure 2-14: Final modified thrust stand with labeled components

2.8 Heating apparatus

Another objective with this research was to test different fuels on the 8 cm model. As previous researchers have discovered, running the valveless pulsejet on fuels other than hydrogen is not a trivial task. One of the successful methods for running the pulsejets on hydrocarbon fuels has been preheating the pulsejet and/or the fuel itself. For this reason, several methods for preheating propane were used on the 8 cm pulsejet.

One popular method used previously was wrapping copper tubing a number of times around the body of the pulsejet and running the fuel through this tubing to take advantage of regenerative heating. Unfortunately, this method was not practical in this case due to the small size of the pulsejet. An analogous method was employed, however, that modified the pulsejet to allow the fuel injector to enter the combustion chamber while running inside the exhaust tube, as detailed in section 2.1.3.

Other than the modified pulsejet, three methods were tested. The first method was running the fuel through a helical section of copper tubing, which was immersed in brake fluid. The pot containing the brake fluid and copper was then placed on a hot plate. Brake fluid was chosen because it offered a high boiling point and a high heat capacity, which would hopefully translate into a large rate of heat transfer into the fuel. The unfortunate drawback of this method was the unexpected result of heating brake fluid. While brake fluid is formulated to withstand high temperatures, it does begin to evaporate even at reasonable temperatures and, in doing so, releases noxious fumes. This method was quickly abandoned as it was deemed ineffective, unpleasant, and probably harmful to the researcher. A similar method was also attempted in which copper tubing was routed through a toaster oven but the oven was not able to reach the desired temperatures.

By far, the best effort used resistive heating and was acquired with the help of Tim Turner. Initially this method was going to employ inductive heating, which could have been much quicker, but this setup proved too difficult to utilize. The resistive heating method used a heating coil embedded in a ceramic jacket. The fuel was routed through a series of connections to a 1-inch diameter steel pipe that was about 12 inches long. This pipe fit into

the U-shaped ceramic jacket and was heated by the coil, which received 220 V. The fuel exited this heated pipe and was transitioned back down to ¼-inch copper tubing that connected to the fuel injector. The tubing beyond the heater could be covered in insulating material to minimize heat losses. The temperature of the steel pipe could be controlled through a thermocouple. Using the large pipe extended the residence time of the gas inside thereby maximizing heat conduction. Gasses leaving the tube were consistently measured at temperatures approaching the set point.

2.9 Sound Level Meter

Sound pressure level (SPL) is one way of defining how loud an object is. For this research, SPL was measured using a RadioShack Sound Level Meter Cat. No. 33-2055. This device uses a 9 V battery and has a digital display that reads out the SPL in decibels (dB). It has several range settings, each reading up to +/- 10 dB of the center value. The 8 cm pulsejets typically operate between 100 and 110 dB (120 dB is considered the threshold of pain for humans), but a few conditions may cause the SPL to extend above or below this range. The meter is generally placed a couple of feet away from the source and at an angle of 30 degrees from the pulsejet centerline.

2.10 Startup procedure

Monitoring the results of experimentation and analyzing the methods critically eventually established a procedure for successfully obtaining results. It is important to stress that small deviations from this procedure could produce inconsistent or erroneous results.

1. Begin charging the air tank. As the tank loses pressure, the flow of air may be reduced causing changes in airspeed exiting the nozzle. This is less likely to occur if the tank is fully charged.
2. Turn the power supply on. The flowmeters will take a few minutes to initialize before accurate flow readings can be taken.
3. Open the valves on the fuel tank to allow fuel flow (Note: The fuel control valves on the control panel should be completely closed at this point).
4. Adjust thrust stand to the desired configuration (inlet, body, fuel injector, etc.). Make sure all screws and clamps are tight enough to restrict movement but do not over tighten. The 2-56 screws that attach the inlet to the upper plate can be especially difficult to unscrew after running an experiment. The fuel line should be hanging down at a 90 degree angle to the injector and should not be touching the base plate or table. Also make sure the injector is placed in the middle of the combustion chamber. Minor variations in injector placement can have significant effects on the pulsejet's operation.
5. Place the air nozzle directly below the inlet at a distance of 2.95 cm. The air should be blowing directly at the inlet. The nozzle should not be touching the thrust stand itself or the balance.
6. Turn on the air and adjust the flow to the desired setting on the rotometer.
7. Tare the balance at this point. This will give the experimenter a zero reading when the pulsejet is not operating. Then, when the pulsejet is running, the experimenter can immediately tell what the thrust output is (a reading of 0.6 g is

about 6 mN). While this is not strictly necessary, because the experimenter can always take the difference of the mass during and after running, it is helpful. Note that it may take a couple of minutes for the balance to stabilize since it is so sensitive. Taring several times may be necessary.

8. Attach the spark and ground wires to the igniter.
9. Flip the ignition switch to On. The spark makes a loud enough noise to be heard although it will not be seen. Another indication that the spark is successful is that the flowmeter reading will go haywire because of the electrical interference.
10. Use ear protection at this point. The 8 cm pulsejets are not quite painfully loud but prolonged exposure may cause hearing damage.
11. Turn the fuel's stop valve 90 degrees to allow flow. Adjust the metering valve, slowly increasing the fuel flow rate, until the pulsejet begins to run.
12. Once the pulsejet has been running well for a few seconds, the ignition switch may be turned Off. The flowmeter will now begin reading the correct flow rate. If the pulsejet stops running at this point, the switch may need to be turned on again.
13. Once the pulsejet has been running without a spark for a few seconds, the ground wire and spark wire may be removed from the igniter. Take great precaution in this step. This ignition switch MUST be turned off. Be careful not to burn oneself on the pulsejet or the thrust stand because these parts will already be very hot. Also, be careful not to disturb the thrust stand's position with respect to the

air nozzle. The alligator clips themselves should not be hot if this step is performed quickly.

14. With the wires removed, the balance should now be reading the correct thrust values.

15. Adjust the fuel flow rate to the desired value. Note that the flowmeter does not react immediately to changes with the metering valve so readjustment may be necessary after several seconds.

16. By monitoring the mass readings, noting the color of the pulsejet, and listening to the pitch of the pulsejet, one can tell once the pulsejet has reached equilibrium. This may take anywhere from 20 seconds to a few minutes depending on a variety of factors.

17. Generally, even at equilibrium, the mass and SPL will oscillate among different values. The experimenter must be judicious in deciding what value to record. One may need to monitor these readings for a minute or more before deciding. Usually, the oscillations are not very great if the pulsejet is resonating and an appropriate median or mean value can be found.

18. The fuel may be readjusted to take new measurements if desired, but note that the procedure must be restarted if a new airflow setting is desired. Unless time is a factor, it is recommended that only a few readings are taken at a time before cutting the fuel and retaring the balance.

19. To stop the pulsejet, turn the stop valve 90 degrees back to the closed position. Make sure to turn the metering valve back to closed as well.

20. The balance should be monitored for a minute or so because the value does not always return immediately to zero. Record the final mass reading, which should at least be near zero.

21. At this point, one may choose to do more runs at these settings or to adjust the air or pulsejet configuration. Be aware that the thrust stand and pulsejet are very hot and will be so for several minutes. If time is a factor, the air should be left on and perhaps even increased to utilize convective cooling. If time is really a factor, one may use pliers and/or gloves to handle the hot parts.

This procedure may seem long and complicated but with experience, can be completed in just a few minutes. When this procedure is followed, it tends to yield very consistent results, which will be discussed in the following section.

3 Forward Facing Configuration

As described above, the majority of the present research was aimed at quantifying results on an 8 cm long valveless pulsejet. Previous research at AERL had yielded many significant results pertaining to chamber pressure, sound pressure level, operational frequency, fuel flow rate limits, fuel types, and even time-resolved thrust. However, net thrust measurements along with thrust specific fuel consumption or specific impulse are conspicuously absent from this list. While knowledge of these other performance characteristics are useful in understanding valveless pulsejet operation, ultimately net thrust and fuel efficiency will determine the applicability of any proposed propulsion system. For this reason, obtaining net thrust was the central goal and getting reasonable and repeatable results was a major victory. The desired procedure was not known a priori, however, and the methodology went through several phases that will be summarized below.

3.1 Evolution of a Methodology

3.1.1 Load Cell

The ambitious initial goal was to obtain both time-resolved and time-averaged thrust. An Omega force sensor with a very high frequency and high sensitivity was purchased and the thrust stand detailed in section 2.7.1 was manufactured. The problem, as expected, was how to account for the external forces imposed by the fuel injector and the spark ignition system. At first, it was not understood how much the spark wire could affect thrust measurements and it was left in place.

The fuel injector problem could potentially be handled by running the injector up through the inlet. As long as the injector did not disturb the pulsejet's operation, this would be ideal because the injector would not create any external forces on the pulsejet. A new pulsejet body could then be made without a hole for the injector in the wall of the combustion chamber. Three inlets were specially constructed for this arrangement with slightly enlarged areas to account for the space occupied by the injector. Also, an XYZ translation stage was used to accurately position the injector in the middle of the inlet. However, repeated attempts revealed that, while operation was in some cases possible, the injector clearly played a detrimental role in the pulsejet's operation. This was but one indication of how sensitive the pulsejet becomes at such small scales. The decision was made to make other arrangements for the fuel injector.

The next iteration saw the fuel injector placed, as usual, in the combustion chamber. The thought was that if it was not held rigidly in place, then it could move or react to the pulsejet and perhaps only minimally interfere with measurements. The load cell was monitored on an oscilloscope. By measuring the time between peaks, some reasonable estimates of the pulsejet's frequency were made. Unfortunately, the nature of the load cell did not lend itself easily to making net thrust measurements. Any DC load imposed on the force sensor would eventually be dissipated. With a time constant of 50 seconds, this was generally accomplished in a matter of minutes. The cell was manufactured to measure a dynamic force with an average voltage output of 0 V.

The crucial realization was that if, somehow, the thrust of the pulsejet could be instantaneously imposed on or withdrawn from the load cell, then the voltage difference

during that short time interval should correspond to the magnitude of the thrust. This could be accomplished by noting the voltage change as the pulsejet is started, but this method poses some difficulties. A spark and air are both necessary for starting the pulsejet and both impose their own forces on the load cell. Furthermore, for most situations, the startup process takes too long to be considered instantaneous. On the other hand, the pulsejet's operation can be suspended almost instantaneously by cutting off the fuel. Additionally, it was noted that the spark and ground wires could be easily removed from the apparatus once the pulsejet was operating on its own. The procedure became clear. The pulsejet would be started as usual while on the thrust stand and with the load cell powered. As soon as the spark was no longer necessary, the ignition switch could be turned off and the wires detached from the igniter. Then, after a few minutes, the DC component of the load cell voltage should return to zero, and only the AC component, representing transient forces, would remain. The fuel supply could then be cutoff and the resulting voltage change during those few seconds would be a direct measure of the thrust. It is important to keep in mind that the force registered by this method would actually be the negative equivalent of the thrust since it measures the absence of thrust.

This method seems straightforward and should have worked but repeated attempts yielded erratic results. One problem was heating of the load cell during operation. The aluminum rods on the thrust stand were replaced by high temperature-tolerant plastic rods to minimize conductive heat transfer from the top plate to the bottom plate that was attached to the load cell. Furthermore, some insulating material was placed over the lower plate to minimize heat transfer from the air around the inlet. It was also around this time that it was

realized that the air nozzle should be placed a good distance away from the inlet to minimize pressure effects (see section 2.2.1). Nonetheless, the results were inconsistent and often difficult to interpret. This is exemplified by Figure 3-1, which shows a typical load cell voltage versus time plot during the period of fuel cutoff. This was the best plot obtained and one can clearly see the change in behavior associated with cessation of pulsejet operation. Trying to extract net thrust data from this profile, however, was not trivial. The usual attempt consisted of finding an average of points before cutoff and an average of points afterward and then taking the difference. This method rarely yielded reasonable results and never yielded the same results. After struggling with this for a short while, the decision was made to look for alternative means of thrust measurement.

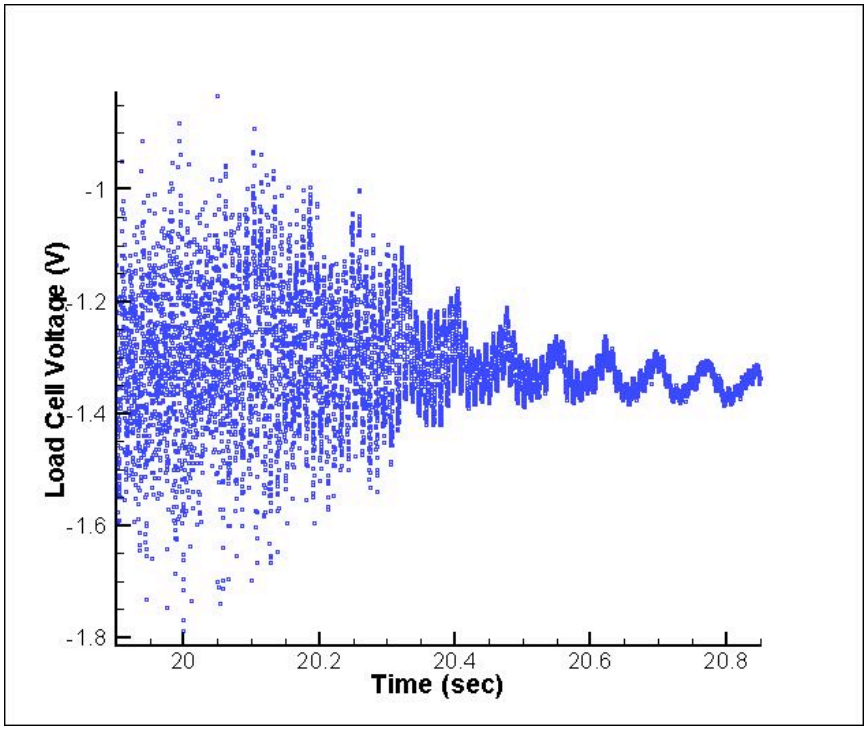

Figure 3-1: Load cell voltage output during fuel cutoff

3.1.2 Electronic Balance

Other methods of thrust measurement were sought. One option was to use a thrust plate. The idea was to use a flat plate hanging in place by wires. If the exhaust of the pulsejet were to be directed at the plate, the momentum of the exhaust would deflect the plate by an amount proportional to the thrust. A few attempts at this method yielded dismal results. The thrust appeared to be much lower than expected at the time and the plate oscillated too much to allow for accurate measurements of its deflection. Also, if measurements with airflow were to be made, the effect of air blowing around the pulsejet and impinging on the thrust plate would have to be countered.

Still another option was to use the electronic mass balance. The thrust stand already positioned the pulsejet vertically so that, if measured on the balance, any positive thrust from the pulsejet should just be measured as an increase in mass. Furthermore, the balance was simple to use and very accurate. The thrust could be measured by noting the difference between the mass while sitting still and the mass while operating. As with the load cell, the spark and ground wires could be removed during operation so they should not interfere with the results.

Again, this method held great promise, but again, the results were disturbing. Generally, once the pulsejet was operating and the wires were detached, the mass readings would increase erratically for several minutes before finally settling down. Then, after cutting the fuel off, the mass readings would again change for several minutes before finally resting, once the pulsejet itself was at room temperature again. Furthermore, the mass

reading before operation and after operation, which should be the same, were almost always different and usually significantly different. It was difficult to interpret these findings. Figure 3-2 shows a typical mass versus time profile for such an experiment. The red sequence shows the change in mass while the pulsejet was operating and the green sequence shows the mass readings once the fuel was stopped. Thus, the final red data point and the initial green data point are of the same mass value. The first thing to notice is that the green sequence clearly does not end at the same value at which the red sequence began. The second aspect to notice is that the profiles both take well over four minutes to stabilize.

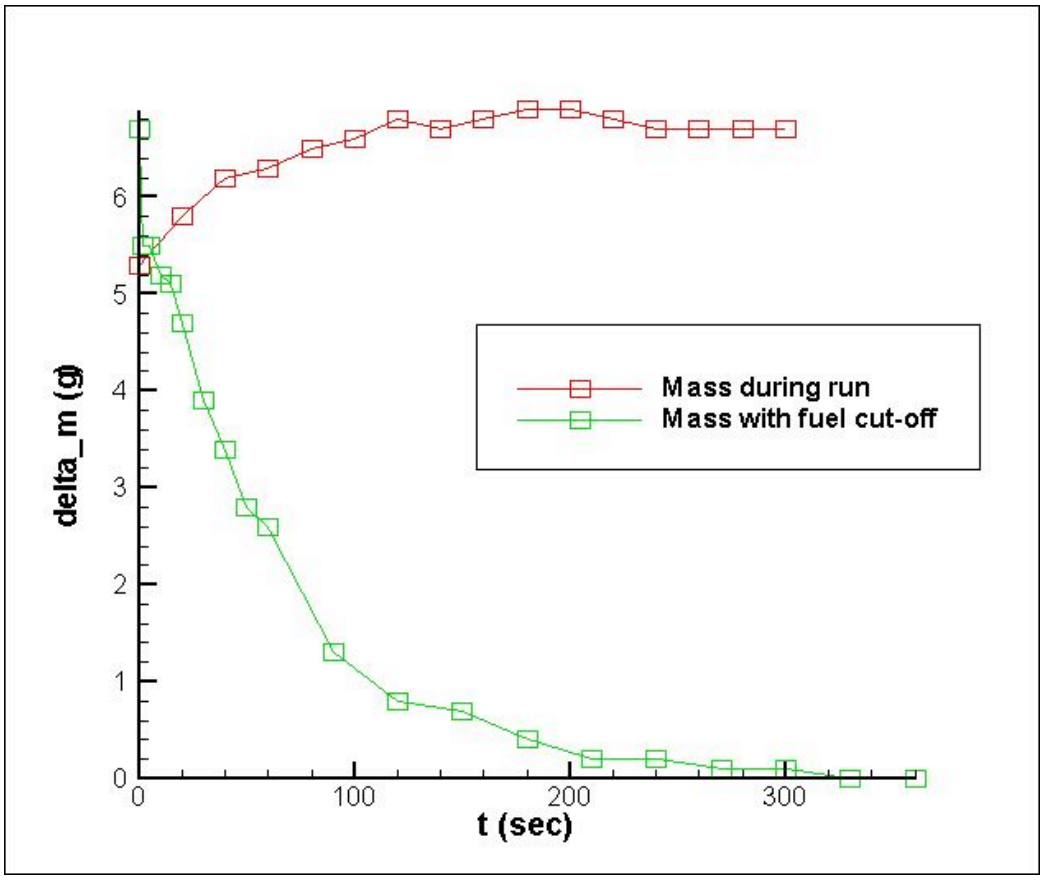

Figure 3-2: Mass versus time profile for typical run in early mass balance testing

Several interpretations were possible. One possibility was that the thrust does indeed change dramatically over a several minute period of operation as the heating of the pulsejet body changes the operating characteristics. In fact, one can discern a change in the pitch of the pulsejet as it begins warming up after startup. Another possibility was that the heating of the pulsejet changes its dimensions in such a way that the air's interaction with the pulsejet is altered, thus affecting the mass readings. Also, it could have been that the electronic balance was simply not adequate for making these measurements. However, the most likely possibility was that interactions with the fuel injector as it was heated were interfering with mass measurements. Nonetheless, some of the trends revealed by using this method made some intuitive sense, and for a while, these results were accepted as reality, although with a high degree of uncertainty. The mass was measured once immediately before fuel cutoff and then again after fuel had been cut and the apparatus cooled sufficiently. The change in mass was then converted to thrust. Thrust values were regularly measured in the 50 mN to 100 mN range.

Being bothered both by the inexplicable behavior of the mass readings during operation and the lack of agreement between experimental results and computational results, a series of tests were performed in an attempt to elucidate the source of the error. Three cases were examined. The pulsejet was operated as usual for a few minutes and the fuel was cut as usual. Then, in the first test, the air was also cut, and the mass balance exhibited the same behavior as in Figure 3-2. In the second test, the air was left running, but the fuel injector was removed, after which little variation in mass readings was seen. Finally, another test was performed in which the air and the fuel injector were removed and the mass readings

stayed steady afterward. This series of tests proved, conclusively, that the problem with the apparatus was the interaction between the fuel injector, as it was heated, and the pulsejet.

3.1.3 Final Apparatus

Since running the injector through the inlet did not work and running it down the exhaust would likely not work either, a way to neutralize the effect of the injector on the thrust measurements was necessary. This was accomplished by fixing the injector and the thrust stand to the same rigid base as described in section 2.7.2. In this way, all forces between the injector and the pulsejet were internal and could not affect the mass measurements. Measurements made with this setup were much more reasonable and very repeatable. Furthermore, the thrust results were much closer to computational predictions. The standard masses described in section 2.5 were used here to test the thrust apparatus for accuracy. Since the pulsejet was not centered on the balance, there was concern that the true value of the thrust may not register. However, the masses were tested in locations all over the base plate and during conditions including no operation, only air operation, and full pulsejet operation. In all cases, the balance registered a reading within 0.02 g of the actual value. For this reason as well, the measurements taken with this apparatus were considered to be valid.

Having solved the fuel injector problem, the ability to obtain dependable results was finally achieved. Two more alterations were made along the way before this setup could achieve the results presented below. First, a new pulsejet was constructed with a fuel injector hole that was much closer in size to the outer diameter of the fuel injector. Previously, a

small obstruction was used in an attempt to plug up the excess area. Results showed that shrinking the size of the hole increased thrust by a factor of four or five on at least one of the inlets (inlet 700-125). An improvement in thrust is not unexpected as the leakage in the chamber results in both an escape of mass in a direction that does not contribute to the momentum thrust and in reduced peak chamber pressure, which directly determines the thrust.

The second alteration consisted of extending the height of the thrust stand by adding 3-inch rod sections, effectively doubling the height. It was found that both the air nozzle and the lower plate interrupted the inlet's flowfield. While the air nozzle still needed to be at the appropriate distance from the inlet, the lower plate could be moved further away and, once it was, increased performance was noted. For static conditions, the air nozzle could be removed once the pulsejet was started. Doing so made drastic differences in the measurable thrust. As a demonstration of how powerful the effect of an obstruction can be, refer to Figure 3-3. Here, a screwdriver handle was used as the obstruction. With no obstruction, the mass reads 0.86 g. Moving the handle into inlet's farfield, roughly 10 cm away, reduces the mass reading to 0.32 g. Moving the handle even closer to the inlet causes a decrease in mass to -0.24 g, showing a very significant detrimental effect on the inlet's ability to entrain fresh air into the pulsejet. For comparison, the handle was also placed at the pulsejet's exhaust plane in which case the mass was reduced but only to 0.74 g, showing that the exhaust is much less sensitive to obstructions and probably is not involved in entraining air into the combustion chamber, as noted by Tao Geng in his dissertation. While this small experiment was very enlightening, it also showed one of the limitations of this apparatus. It is very

likely that, for the inlet (700-125) used in this example at least, the lower plate of the thrust stand is consistently interrupting the inlet's flowfield.

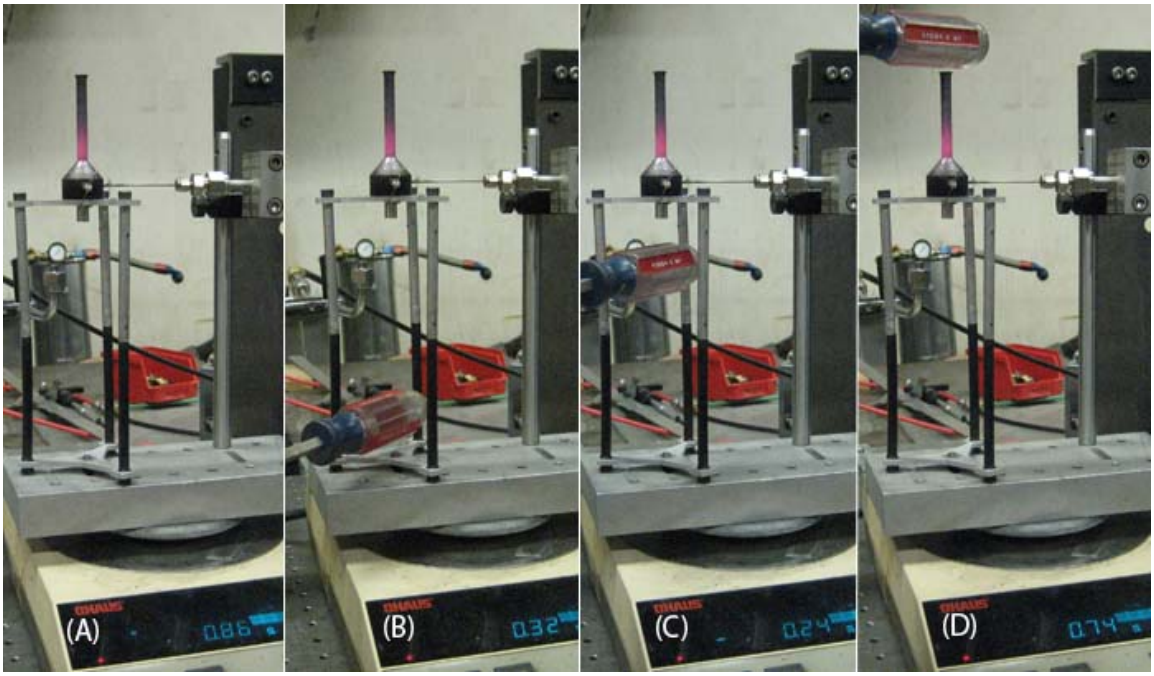

Figure 3-3: Effects of obstruction location in pulsejet flowfield for inlet 700-125. (A) No obstruction, (B) Obstruction in inlet farfield, (C) Obstruction in inlet nearfield, (D) Obstruction in exhaust nearfield

3.1.4 Difficulties and Considerations

One inescapable reality of working with valveless pulsejets at this scale is that results and operation are quite sensitive to variations in the setup. The researcher must pay close attention to details such as fuel injector orientation and air nozzle location. The location in which the pulsejet is attached to the apparatus may have profound effects on its performance. Figure 3-4 shows similar air and fuel conditions for a pulsejet during operation. The only difference between the two pictures is the way the body is held in place, but the visible effects of doing so are dramatic. The pulsejet clamped along the exhaust tube has bright red

spots in the combustion chamber and near the end of the exhaust tube. On the other hand, the pulsejet clamped along the inlet shows a bright red spot only along the exhaust tube. This evidence indicates that the two situations may have significantly different consequences for heat distribution along the pulsejet body, and possibly also for thrust measurements. To have repeatable and comparable measurements, a strict procedure was created and followed carefully. This procedure can be found in Section 2.10.

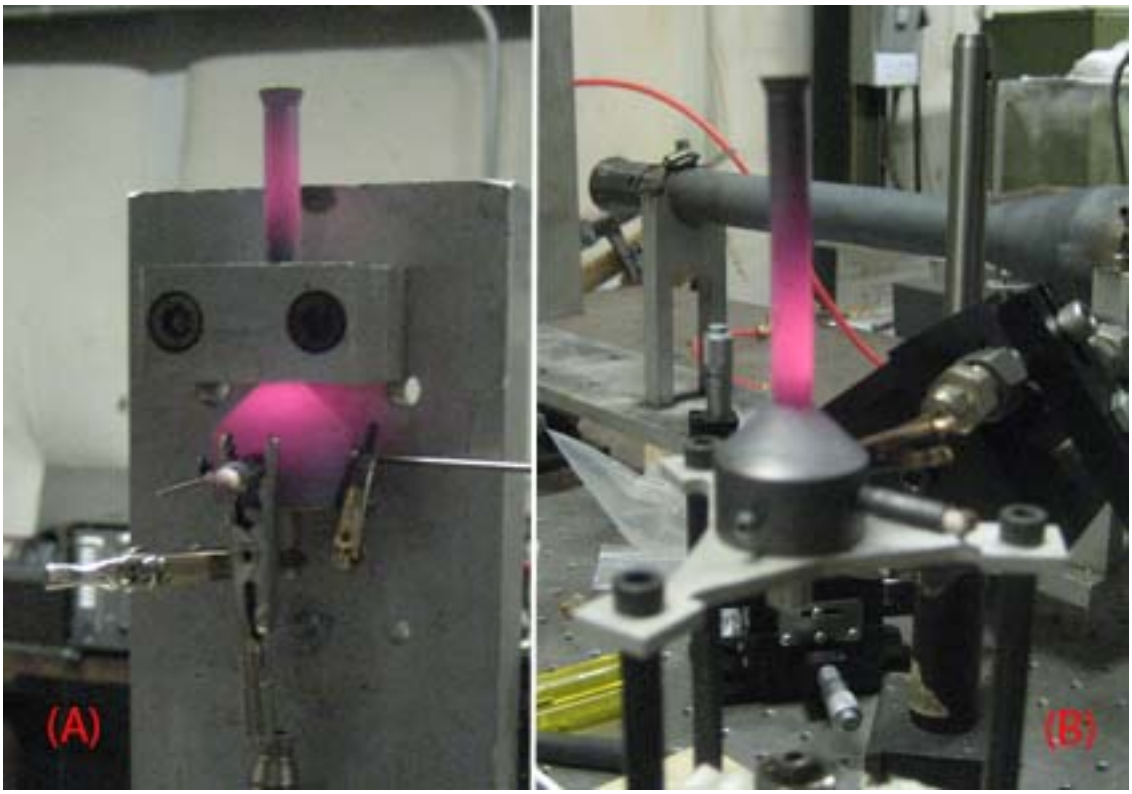

Figure 3-4: Evidence of effects of clamping location. (A) Clamped behind combustion chamber, (B) Clamped at inlet

Degradation of the pulsejet over time is inevitable. Even though there are no moving parts, the pulsejet is subjected to continuous heating and cooling as it is tested. This has a detrimental effect on the physical condition of the pulsejet and likely has some negative

effect on performance. Small chunks of metal can be seen separating from the interior and exterior from time to time while operating. Also, extended use has begun to curve the exhaust tube slightly creating some unintentional thrust vectoring. It is unclear why the exhaust tube curves but it may have something to do with the uneven convective cooling by the forced air on the exterior of the pulsejet as a results of the asymmetrical shape of the thrust stand upper plate.

As a final consideration, it should be noted that the balance does not always return to a zero mass reading once the fuel flow has ceased. One would expect that if the mass reads zero grams before starting, then it should read zero again afterwards, but this is not the case. The reason why is not exactly clear but may be related to minor shifting in the fuel line's position. At any rate, the discrepancy is never greater than 0.20 g or 2 mN, which may be considered the maximum uncertainty associated with the apparatus. In cases where the final mass reading was not zero, the final mass was subtracted from the recorded mass and the difference was used to calculate thrust. As for the readings themselves, the balance rarely stayed constant at a single value. Usually, the readings would oscillate steadily between two extreme values that were only occasionally more than 0.10 g apart. The value recorded was a good mean or median value considering the range of the oscillation. For many of the data points, two or more readings may have been taken. In most cases, these readings were averaged or a reasonable representative value has been used for the findings below.

3.2 Thrust and Specific Impulse Results

A total of seven different inlets were tested in the forward facing configuration. Four of these have the same diameter and four have the same length (one is in both groups). The inlets are referred to by their dimensions (in thousandths of inches). Table 3-1 gives the length and diameter of each inlet in centimeters along with its name. This section presents the full data and performance characteristics for each inlet. Each inlet was tested over the entire operational fuel range at six velocities ranging from 0 to 50 meters per second at intervals of 10 m/s. Future sections will proceed to analyze the patterns and trends among the different inlets.

Table 3-1: Dimensions of inlets tested

Inlet	Length (cm)	Diameter (cm)	Area (cm^2)	CC area/Inlet area	Exhaust area/Inlet area
300-125	0.762	0.318	0.079	36.0	1.97
415-125	1.054	0.318	0.079	36.0	1.97
550-125	1.397	0.318	0.079	36.0	1.97
700-125	1.778	0.318	0.079	36.0	1.97
700-100	1.778	0.254	0.051	56.2	3.08
700-081	1.778	0.206	0.033	85.7	4.69
700-150	1.778	0.381	0.114	25.0	1.37

The first inlet to be analyzed is inlet 300-125. This inlet is very short with a wide diameter. In fact, the length is barely greater than the width of the inlet base so that the protruding portion of the inlet is not even long enough to span the entire width of the upper plate on the thrust stand. It is unclear if this complication interfered with the results of the tests. Figure 3-5 and Figure 3-6 are plots of the thrust and specific impulse of inlet 300-125 respectively. The maximum thrust achieved was about 7 mN and specific impulse never

exceeded 100 sec. The most striking characteristic of both plots is how the data at 20 m/s stand out from the rest. With all other velocities, the thrust rises steadily with fuel flow rate and specific impulse stays virtually constant over the entire fuel range. At high fuel flow rates, higher velocity tends to contribute to the highest attainable thrust, but below 7 SLPM, the thrust at 20 m/s dominates. As far as efficiency, the plot of specific impulse shows that this inlet clearly prefers running at 20 m/s. One interesting thing to note is that this inlet barely runs at 10 m/s so no data was taken at this condition. This is likely due to interference with the air nozzle (see Figure 3-3). Another operating characteristic of this inlet that was noted during operation was the amount of warm air in the vicinity of the inlet itself. The general understanding of valveless pulsejets is that you want combustion products leaving out the exhaust as opposed to the inlet so the presence of warm air indicates that much of the combustion products are exiting by way of the inlet. This leads to poor engine performance and, indeed, the performance of this inlet is quite poor compared to others that were tested. The short and wide inlet is not very efficient at forcing products to leave through the exhaust tube.

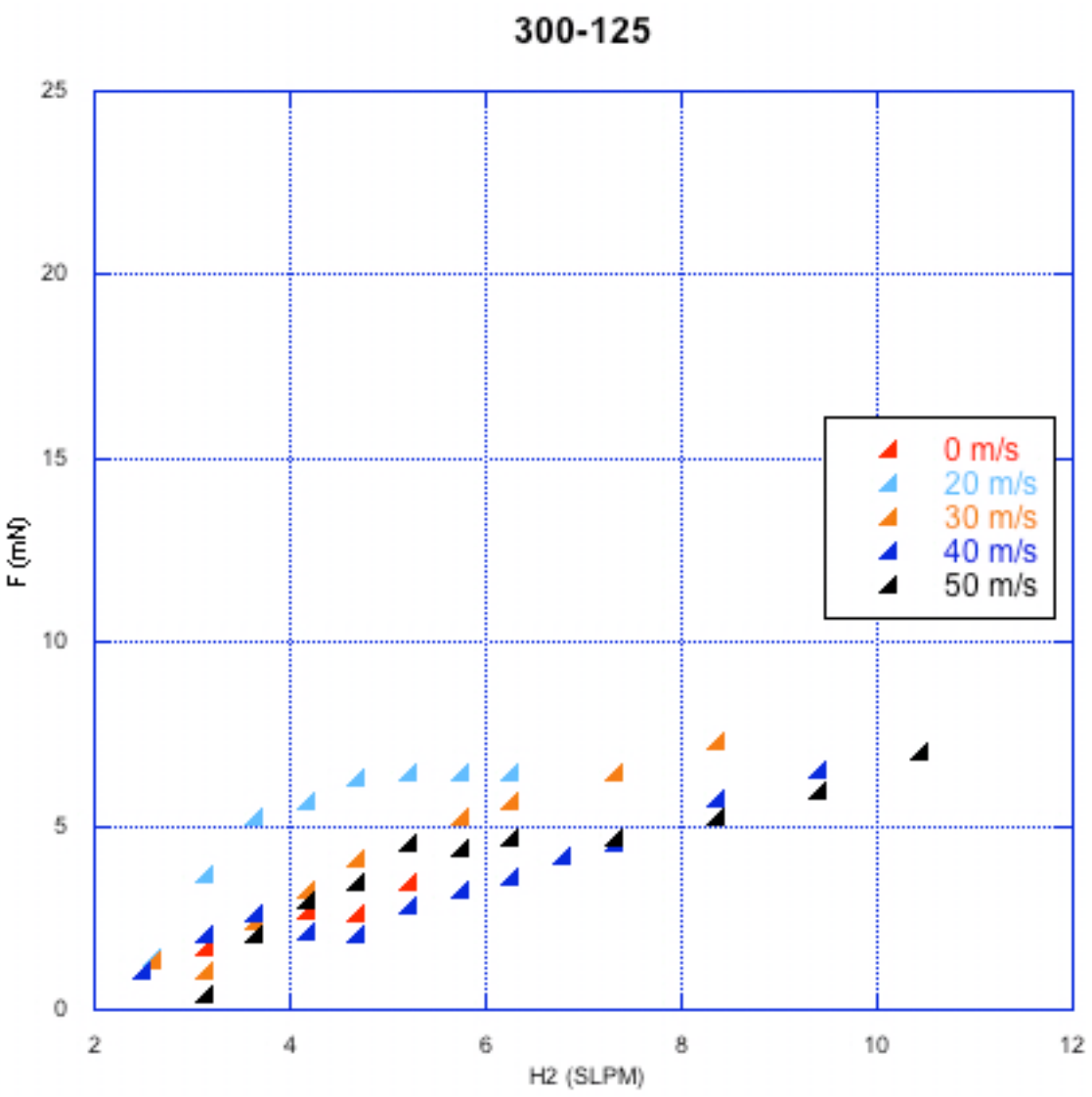

Figure 3-5: Thrust data for inlet 300-125

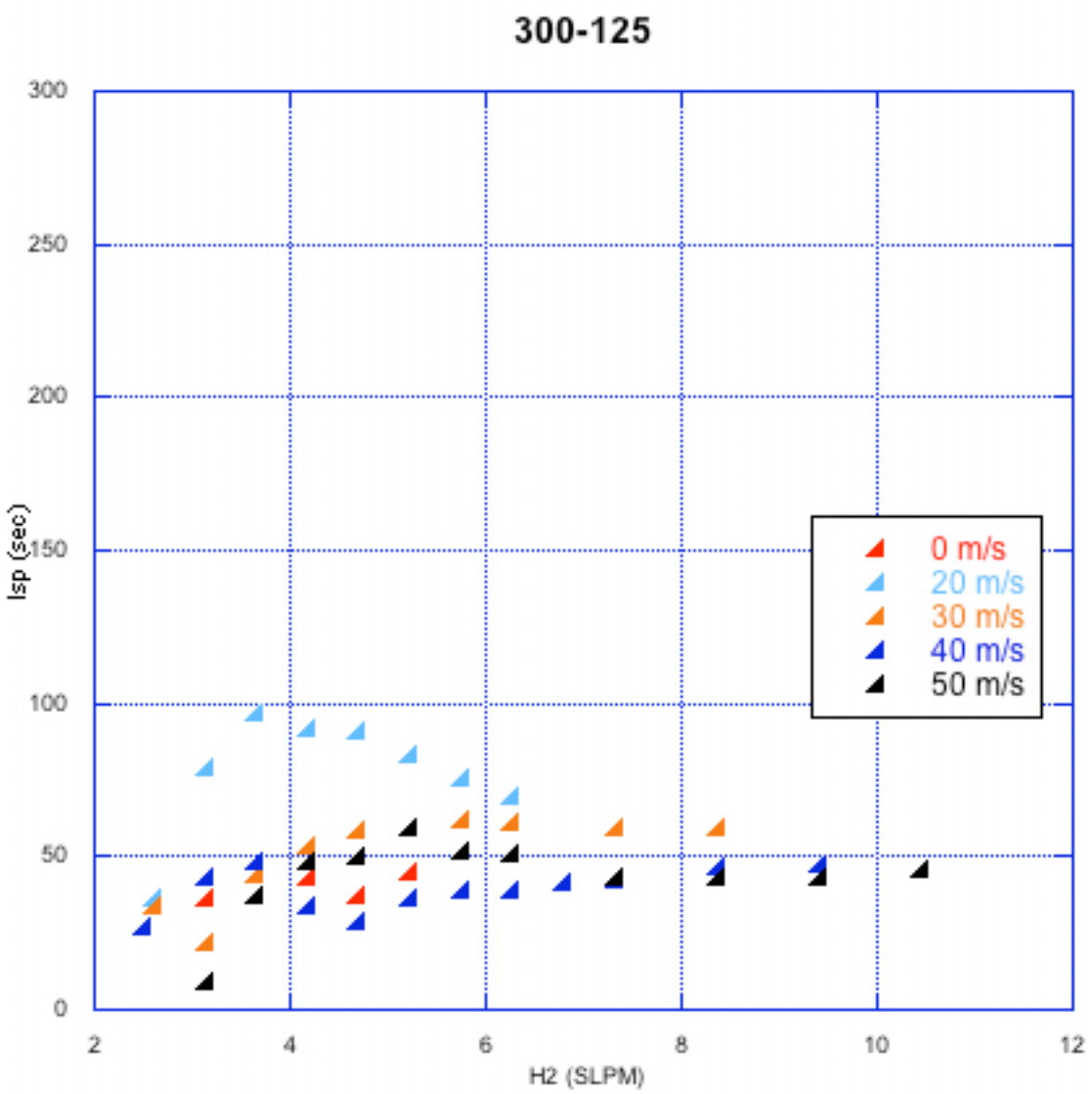

Figure 3-6: Specific impulse data for inlet 300-125

Inlet 415-125 is the inlet that Adam Kiker had manufactured previously and found to work on the forward facing pulsejet. This inlet is preferred as an experimentalist because of its ease in running at all conditions. Figure 3-7 and Figure 3-8 depict the thrust and Isp results respectively. In the 4 to 8 SLPM range, the performance at 30 m/s clearly dominates having both the highest thrust and highest Isp. For fuel flow rates lower than 4 SLPM,

performance at high velocities drops off and the performance at 20 m/s is best. Maximum Isp is between 130 and 150 sec and thrust is highest above 6 SLPM at 30 m/s with magnitudes around 11 mN. Again, the data at 10 m/s does not follow the trend and is likely erroneous due to interference with the air nozzle.

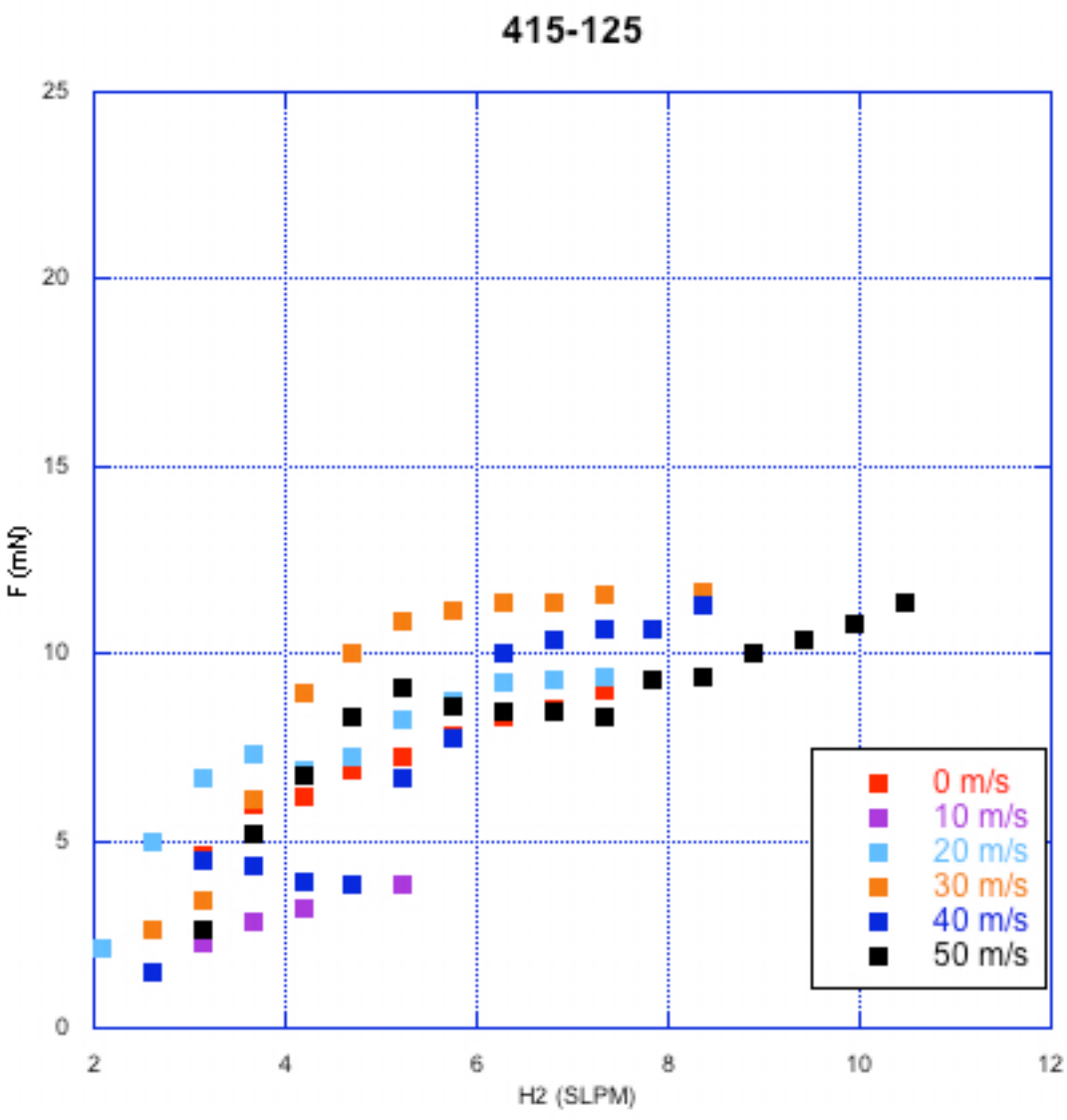

Figure 3-7: Thrust data for inlet 415-125

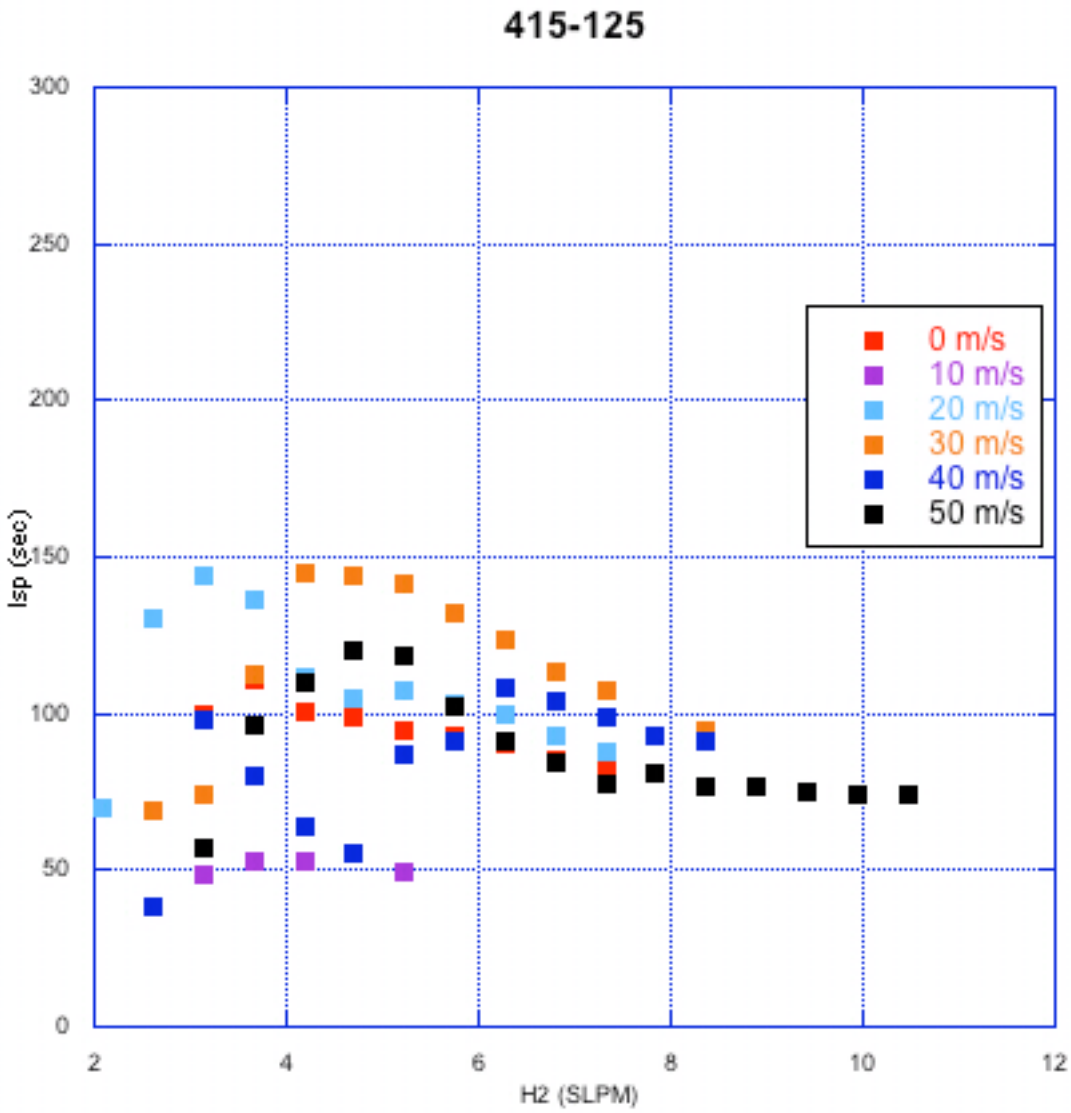

Figure 3-8: Specific impulse data for inlet 415-125

Inlet 550-125 is slightly longer but with the same inlet diameter. The thrust profiles are shown in Figure 3-9. Above fuel flow rate of 7 SLPM, the thrust is maximized at the top air speed. However, below 6 SLPM, the thrust appears to be highest at 30 m/s, which is similar to the case for the previous inlet. As a result, the highest Isp occurs at 30 m/s as revealed by Figure 3-10. As with the previous two inlets, the highest Isp takes place around

4 SLPM, but with inlet 550-125, the value is 180 seconds, which is much higher than the Isp achieved by either of the other inlets. This inlet was not attempted at 10 m/s because the performance on other inlets was so poor.

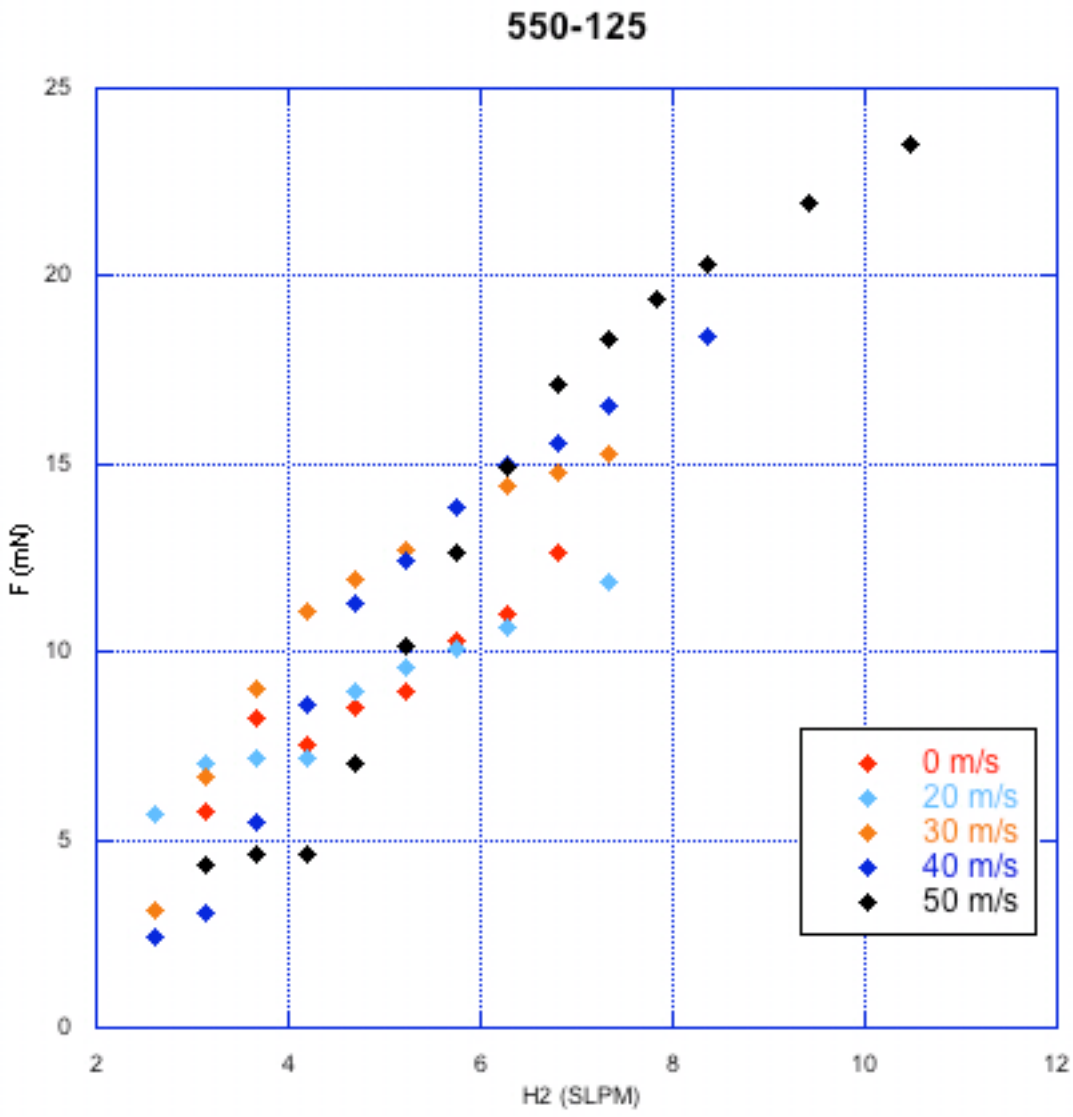

Figure 3-9: Thrust data for inlet 550-125

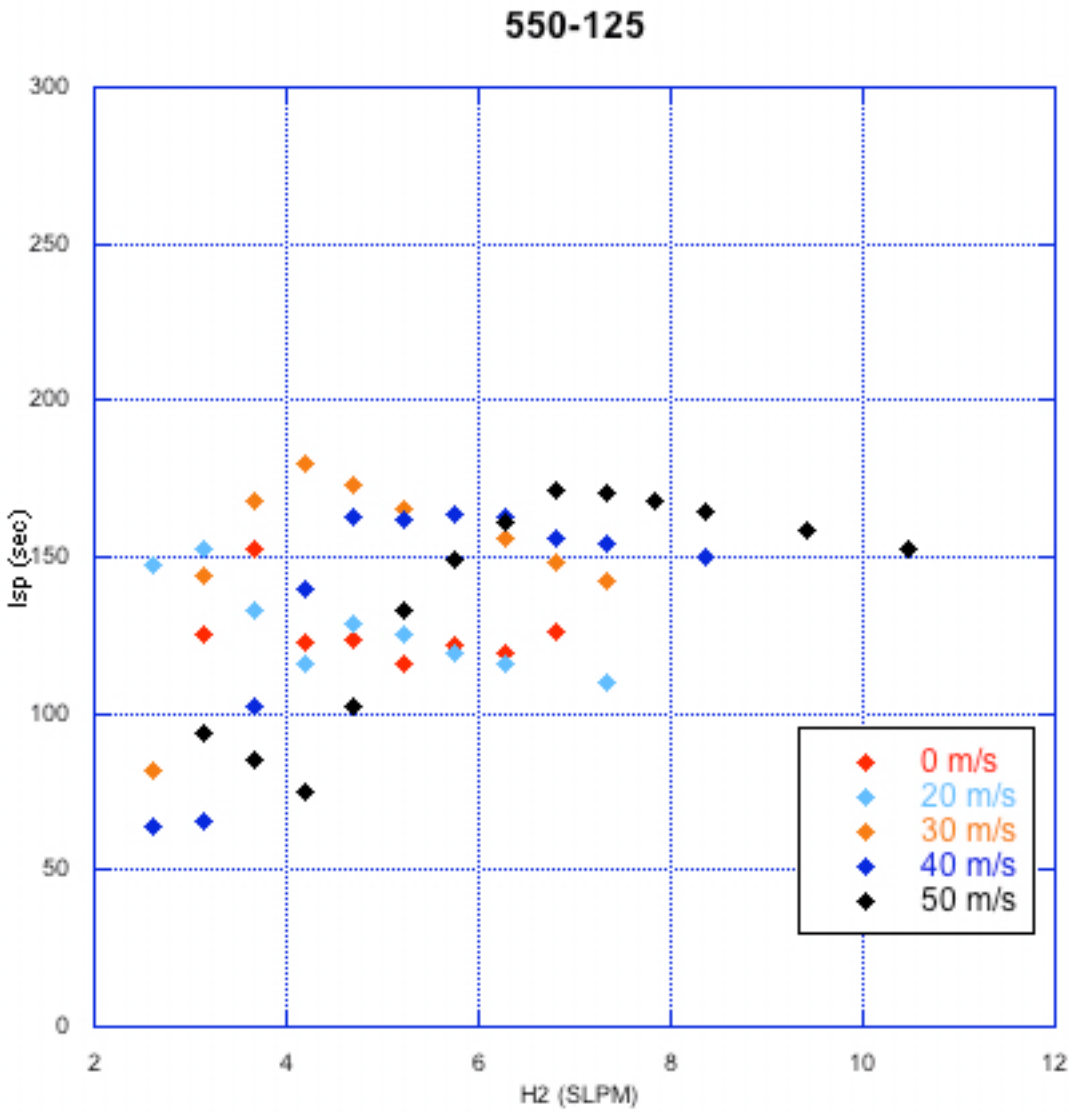

Figure 3-10: Specific impulse data for inlet 550-125

Inlet 700-125 was the second forward facing inlet tested ever tested at AERL. It was designed around inlet 415-125 thinking that increasing the length might result in increased performance. Indeed, even the early evidence well before reliable thrust data, such as sound pressure levels, indicated superior performance. The thrust profiles shown in Figure 3-11 must be very pleasing to any mathematical mind that prefers patterns. Every profile has a

positive slope that tapers off as the fuel flow rates increase. Figure 3-12 shows the Isp profiles for this inlet and they exhibit very regular structures as well. Each profile tends to peak in the middle of the fuel range with Isp dropping off symmetrically with either an increase or decrease in SLPM. Thrust at low fuel rates is highest at 30 m/s, whereas the best thrust at medium flow rates occurs at 40 m/s, and at high rates, the winner is 50 m/s with thrust peaking at about 24 mN. Maximum Isp is over 290 seconds. For this inlet, the results for both 10 m/s and 20 m/s are worse than the case for static. This is probably due to nozzle interference again. The detrimental effect of the nozzle was first noticed while testing this inlet and the effect appears to be greater with this inlet than with others.

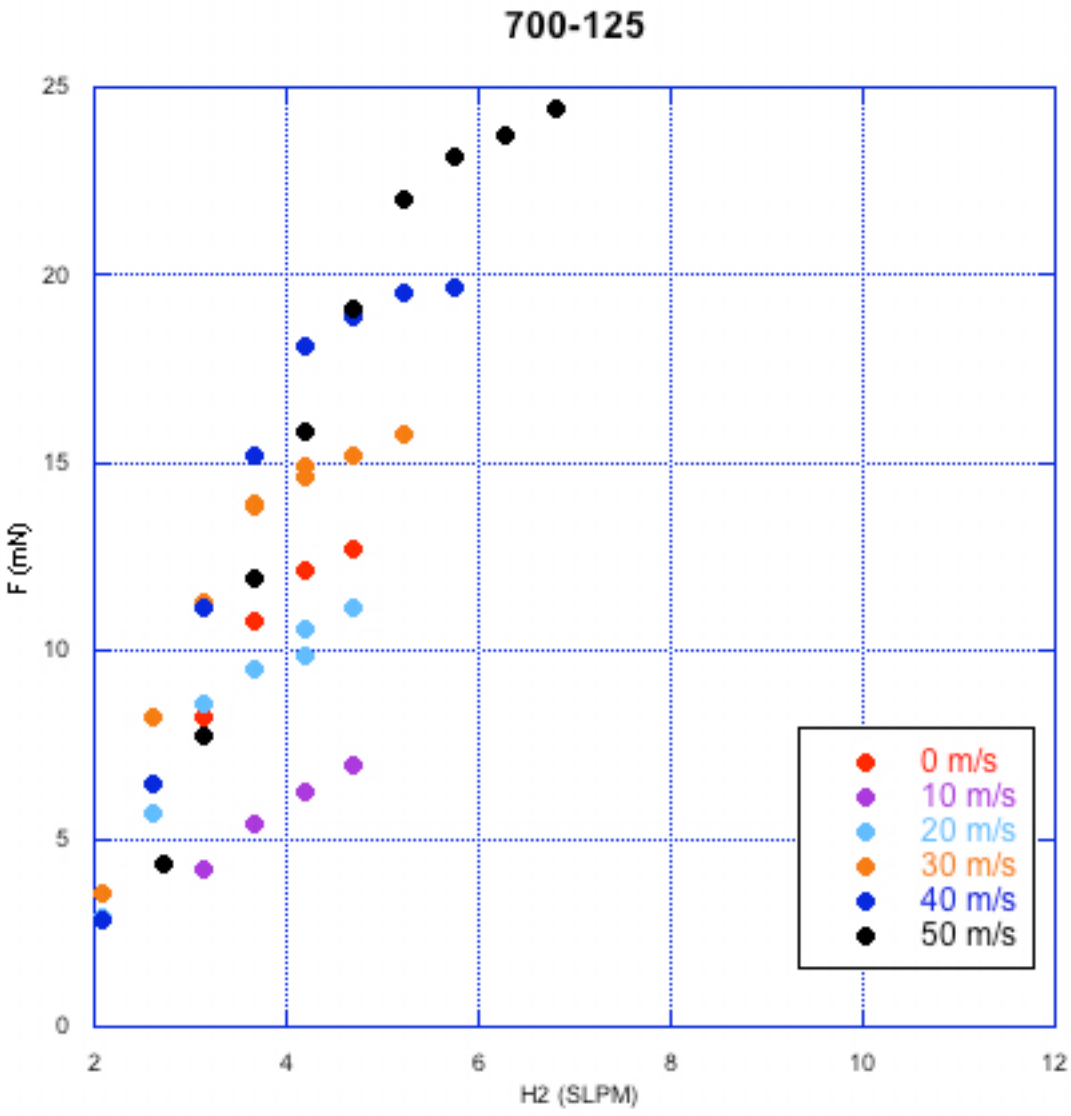

Figure 3-11: Thrust data for inlet 700-125

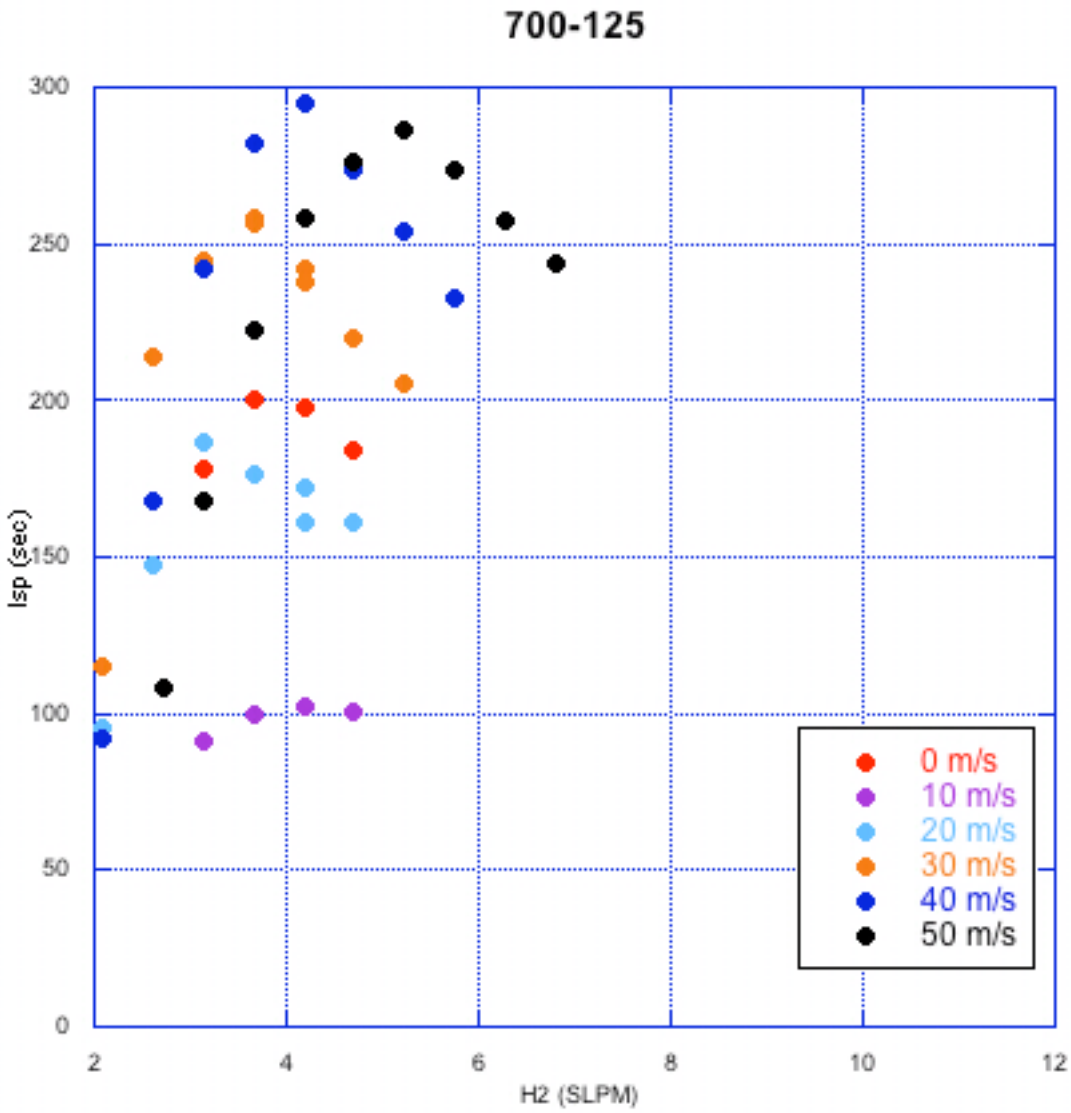

Figure 3-12: Specific impulse data for inlet 700-125

The data taken with inlet 700-100 is displayed in Figure 3-13 and Figure 3-14. Perhaps the most salient feature of these figures is how narrow the fuel flow rate range is for this inlet. This inlet caused the pulsejet to be very limited in the amount of fuel it could process, due to the smaller area of the inlet, which resulted in reduced mass flow of air. Furthermore, the pulsejet with this inlet would only work with forced air and no conditions

below 30 m/s allowed operation. For these reasons, there is much less data with which to work. A few conditions resulted in Isp over 200 sec and maximum thrust was just over 11 mN. The three points above 3 SLPM at 40 m/s are data taken while the pulsejet was in "torch mode". This mode occurs when fuel flow rates are too high for the inlet and operation in this mode is clearly suboptimal.

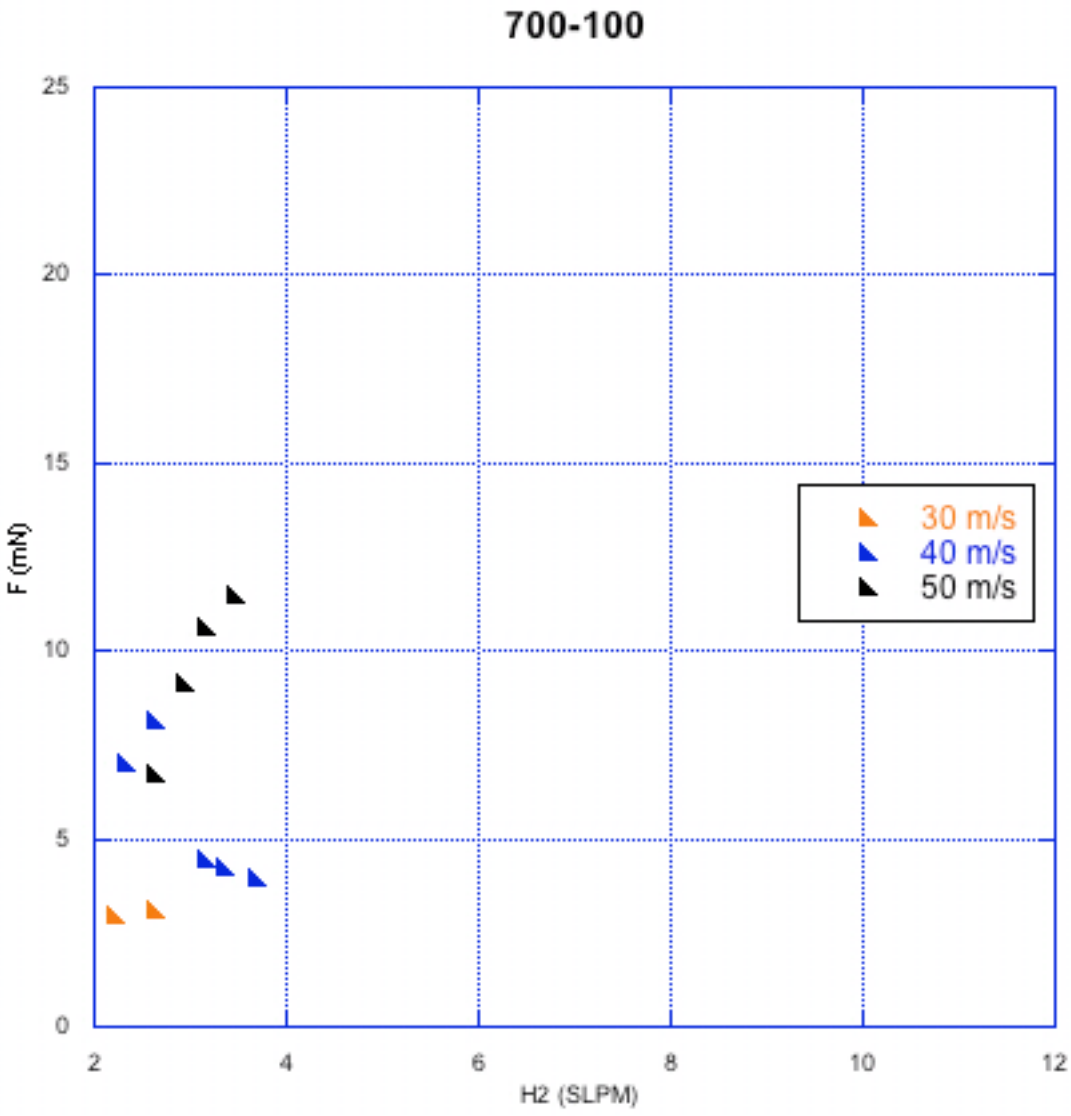

Figure 3-13: Thrust data for inlet 700-100

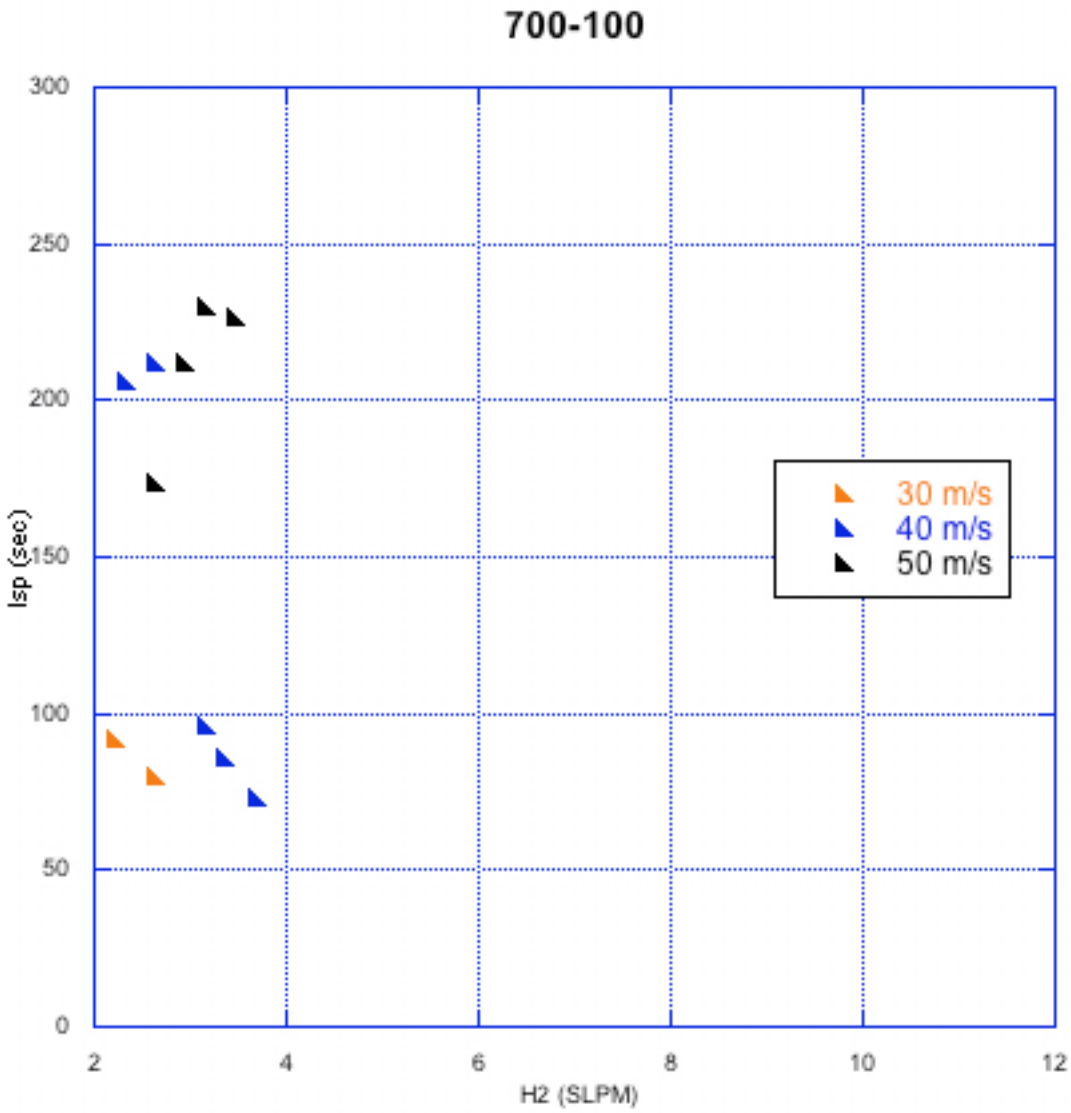

Figure 3-14: Specific impulse data for inlet 700-100

Inlet 700-081 has the smallest inlet of all inlets tested. It may be expected that this inlet would have a hard time respirating and testing showed this to be the case. During testing, the pulsejet ran very cold and sound pressure level was considerably lower than with other configurations. Figure 3-15 shows the data that was obtainable. Results were only recorded at 50 m/s since the pulsejet could not run without a significant amount of forced air.

Another consequence of the small diameter is the short fuel flow rate range that was possible. Furthermore, notice that the thrust measurements are all between 7 mN and 8 mN so changing the fuel flow rate had little impact on thrust performance. However, Figure 3-16 indicates that the Isp was as high as 225 seconds because the thrust occurred at such low fuel flow rates. This inlet was, by far, the most difficult to start and by normal operation standards it was probably never truly resonating. An attempt was made to inject fuel through an open ended tube into the combustion chamber to see if the pulsejet could run easier without the fuel injector blocking incoming air, but the pulsejet would not operate at all in this configuration.

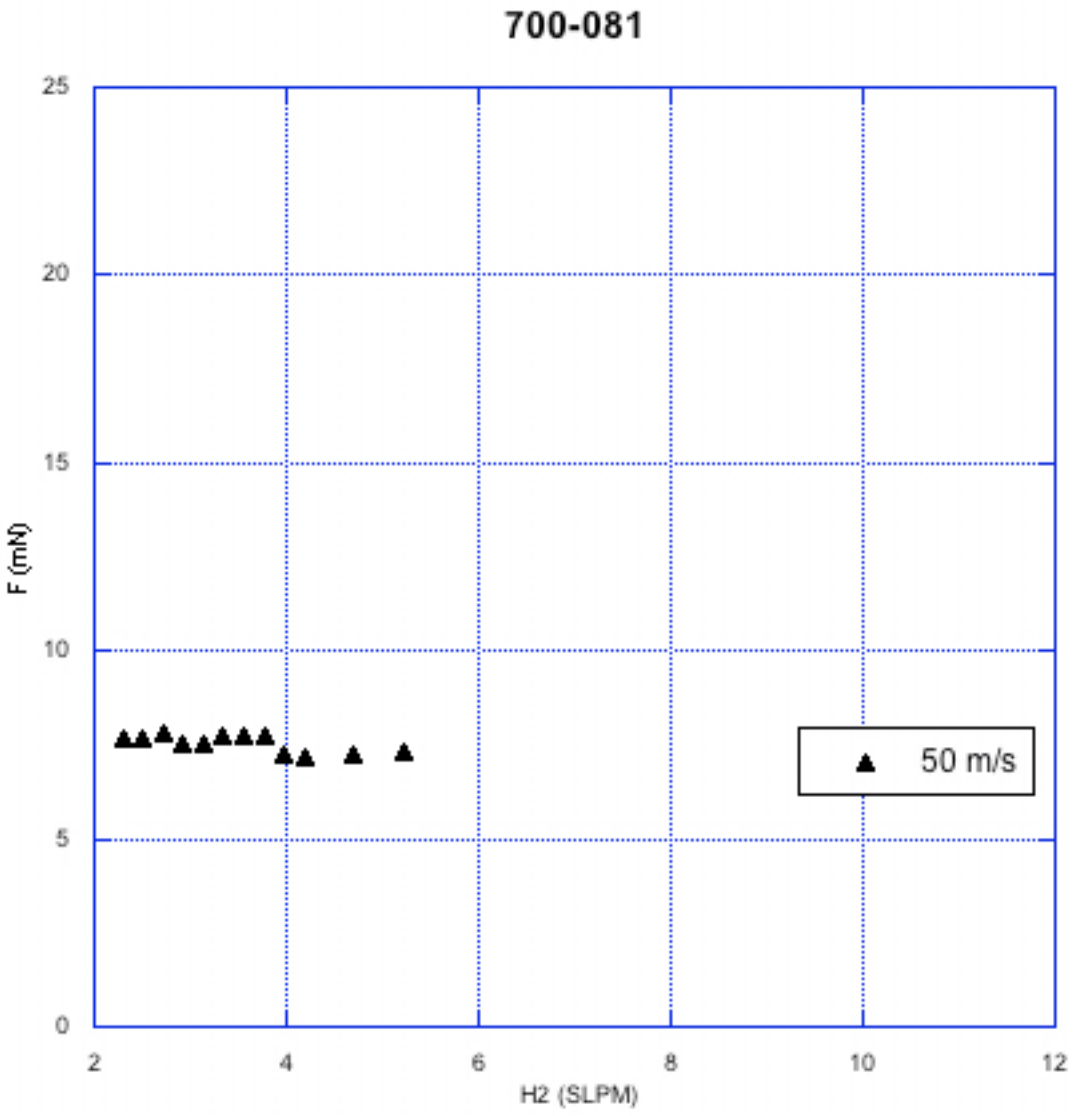

Figure 3-15: Thrust data for inlet 700-081

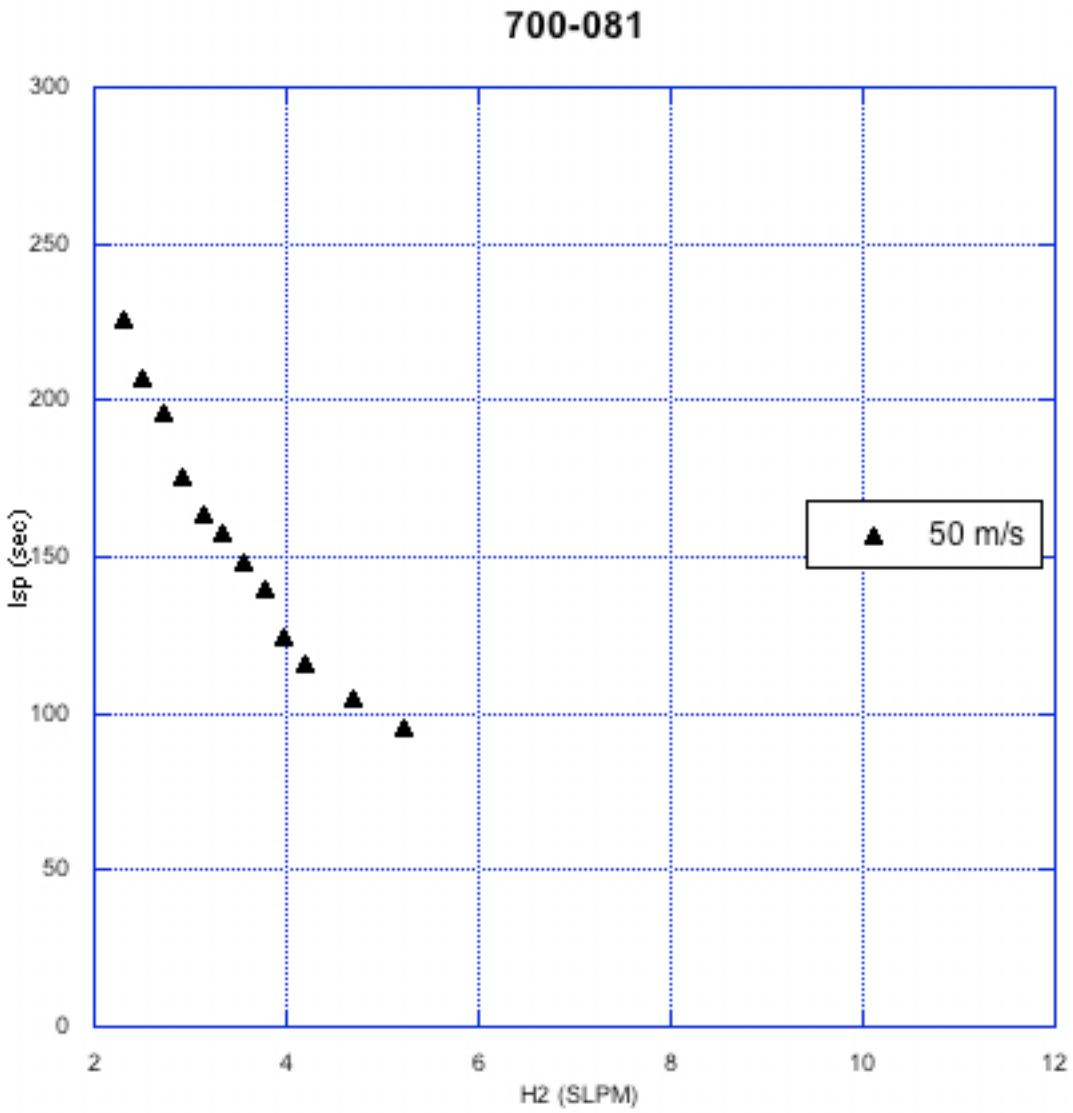

Figure 3-16: Specific impulse data for inlet 700-081

The last inlet to be presented here is inlet 700-150 which has the largest area of all seven inlets. The behavior of this inlet was very surprising. The expectation was that it would be easy to run but with poor performance. It turned out to be quite difficult to operate. With this inlet, the pulsejet takes a relatively long while to heat up and transition to resonance mode. The spark had to be used several times to essentially preheat the pulsejet so

that it could run. Part of the reason may be the large amount of cold air being forced into the inlet. After all, the inlet diameter is larger than the diameter of the nozzle used to feed air to the pulsejet. The thrust data that was collected is displayed in Figure 3-17. No data was taken below 40 m/s because of the starting difficulties with this inlet. Even at 50 m/s, the pulsejet begins transitioning to torch mode above 6.5 SLPM, which is why the two data points above this value have diminished thrust magnitudes. Another surprising result from this inlet is that some negative thrust values were recorded. Figure 3-18 shows the specific impulse data for this inlet. Specific impulse peaks at about 125 seconds.

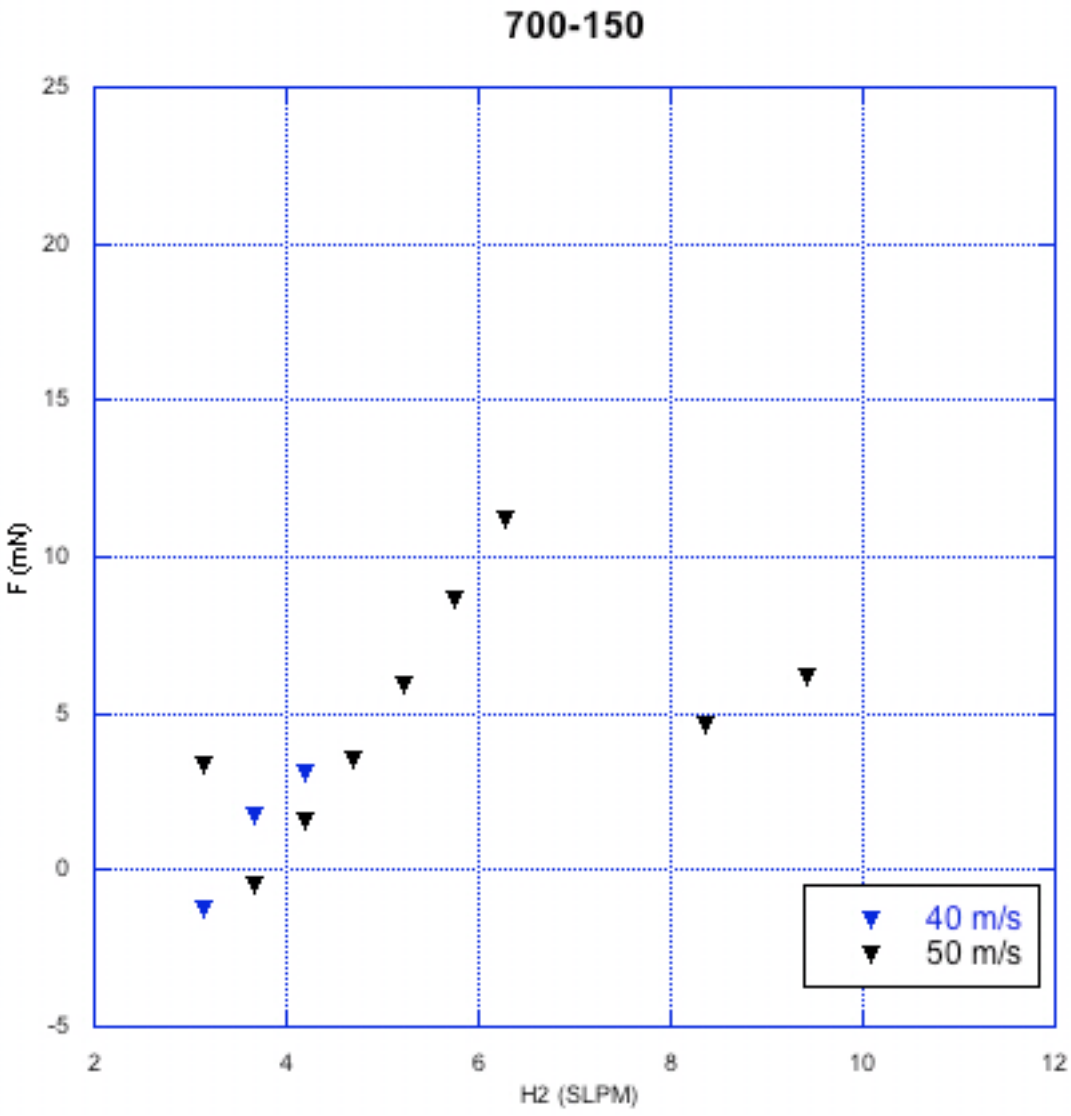

Figure 3-17: Thrust data for inlet 700-150

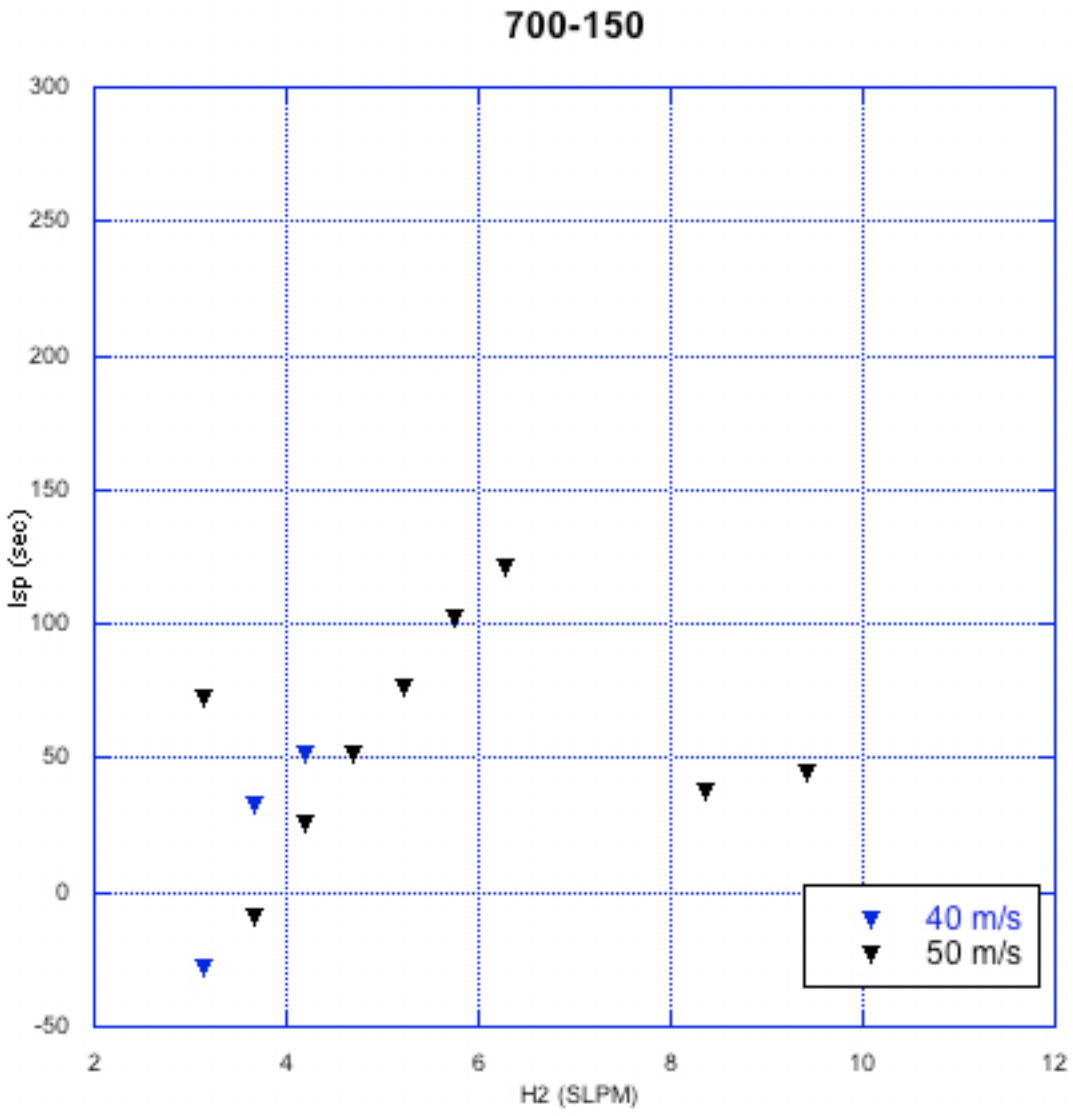

Figure 3-18: Specific impulse data for inlet 700-150

3.3 Performance as a Function of Inlet Diameter

To study the effect of inlet diameter on the performance of forward facing valveless pulsejets, four inlets with constants lengths were studied. The inlets all had a length of 1.778

cm. The trend with inlet diameter is difficult to ascertain with the above information. The main problem is that inlet 700-125 was the only inlet that worked well enough to yield results at all speeds being tested. Inlet 700-081 and inlet 700-100 both had such a narrow fuel flow range that few data points were possible. Furthermore, inlet 700-081 only worked at 50 m/s and barely worked at all. Nonetheless, all inlets yielded specific impulses above 200 seconds except inlet 700-150, the largest inlet.

The paucity of data in this category makes drawing definite conclusions tricky. The evidence appears to indicate, however, that reduction in inlet area is beneficial. But one must be careful since narrow inlets limit the amount of air that can be ingested per cycle so any reduction in inlet area will come with a reduction in fuel flow range. This, in turn, will probably limit the maximum possible thrust. If the area is reduced too much, the restriction may be too great to allow for adequate operation and so may be quite detrimental to performance. This is probably what happened with the two smaller inlets. The inverse also appears to be true in that if the area is too large, the excess air may make operation difficult.

Performance is also a function of inlet length, as will be discussed below. This research indicates that performance is more sensitive to changes in diameter than in changes in inlet length. This is not unexpected if the inlet frequency is to be modeled as a Helmholtz resonator as discussed in Section 1.4. Since frequency is a function of the square root of the inlet area, it is a linear function of the diameter but a function of the inverse square root of inlet length. Also, beyond frequency considerations, inlet area has a strong influence on the mass flow of air that is allowable whereas the inlet length has a very weak influence on this factor.

To investigate this connection further, one recommendation would be to look at inlets with areas much closer to the area for inlet 700-125. This inlet works well at all conditions and perhaps even small changes in inlet area could produce a convincing trend. Another recommendation would be to focus on shorter inlets. For instance, one could produce three inlets with a length of 1.397 cm and compare them with inlet 550-125. The pulsejet may be more forgiving of significant area changes at shorter inlet lengths.

3.4 Performance as a Function of Inlet Length

As with inlet diameter, four of the inlets presented above had a diameter of 0.318 cm with lengths ranging from 1.778 cm to 0.762 cm. Fortunately, all four of these inlets were able to run at every airspeed from static to 50 m/s (omitting 10 m/s) yielding a wealth of data with which to draw conclusions about the effect of inlet length on pulsejet performance.

Figure 3-19 compares the thrust values at an airspeed of 50 m/s for all four inlets. The trend is very clear. The thrust profiles stack up neatly in order of increasing length with the longest inlet (700-125) having the greatest thrust and the shortest inlet (300-125) having the lowest thrust at every single fuel flow rate tested. There is a small amount of overlap with the two medium length inlets around 4 SLPM, but otherwise, they too stack according to inlet length. If one looks specifically at the points around 6 or 7 SLPM, one can see an almost linear increase in thrust with an increase in length.

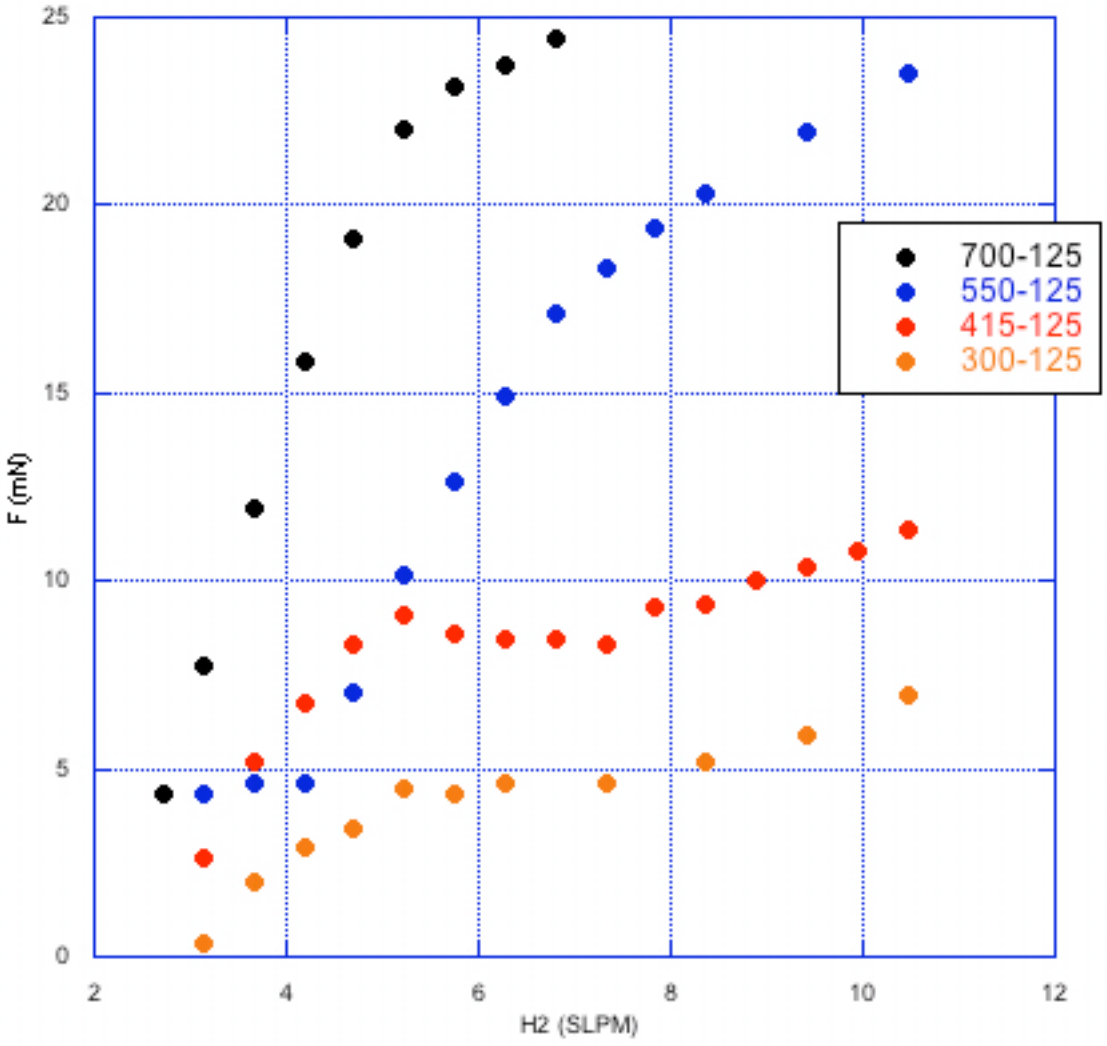

Figure 3-19: Thrust data for inlets of same area at 50 m/s

Because the above trend may only apply to the 50 m/s condition, Figure 3-20 plots the thrust data for these four inlets at static conditions. Here, the trend is equally convincing. No overlap exists at any point on the plot. The other trend noticeable with this plot and the previous figure is that the shorter inlets tend to allow greater fuel flow rates. This is a result that has been seen many times both experimentally and computationally.

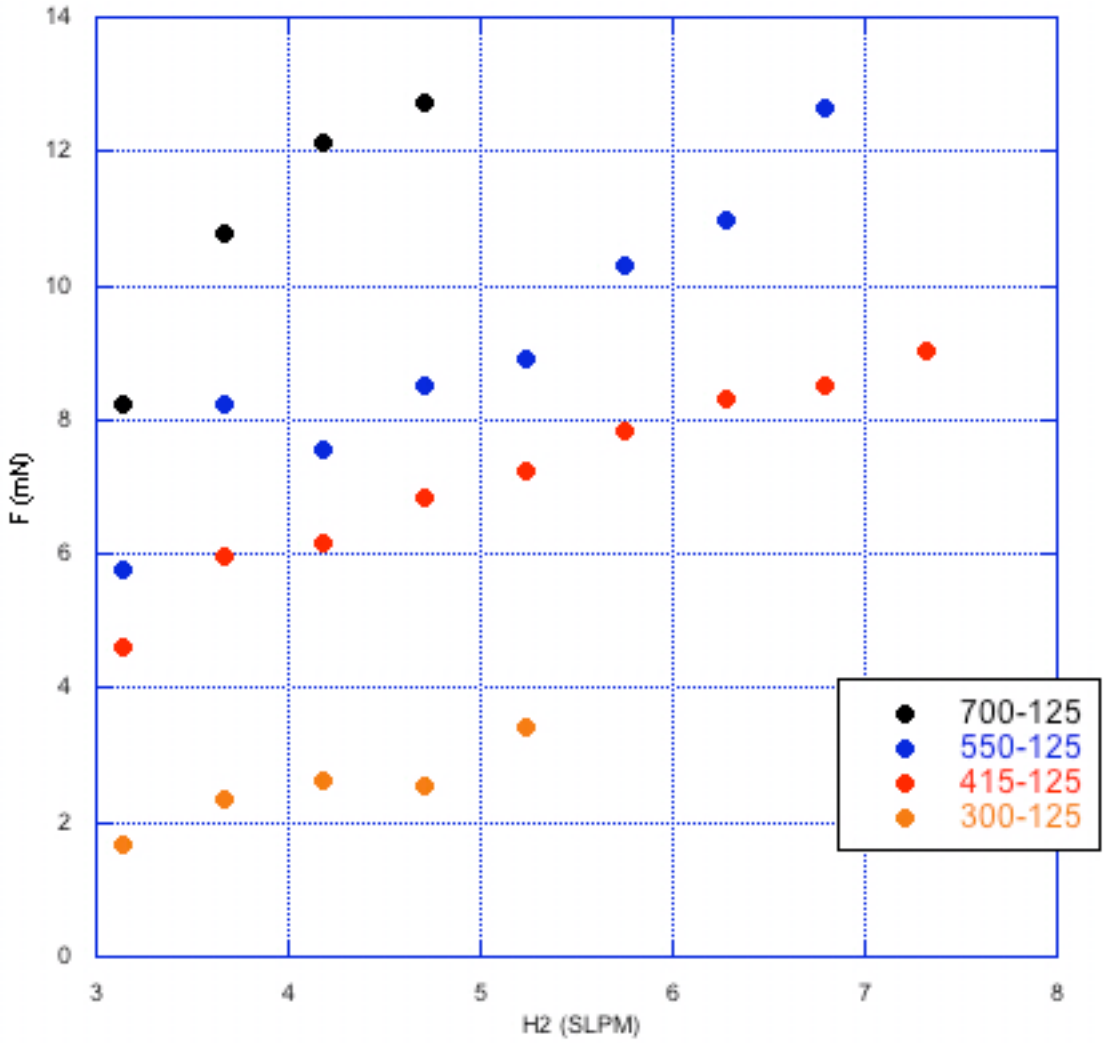

Figure 3-20: Thrust data for inlets of same area at 0 m/s

Finally, just to drive the point home, the maximum thrust and maximum Isp achieved for these four inlets at any condition is plotted as a function of inlet length in Figure 3-21. Again, it is shown that with an increase in length, the achievable thrust and specific impulse both improve. In fact, the thrust profile here would be even more dramatic if these values occurred at equal fuel flow rates. The maximum thrust for inlet 550-125 occurs at over 10

SLPM whereas the maximum thrust for inlet 700-125 occurs at only 7 SLPM. Two other things should be noted about this plot. First of all, maximum thrust and maximum Isp do not necessarily occur at the same condition. In fact, they almost never do. Secondly, the maximum Isp does not occur at the same airspeed for each inlet. This issue is explored in section 3.6.

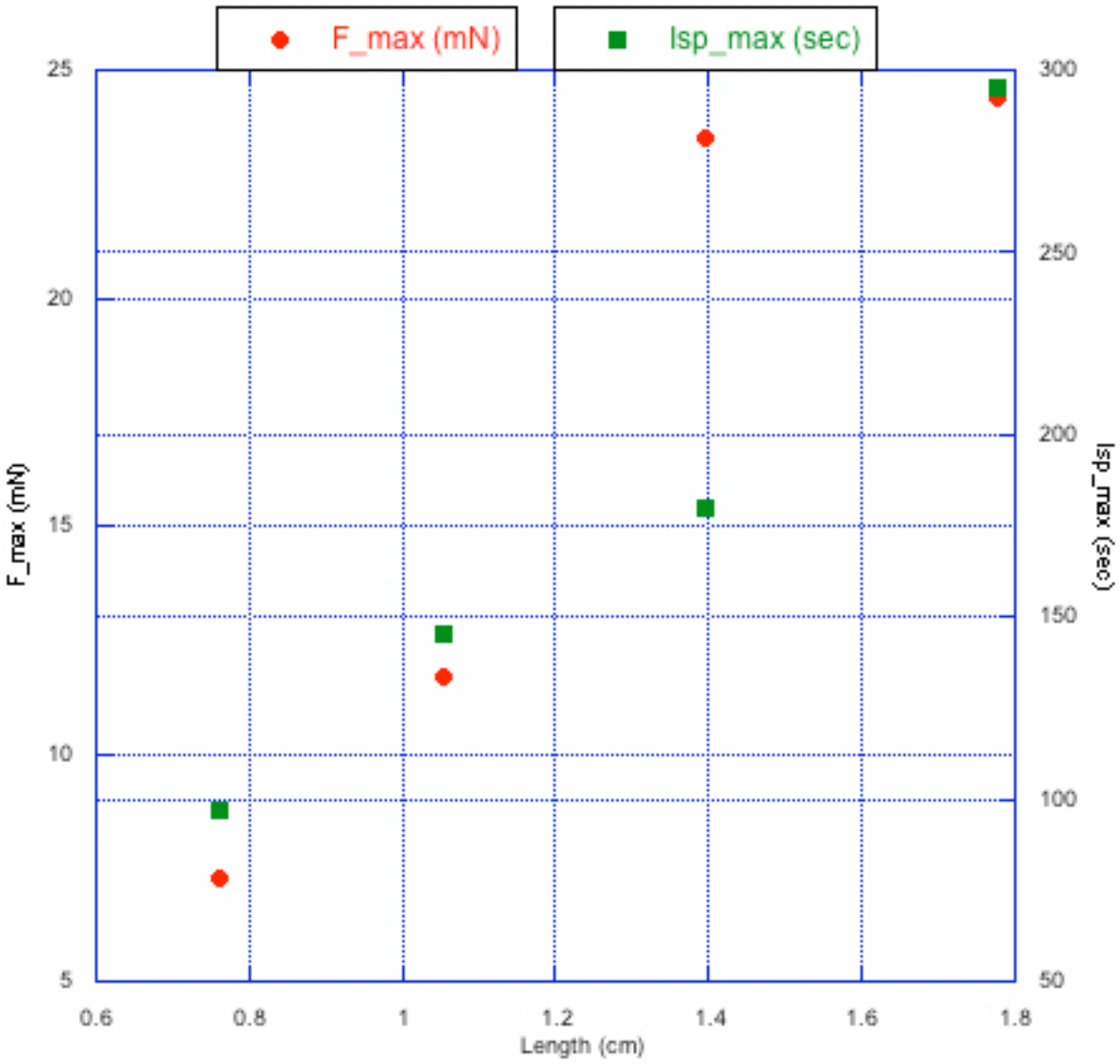

Figure 3-21: Maximum thrust and Isp for inlets of varying length

These results are not unexpected. Lengthening the inlet appears to diminish the combustion products' ability to leave via the forward facing inlet. Foa describes the flow leaving through the inlet as a series of weak compression waves. With an extended length, there is more distance over which these waves may be weakened by the pressure of outside

air. This is particularly true for inlets facing a forward flight speed. One may also make an analogy with oil pipelines, in which ever greater pump pressures are needed to pump oil greater lengths. If indeed the combustion products have a harder time leaving through the inlet, one would expect an increase in thrust and, clearly, that is seen here.

3.5 Performance as a Function of Fuel Flow Rate

For the majority of conditions tested, an increase in fuel flow rate results in a corresponding increase in thrust. Generally, as the fuel flow rate gets very high, the increase in thrust becomes less pronounced. For a few conditions studied, there may be a small interval over which increases in fuel flow rate actually result in decreases in thrust. It is difficult to explain this dip in the thrust profile without more information but the dip normally occurs at very low fuel flow rates.

The maximum thrust obtained at each flow rate, regardless of airspeed, can be plotted for the four inlets that had complete data sets. This plot is given as Figure 3-22. The general trend for all four inlets is an increase in the achievable thrust as the fuel flow rate rises. The two shorter inlets have positive slopes that essentially level out around 6 SLPM while the longer inlets continue increasing throughout the entire tested range. Note also that this plot reinforces the idea that longer inlets can achieve greater thrust.

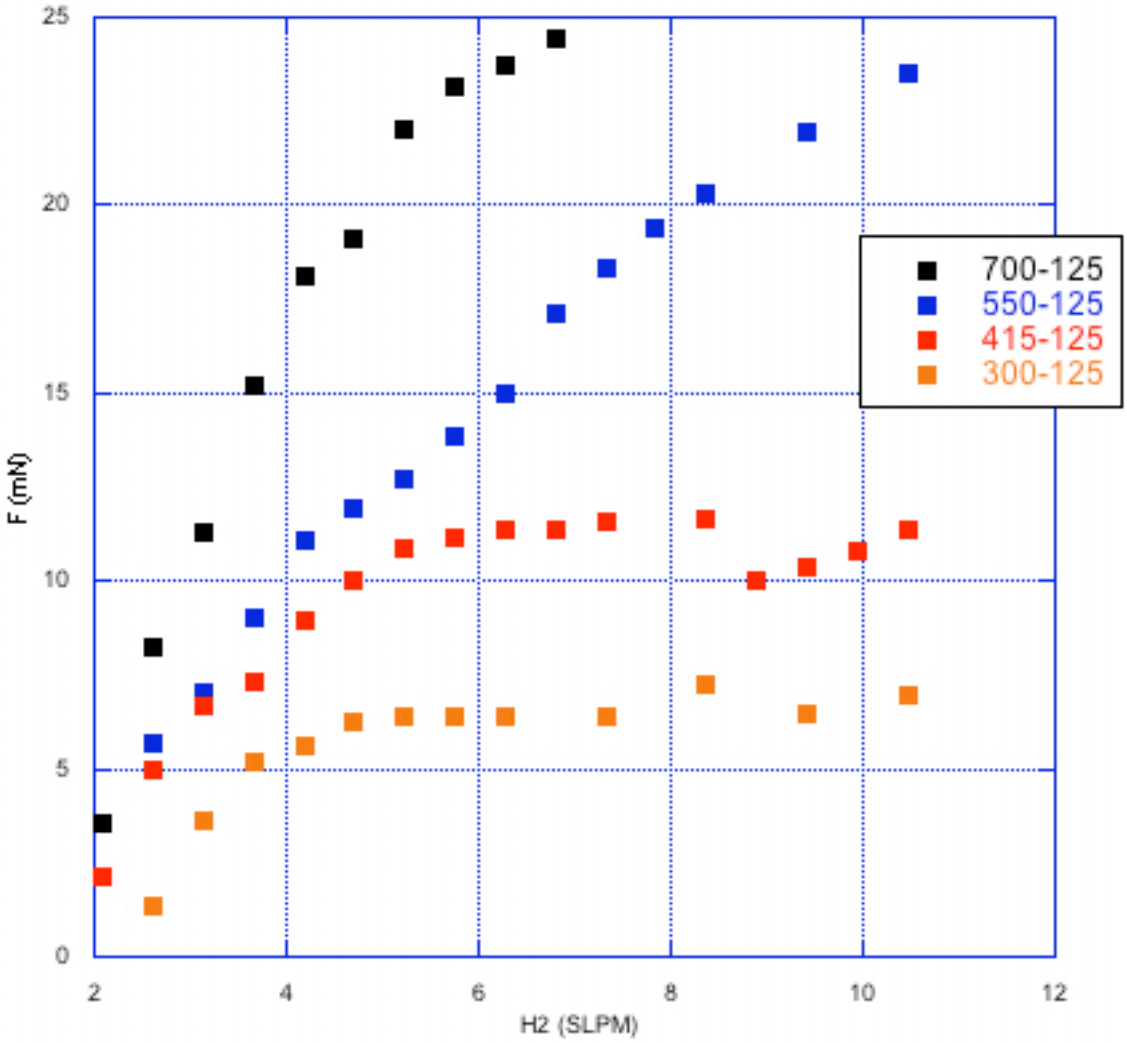

Figure 3-22: Peak thrust for each fuel flow rate

Specific impulse profiles, on the other hand, almost all exhibit a bell-shaped profile. The peak Isp generally occurs near the middle of the fuel flow rate range. In fact, for all of the inlets with a full set of data, the Isp peak occurs between 3 and 5 SLPM. This is to be expected since Isp is an inverse function of the fuel mass flow. Thrust must increase appreciably with incremental changes in fuel flow rate at the high fuel flow rates in order for

specific impulse to increase. This typically does not happen. The point of peak Isp at each fuel flow rate, regardless or airspeed, can also be plotted and is done so in Figure 3-23. Of course, each point on this plot corresponds to a point in Figure 3-22 since the peak thrust at a given fuel flow rate is also the peak specific impulse.

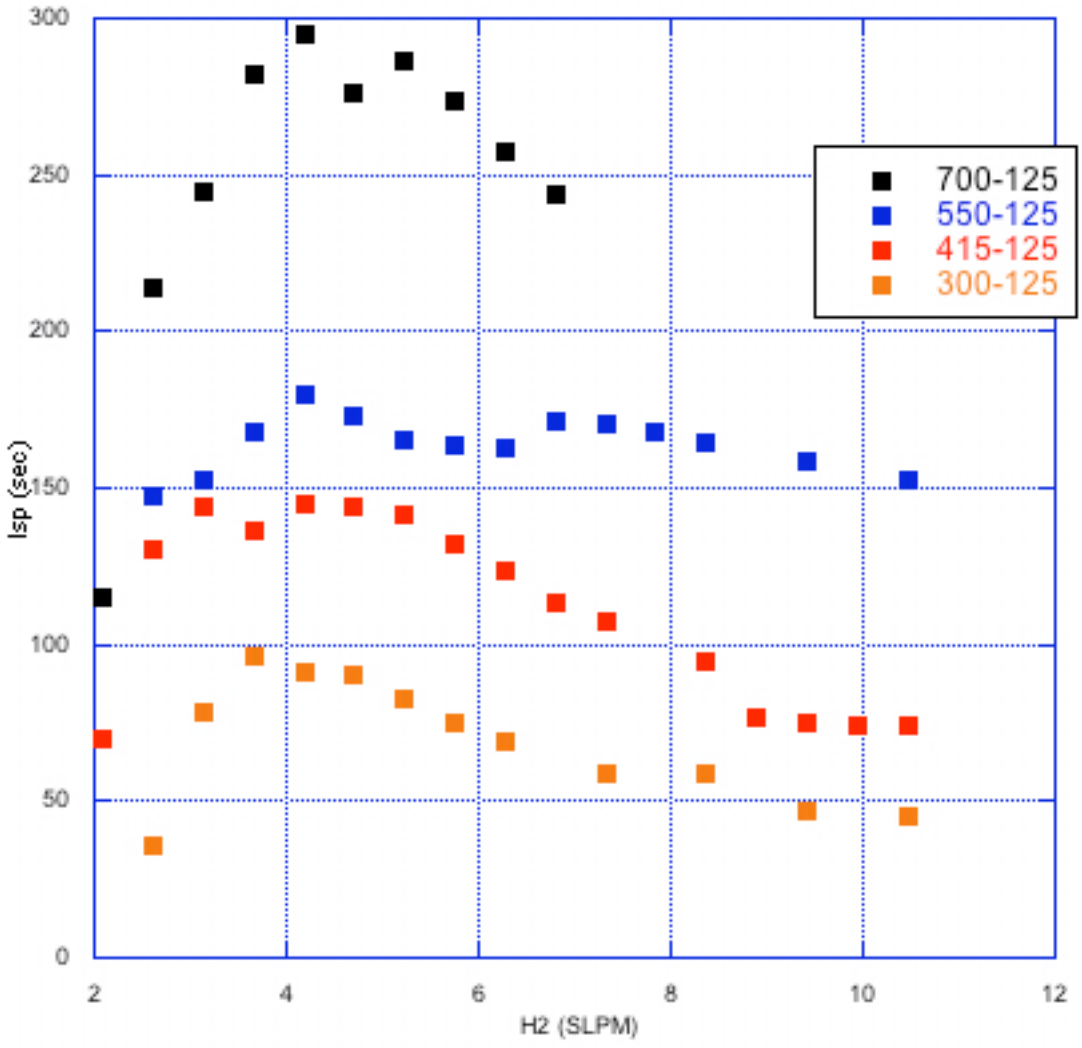

Figure 3-23: Peak specific impulse for each fuel flow rate

3.6 Performance as a Function of Simulated Forward Velocity

One of the central questions raised before this research began was whether one would expect better performance out of a forward facing configuration or a rearward facing configuration at a given velocity. At static conditions, one certainly expects better performance out of the rearward facing configuration since there can be no momentum loss out of the inlets. On the other hand, there is no reason to expect better performance with forward flight speed. If anything, one might expect worse performance because it becomes more difficult to entrain fresh air into the inlet. If the inlets were facing forward, however, an increase in performance may be possible. The theory is that the increase in ram pressure (though small at these speeds) might both increase the pressure before combustion, and thus increase the combustion efficiency, and may also serve to block combustion products that would otherwise escape through the inlet. An additional benefit would be the air's ability to push combustion products out of the inlet's flowfield making it easier to entrain fresh air into the combustion chamber with each cycle. These ideas provided the impetus for studying pulsejet behavior as a function of forward flight speed.

The discussion in this section will focus primarily on inlets 700-125, 550-125, 415-125, and 300-125 because these inlets have data at static conditions as well as 50 m/s and all of the speeds in between. These just happen to be the four inlets with the same inlet area as well. The general trend seems to be an increase in the thrust as the airspeed increases, but the trend is quite complicated.

For inlet 300-125 (Figure 3-5), the maximum thrust at low fuel flow rates occurs at 20 m/s. Then, as the fuel flow rate increases, the maximum thrust occurs at 30 m/s, 40 m/s, and finally 50 m/s. For inlet 415-125 (Figure 3-7), maximum thrust occurs at 20 m/s below 4 SLPM and then at 30 m/s above this value until the data at 30 m/s ends. Inlet 550-125 (Figure 3-9) has maximum thrust at 30 m/s below 6 SLPM and at 50 m/s above this flow rate. Inlet 700-125 (Figure 3-11) has maximum thrust occurring at 30 m/s at low flow rates, at 40 m/s at medium flow rates, then at 50 m/s at high flow rates. The general trend, then, is to benefit from high speeds only at high fuel flow rates.

The maximum thrust at each fuel flow rate was plotted previously in Figure 3-22. This figure excluded data about airspeed. Figure 3-24 takes each point on that plot, a point of maximum thrust, and plots the forward flight speed at which peak thrust was obtained as a function of fuel flow rate. The first thing to notice is that at no point in all the tests on forward facing inlets was the peak thrust recorded at static conditions. This plot provides incontrovertible evidence that some benefit is seen with forward flight speed. Of course, there are no points at 10 m/s either but, as mentioned previously, this appears to be because the nozzle is more of an obstruction than an assistant to the pulsejet at this low air flow rate. Another important point to make about this figure is that, for each inlet, as the fuel flow rate increases, the airspeed at which peak thrust occurs tends to increase. And according to Figure 3-22, the thrust also increases with fuel flow rate. Therefore, the thrust does increase as the airspeed increases, provided that more fuel is supplied to the pulsejet. The manner of progression of this trend depends on the length of the inlet as well. For each airspeed, the inlets are ordered according to length with the longest inlet at the lowest fuel flow rates and

the shortest inlet at high fuel flow rates. So the transition to higher performance at higher speeds takes more fuel as the inlet gets shorter. The few points that seemed to interrupt the trend were omitted. It should be noted that each of these points represents a condition at which data is missing. So while it may look like thrust peaked at 40 m/s, this could only be because data was not taken for 30 m/s at this fuel flow rate. With more data, it is expected that the trends will smooth out even more. This goes for the number of velocities tested as well. Had the velocities been tested at 5 m/s or 2 m/s intervals, these profiles could take on a more linear structure.

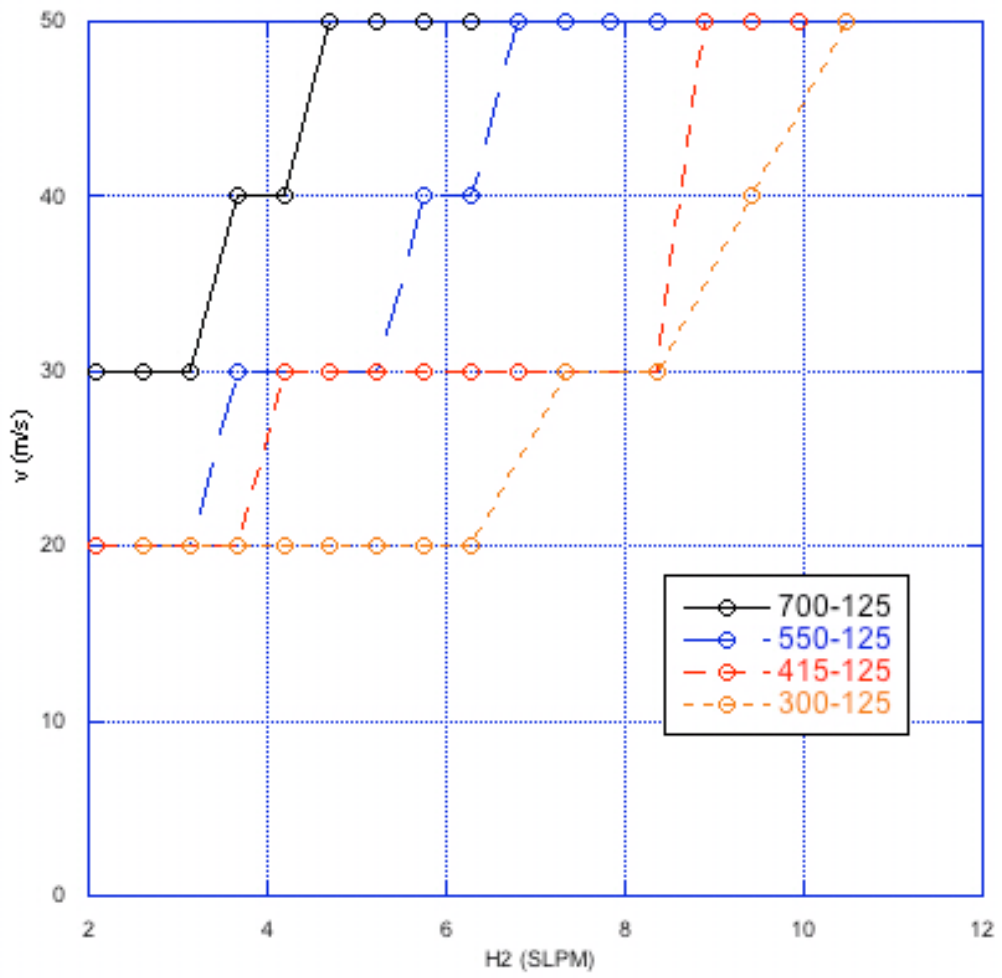

Figure 3-24: Forward flight speed at which peak thrust occurs by fuel flow rate

Looking at the specific impulse as a function of airspeed may provide a clearer picture of what is happening. With each inlet, the maximum Isp occurs at a slightly different speed. This phenomenon is summarized in Figure 3-25. For inlet 300-125, the superior efficiency clearly occurs at a forward flight speed of 20 m/s. Inlet 415-125 has two points of maximum Isp, one at 20 m/s and the other at 30 m/s. Inlet 550-125 has a clear maximum at 30 m/s. Finally, the longest inlet, inlet 700-125 has two points which are essentially tied at

about 290 seconds. These points occur at 40 m/s and 50 m/s. The trend here is that longer inlets have peak efficiencies at higher forward flight speeds. With some testing of intermediate speeds, this plot could turn out to be a fairly linear line.

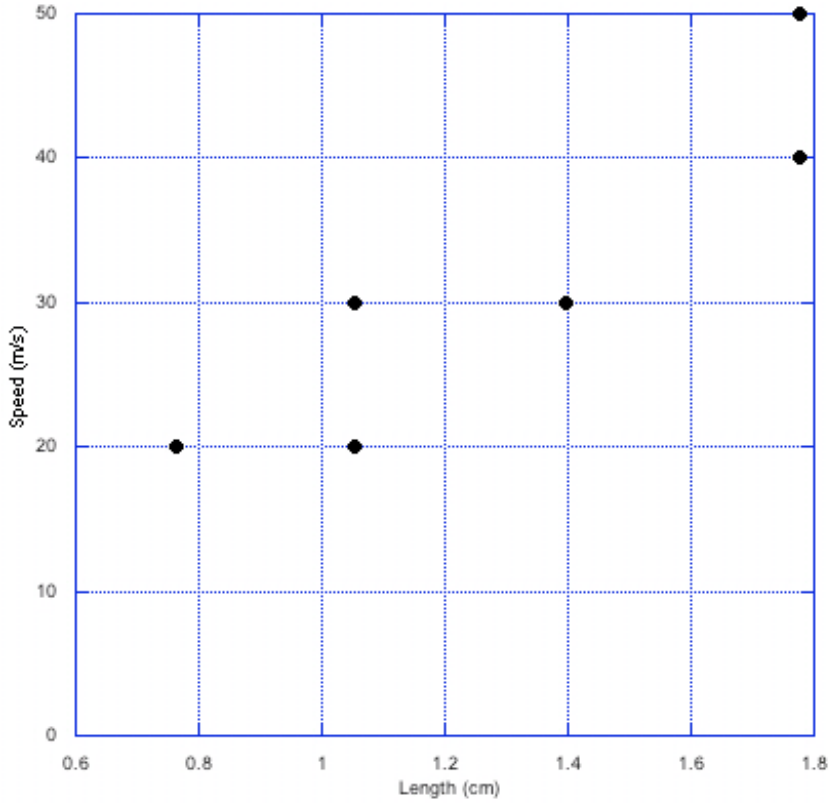

Figure 3-25: Airspeed for which maximum Isp occurs as a function of inlet length

The picture now coming into focus indicates that forward flight speed necessary for peak efficiency is a function of the inlet. One may expect that an inlet longer than inlet 700-125 could have peak fuel efficiency at speeds greater than 50 m/s. More testing would be necessary to understand how the inlet area plays a role in this phenomenon. It is not clear why this is the case.

One reason may be that the pulsejet has an ideal frequency at which it can process the fuel most efficiently. Other researchers have shown that frequency does change as a function of fuel flow rate. There is also anecdotal evidence that the frequency may be a function of forward flight speed, in that the pitch of the pulsejet while operating will usually go up if airflow rates are increased. If there is an ideal frequency for the pulsejet, perhaps the right combination of fuel and air will force the pulsejet into that frequency. When this occurs, one may expect optimal efficiency.

Another reason may be that the forced air assists the inlet as it entrains air into the combustion chamber. While it is understood that disallowing combustion products from leaving through the inlet is advantageous, the pulsejet still needs to bring in fresh reactants through the inlet of course. At static conditions, the sub-atmospheric pressure in the combustion chamber following the combustion event accomplishes this work. Air forced at the inlet may help to compensate for this work. Since longer inlets may require faster velocities to move reactants into the chamber, it stands to reason that longer inlets benefit more from higher flight speeds. Of course, the velocity at which reactants move into the chamber depends on the frequency also. So, achieving this velocity may just be a matter of allowing the pulsejet to run at a particular frequency, in which case this argument is simply another way of looking at the previous one.

The notion that this trend is an artifact of the experimental method and apparatus must also be addressed. The upper plate of the thrust stand presents a large flat surface area immediately downstream of the inlet face. In fact, for inlet 300-125, the inlet is so short that the inlet face sits within the upper thrust plate itself. It was earlier demonstrated how

detrimental obstructions upstream of the inlet can be. Perhaps obstructions downstream of the inlet play a role in the pulsejet's performance as well. Considering the unsteady, subsonic nature of the flow associated with pulsejet operation, this is likely. Moreover, as the speed of the airflow increases, the thrust plate may have an increasingly significant effect. And as the inlet gets shorter, the plate is that much closer to the inlet face. Therefore, it is entirely possible that the thrust stand itself has a significant effect on the inlet's flowfield and, consequently, on the pulsejet's measured performance.

4 Frequency and Temperature

As discussed above, frequency measurements have been an important component of previous pulsejet work at AERL. Furthermore, a method for predicting the operating frequency of valveless pulsejets has already been developed and was successful in a number of instances. Therefore, it was useful to continue this line of research with the 8 cm models. Furthermore, this was an opportunity to investigate any correlation between frequency, temperature, and performance.

4.1 Measured Frequency

For a wide range of conditions, a spectrum analyzer was used to measure the frequency of the valveless pulsejet. The four inlets with the same length were used because of the wide range of operation.

Inlet 300-125 exhibited frequencies between 1650 Hz and 1900 Hz. These results are displayed in Figure 4-1. In general the frequency tends to increase as fuel flow rate increases although this trend levels off at higher fuel flow rates. The other noticeable trend is a reduction in frequency as the speed of the incoming air increases.

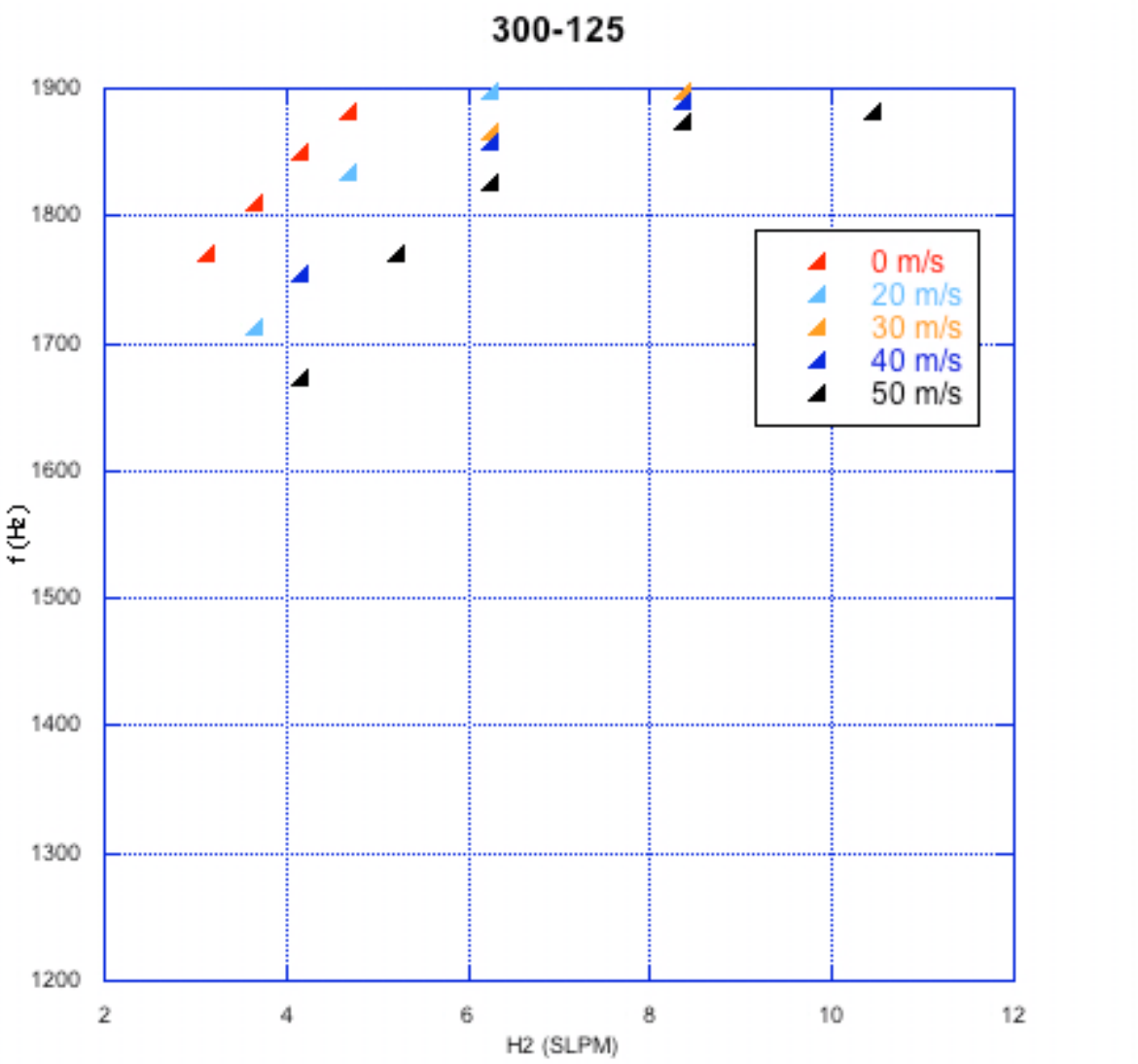

Figure 4-1: Frequency measurements for inlet 300-125

The frequencies of inlet 415-125 are shown in Figure 4-2. In this case, all frequencies fall between 1500 Hz and 1800 Hz. Again, frequency tends to increase as the fuel flow rate is increased with the frequencies peaking around 1750 Hz. In general, the frequency decreases as airspeed increases with a couple of exceptions at 30 m/s and 40 m/s.

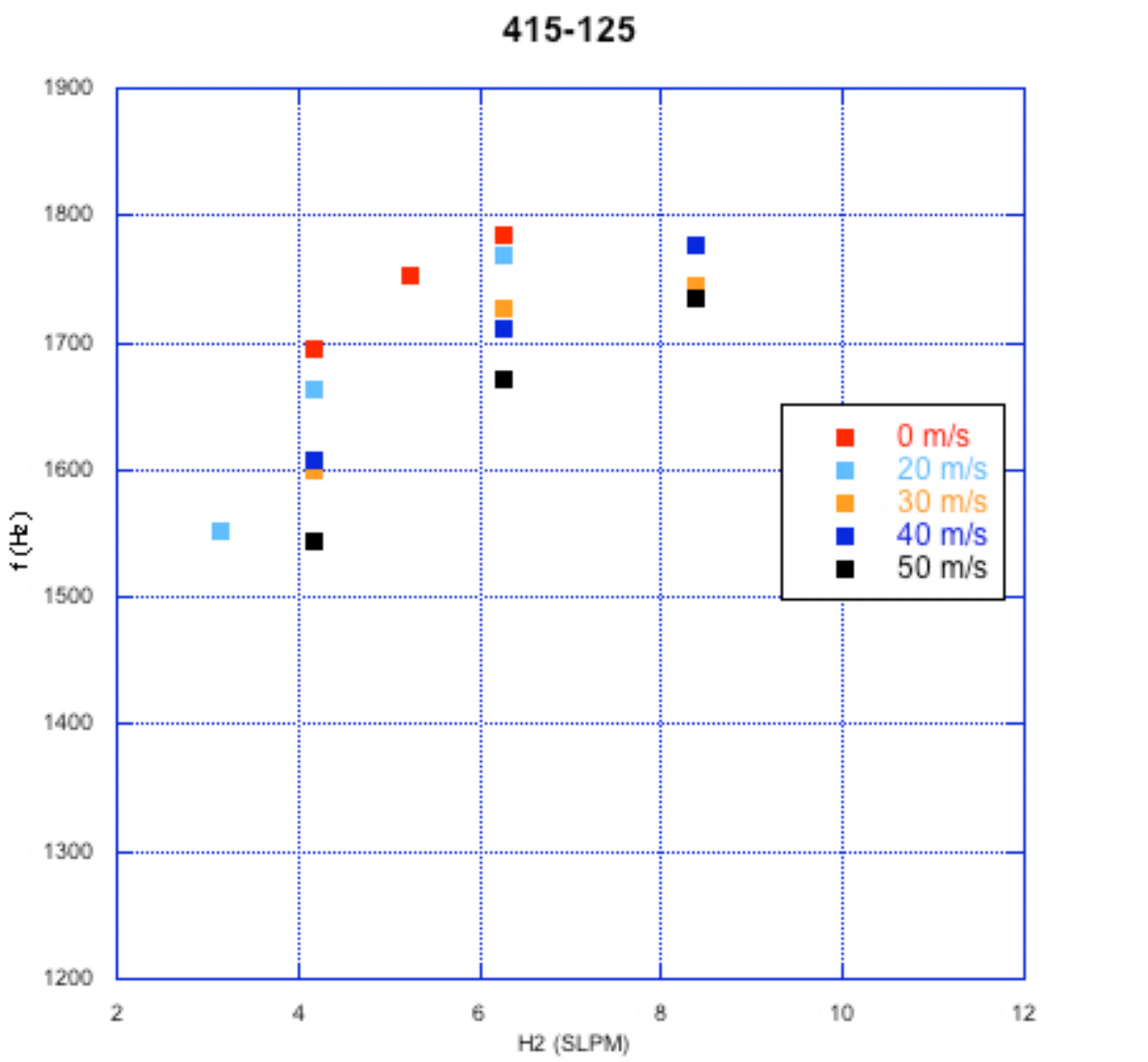

Figure 4-2: Frequency measurements for inlet 415-125

Figure 4-3 shows that the frequencies for inlet 550-125 fall within the range of 1400 Hz to 1600 Hz, a somewhat narrower range than the other two inlets discussed thus far. The trends with fuel flow rate and airspeed are similar to the trends found with other inlets. With this inlet, frequency appears to maximize at about 1580 Hz.

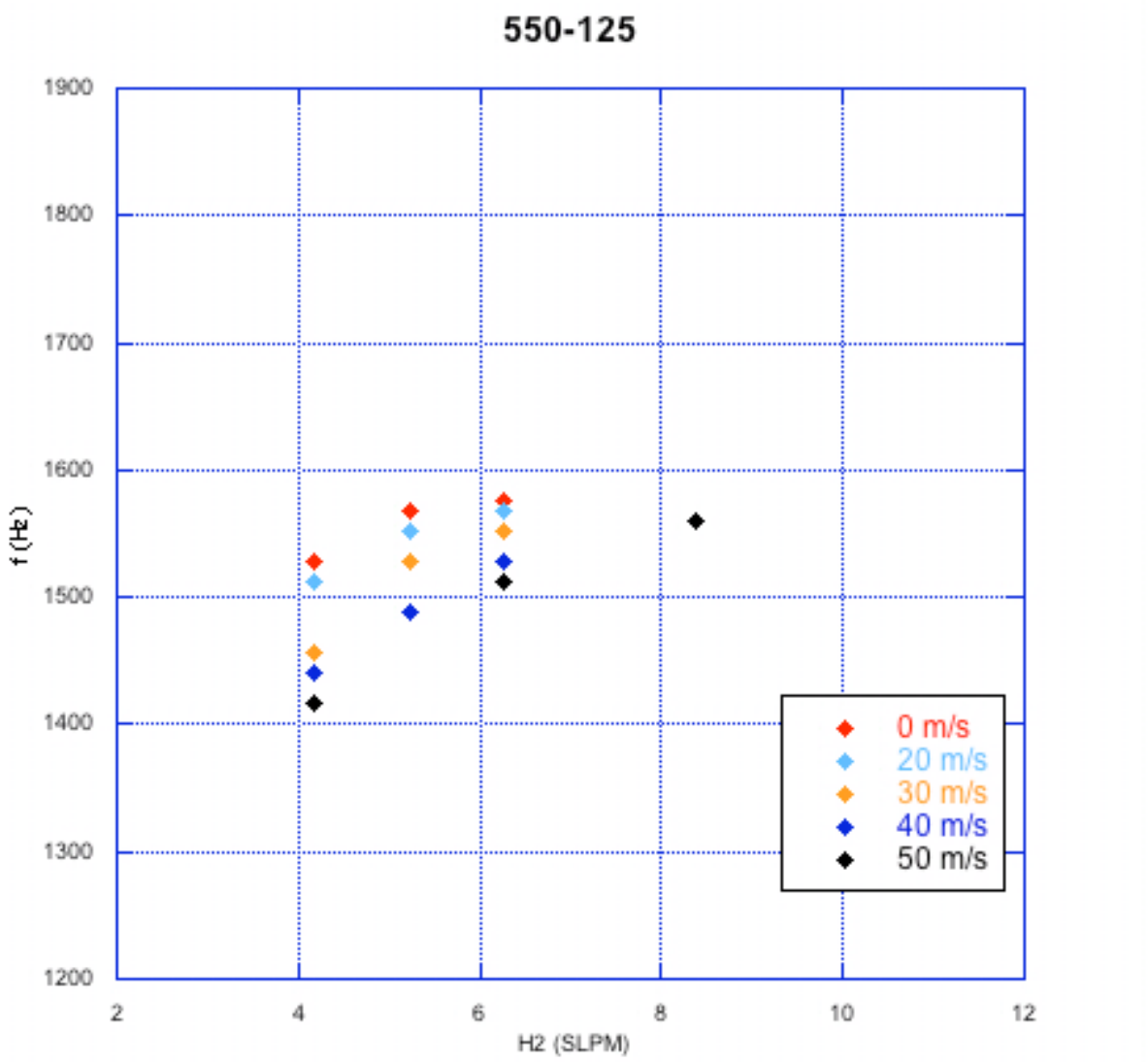

Figure 4-3: Frequency measurements for inlet 550-125

The final inlet for which frequency measurements were taken was inlet 700-125 and the results of these measurements are given in Figure 4-4. A large number of data points were taken with this inlet since it outperformed the other inlets in general and an effort was made to associate frequency with performance. This inlet, being the longest, had frequency measurements in the range of 1200 Hz to 1450 Hz.

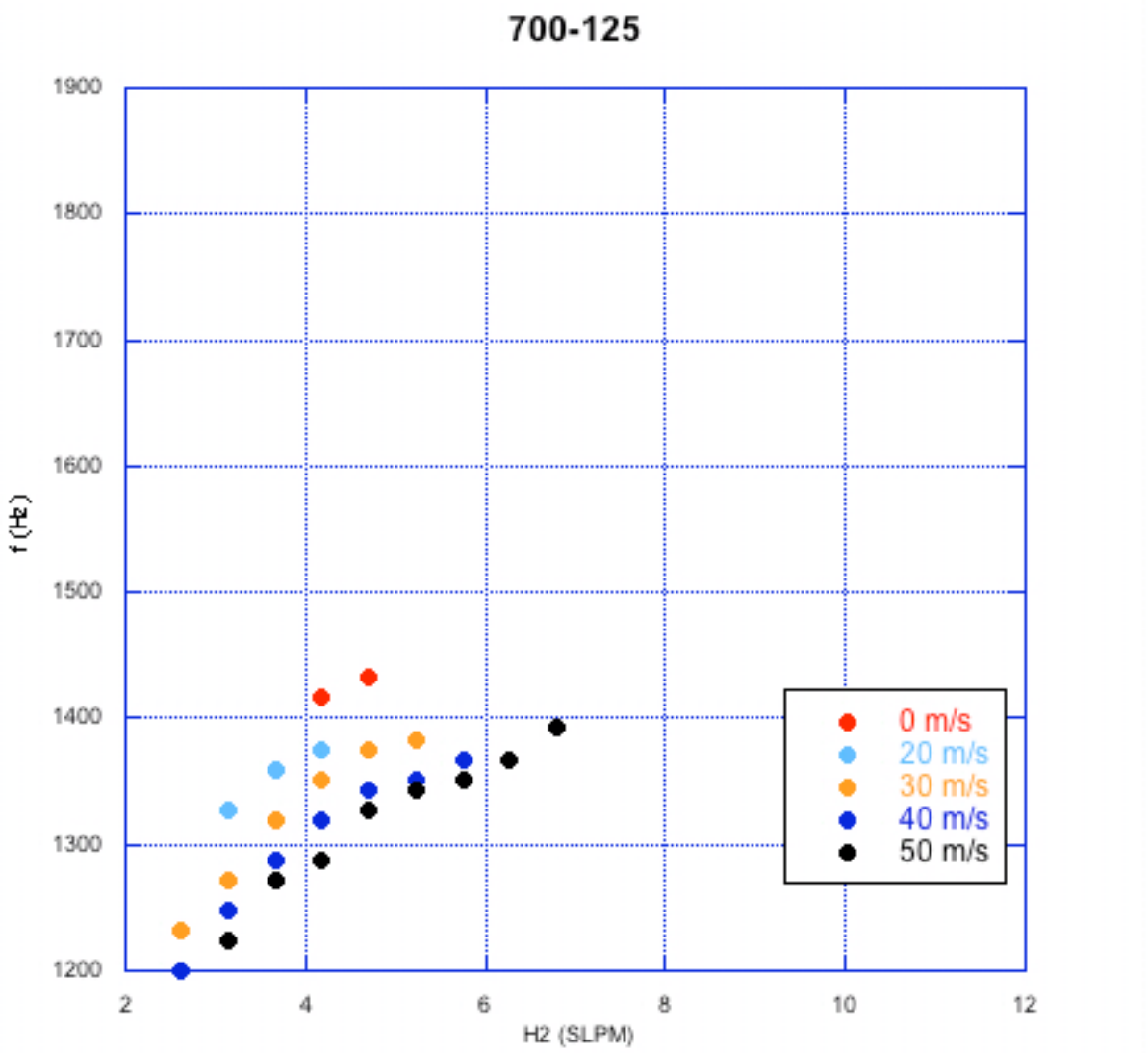

Figure 4-4: Frequency measurements for inlet 700-125

A few generalized trends may be established from the four inlets tested here. First, increasing the fuel flow rate is seen to increase the frequency. This may be a consequence of increasing combustion chamber temperatures. Second, increasing the incoming air speed has the effect of decreasing the pulsejet's operating frequency. This may be a consequence of lower combustion chamber temperatures as more cool air is forced into the combustion zone.

The third trend is that increasing the length of the inlet decreases the operating frequency of the pulsejet. This is to be expected if the inlet can be modeled as a Helmholtz resonator, as had been done previously (see Section 1.4). This is discussed in further detail below.

4.2 Exit Temperature

In addition to frequency measurements, exit and inlet temperature measurements were also taken for the same conditions. It is clear that the temperature of the combustion products as they are expanded through the exhaust tube plays a role in determining frequency. Actually gathering temperature data was considerably more challenging than taking frequency measurements. The thermocouple had to be held in roughly the same location of the exit plane despite the hot gases flowing past it. It could not be permanently attached to the pulsejet in one location because in some cases, the pulsejet would stop operating due to the obstruction. The task was even more challenging when taking inlet measurements as the pulsejet is extremely sensitive to obstructions at the inlet plane.

The exit temperature data are too scattered to look at on an inlet-by-inlet basis. However, a noticeable trend can be seen if one looks at the entire data set with grouping by inlet. This is done in Figure 4-5. The relationship between measured frequency and measured temperature looks to be almost linear with a positive slope. As a result, higher frequencies tend to be associated with higher exit temperatures. Since higher frequencies have been found with shorter inlets, it follows that the inlets line up in a fairly orderly fashion from 700-125 at the bottom left corner to 300-125 at the top right. There is some significant overlap between the two shortest inlets and a few outliers exist for inlet 550-125.

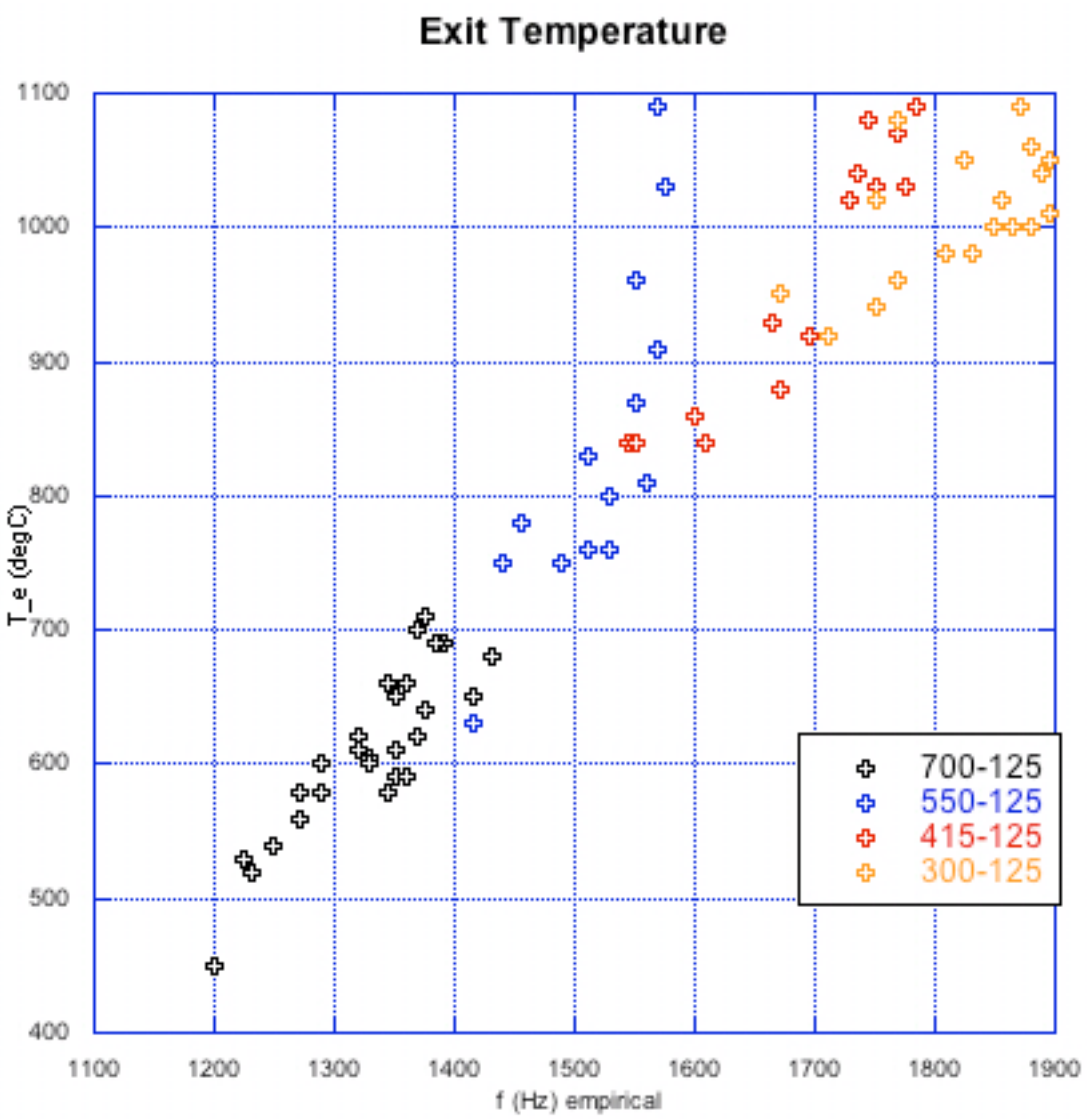

Figure 4-5: Temperature as a function of frequency

4.3 Analytical Frequency

As discussed in Section 1.4, previous research at AERL has shown that the operating frequency of a pulsejet can be predicted by averaging the inlet frequency with the exhaust

frequency. The inlet is modeled as a Helmholtz resonator and the equation for frequency is given as:

$$f = \frac{c}{2\pi}\sqrt{\frac{S}{VL}}$$

where the only variable for the inlets with measured frequencies was the length L, assuming that the speed of sound is the same in each case. Similarly for the exhaust tube, where L is the length of the exhaust;

$$f = \frac{c}{6L_b}$$

In analyzing the current set of data, it was found that this model fails to accurately predict the operating frequency of the valveless pulsejet. However, by slightly modifying the exhaust tube equation to a 1/8 wave tube, very accurate results are obtained. This modification may be justified by noting that the relative size of the combustion chamber is much greater than in previous pulsejets. It may also be noted that the speed of sound in the exhaust tube was calculated from the exhaust temperature data obtained. Also, the speed of sound in the inlet was based on a combustion chamber temperature of 1575 K. While this value is below the theoretical adiabatic flame temperature of a combusting hydrogen-air mixture, it is noted that the actual pulsejet is far from adiabatic in nature. Furthermore, the speed of sound should be some representative value somewhere between that of the combustion chamber and that of the inlet.

Table 4-1 shows the averaged analytical and measured frequencies for each inlet tested. One interesting feature of this table is that the difference between the inlet frequency

and the exhaust frequency appears to become closer as the inlet length gets longer. It is also noted that the average percent error is quite low. In most cases, the calculated frequency overestimates the measured frequency and the largest single percent error was under 12%.

Table 4-1: Averaged analytical and measured frequencies

	300-125	**415-125**	**550-125**	**700-125**
Number of data points	18	15	15	27
Inlet speed of sound	816	816	816	816
Comb. chamber volume	3.16E-06	3.16E-06	3.16E-06	3.16E-06
Inlet cross-sectional area	7.92E-06	7.92E-06	7.92E-06	7.92E-06
Inlet length	7.62E-03	1.05E-02	1.40E-02	1.78E-02
Calculated inlet freq.	2350	2000	1740	1540
Exhaust speed of sound	737	722	684	612
Exhaust tube length	6.52E-02	6.52E-02	6.52E-02	6.52E-02
Calculated exhaust freq.	1410	1380	1310	1170
Exhaust freq./Inlet freq.	0.60	0.69	0.75	0.76
Average calculated freq.	1880	1690	1520	1360
Measured freq.	1820	1690	1520	1330
Percent error	3.59	0.40	0.43	2.23

Since this analysis is the first to look at the effects of forward flight speed, it is instructive to look at how velocity affects the analytical model. To this end, Figure 4-6 presents the percent error in frequency prediction for each individual case, broken down by forward flight speed and plotted against fuel flow rate. The most obvious trend is that the analytical model works best at higher fuel flow rates with percent errors being largely above 4 percent when the fuel flow rate is below 4 SLPM. There is also slightly improved agreement when the forward flight speed is low. It is possible that any deviation with respect to fuel flow rate or flight speed may be due to bad estimations of the combustion chamber speed of sound. For instance, both high velocities and low fuel flow rates may be expected to cool off combustion chamber temperatures, in which case the expected inlet frequency

would be lower and the resulting positive percent error would be reduced to a value closer to zero.

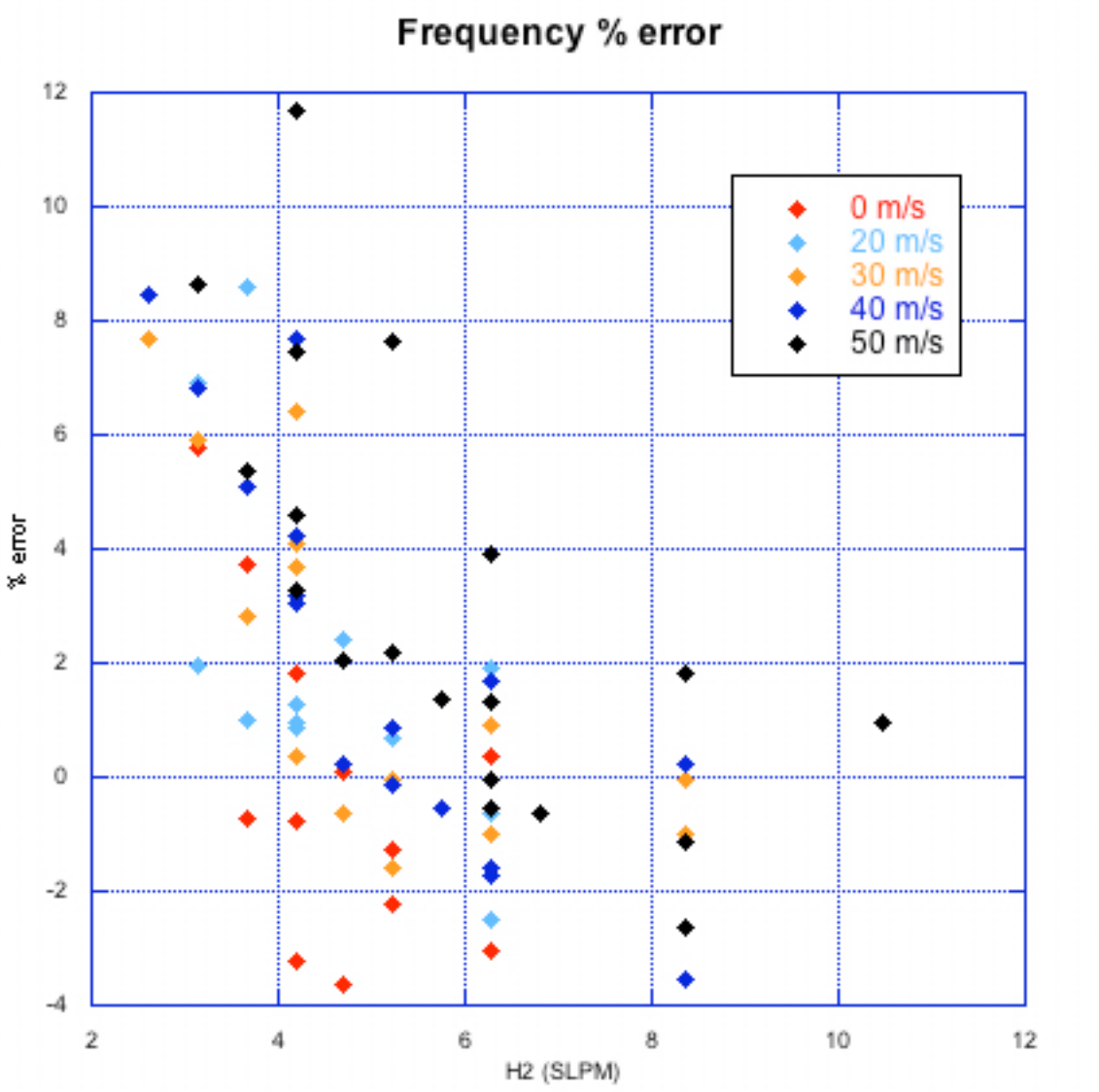

Figure 4-6: Percent error in frequency

4.4 Frequency, Temperature and Performance

Although frequency and temperature measurements were not taken at the same time as thrust and specific impulse, both sets of data were taken for identical conditions (ie. flight speed and fuel flow rate). Therefore, an attempt will be made to correlate the frequency and particularly the temperature data with the performance characteristics discussed in the previous chapter. Table 4-2 lists the average values for the performance characteristics associated with the conditions used in the frequency measurements.

Table 4-2: Average performance characteristics for 4 inlets

	300-125	**415-125**	**550-125**	**700-125**
Inlet length (m)	7.62E-03	1.05E-02	1.40E-02	1.78E-02
Inlet temperature (C)	394	425	271	157
Exhaust temperature (C)	1008	959	833	612
Measured freq. (Hz)	1820	1690	1520	1330
Thrust (mN)	4.37	8.41	11.26	14.84
Specific Impulse (sec)	52.8	103	139	231
Exhaust freq./Inlet freq.	0.60	0.69	0.75	0.76

As was discussed previously, thrust and specific impulse to tend increase as the inlet length increases. This table indicates a few other trends as well; namely, that inlet temperature and exit temperature tend to decrease as inlet length increases. Decreasing inlet temperatures seem to indicate that less of the hot combustion products are escaping out the inlet, meaning more products are exiting through the exhaust tube where they would contribute to the thrust rather than detract from it. At the same time, the exhaust temperature data indicates that the combustion products are cooler as they leave the pulsejet when the inlet is relatively long. The conservation of energy shows that the energy leaving the pulsejet is composed primarily of static enthalpy, which is proportional to static temperature, and

kinetic energy, which is proportional to the square of the velocity. Since the sum of these quantities is conserved, any decrease in temperature should be accompanied by an increase in velocity. Since thrust is a strong function of exit velocity, increases in exit velocity tend to increase the thrust. In fact, this conversion of static enthalpy into kinetic energy is exactly the point of a diverging nozzle on a supersonic jet engine or a rocket. In this case, the lower exhaust temperature for inlet 700-125 indicate higher exit velocities which should translate into higher thrust, and that is, in fact, the case. Additionally, since the total energy is associated linearly with the temperature and with the square of the velocity, it may be shown that decreases in temperature will result in diminishing increases in velocity. Thus, even though the temperature decrease grows with each inlet length increase, the thrust gains are roughly linear.

Now, a cause-and-effect relationship between these characteristics may be outlined. The cause, of course, is increasing the length of the inlet. This has the acoustic effect of decreasing the inlet frequency and the fluid mechanical effect of impeding the backflow of combustion products through the inlet. This results in lower inlet temperatures and higher mass flow rates through the exit plane. Higher mass flow rates mean higher velocities since the exit plane area is constant and the density may be assumed constant. Higher exit velocities mean lower exit static temperatures assuming the stagnation temperature is constant for all sets of conditions. Higher exit velocities also mean higher thrust and, for equivalent fuel flow rates, higher specific impulse. Lower exhaust temperatures also result in lower speeds of sound, which then results in lower exhaust tube frequencies. Finally, since the inlet frequency and the exhaust frequency are both lower, the operating frequency is

lower. This is why inlet 700-125 has the lowest frequency and the highest thrust while inlet 300-125 has the highest frequency and the lowest thrust and inlets 415-125 and 550-125 fall somewhere in between.

As a side-note, computational results have shown that performance tends to peak when inlet frequency and exhaust frequency are closest in value. According to Table 4-2, this analysis appears to support that conclusion, though not very strongly.

5 Hybrid Configurations

Unfortunately, during this research, no pulsejets with only rearward facing inlets were able to undergo testing while on the thrust stand. The configuration described in section 2.1.2 with two 180 degree inlets was preferred by Adam Kiker but the pulsejet would not start while positioned for thrust measurement. The explanation for this may be the way in which the pulsejet was clamped to the thrust stand, that being at the front of the combustion chamber instead of along the exhaust tube.

The modified configuration described in section 2.1.3 with two 125 degree inlets was able to start in its rearward-only configuration but after running for a couple of minutes, its operation ceased. Since it did not reach steady state (steady here refers to the operating frequency and thrust output; the flow is still unsteady), its performance was not recorded. For this configuration, the pulsejet thrust began at about 14 mN and continually decreased below 10 mN until it finally transitioned to torch mode. The reason for this appears to be related to the heating of the pulsejet body. As the heat builds, the frequency increases until, eventually, the kinetics of the fuel cannot keep up. The design of this configuration gives it a much thicker body than other designs. This may have important implications for heat transfer, both at static conditions and at high air flow rates. It should be noted that the highest recorded static thrust for a forward facing inlet pulsejet was almost 13 mN (see Figure 3-11) so the advantage of rearward facing inlets at static conditions was never verified.

A third possibility that had never been tested to my knowledge is creating a hybrid engine that has a forward facing inlet as well as rearward facing inlets. One might be able to benefit from the advantages of both configurations. Early testing showed that a pulsejet could indeed operate in this configuration. Once the method for measuring thrust was established, some data was taken for a few hybrid configurations as well.

5.1 Thrust and Specific Impulse Results

The first example presented here has an inlet ,which was not tested in a forward facing configuration. Inlet 500-088 has a length of 1.270 cm and a diameter of 0.224 cm making it quite narrow but of medium length. The results of using it with the configuration detailed in section 2.1.2, with 180 degreed rearward inlets, are given in Figure 5-1 and Figure 5-2. The thrust for this configuration is very impressive, eclipsing the 30 mN mark. The specific impulse is also impressive but a number of the points tested with the 700-125 forward facing inlet were higher. This indicates that the tradeoff for high thrust has been high fuel flow rates. The reason for this is the high total area of the inlets. This configuration did not run at static conditions.

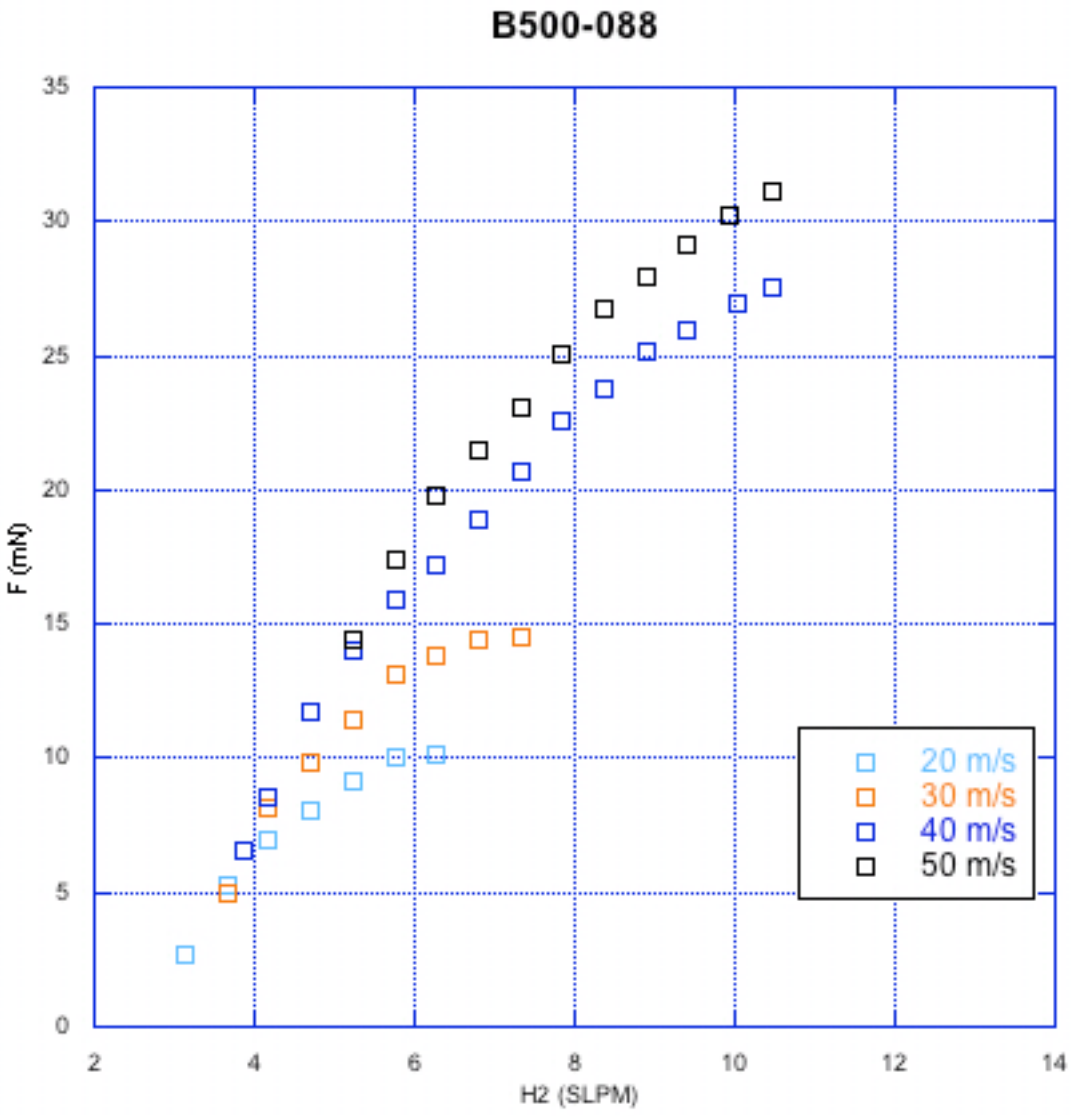

Figure 5-1: Thrust data for inlet 500-088 + 180 deg hybrid

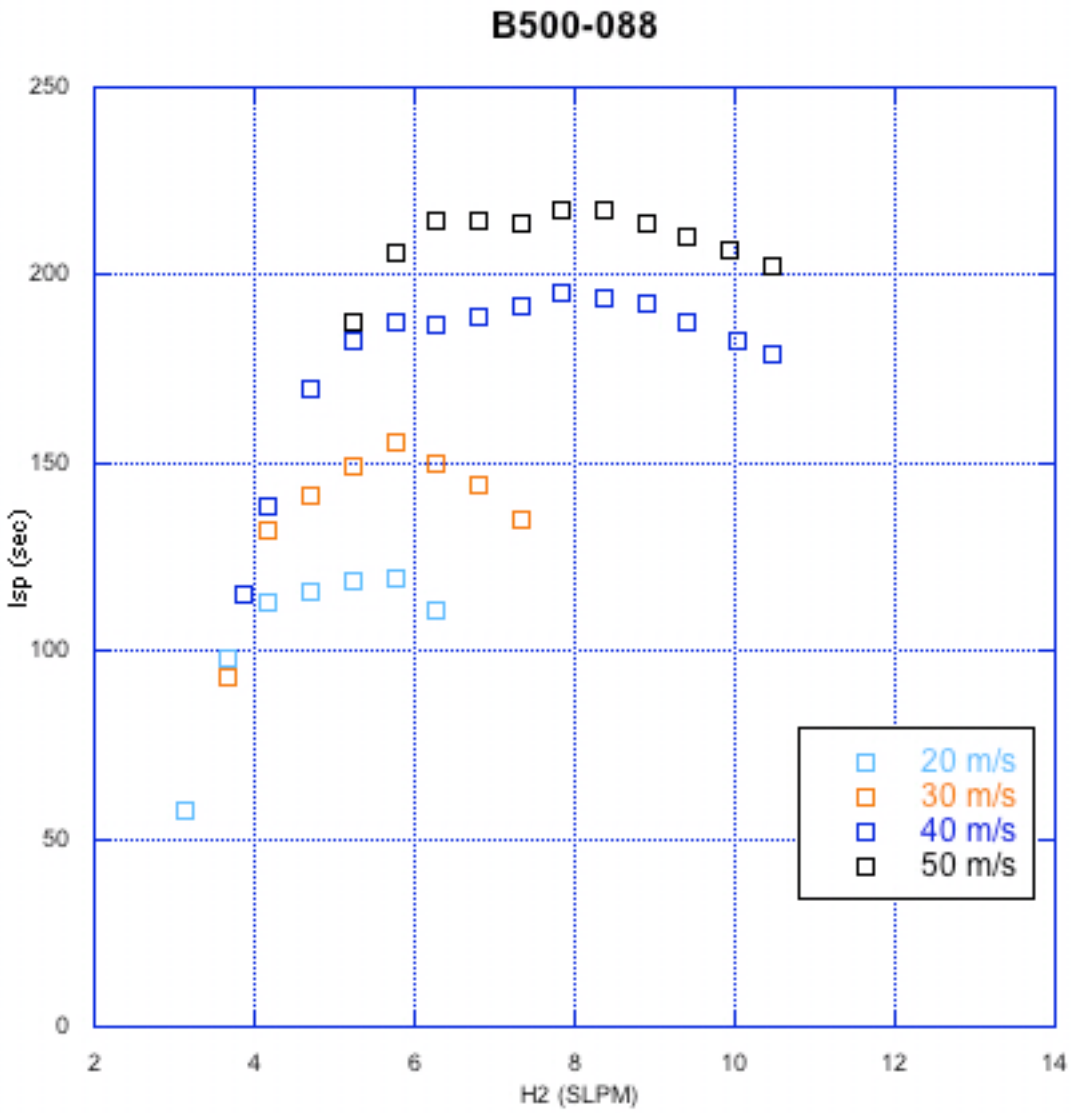

Figure 5-2: Specific impulse data for inlet 500-088 + 180 deg hybrid

Inlet 700-081 and the body described in section 2.1.2 with two 180 degree rearward inlets were also combined and tested. The results are given in Figure 5-3 and Figure 5-4. For all speeds tested, the thrust profile shows a very linear increase in thrust as fuel is increased. Very high fuel flow rates are possible with this configuration because of the large overall inlet area. Thrust ultimately reaches almost 30 mN at 10.5 SLPM. While high thrust

values are obtained, they are generally at the expense of high fuel flow rates. Isp peaks around 230 sec at both 40 m/s and 50 m/s. This configuration would not operate below 20 m/s.

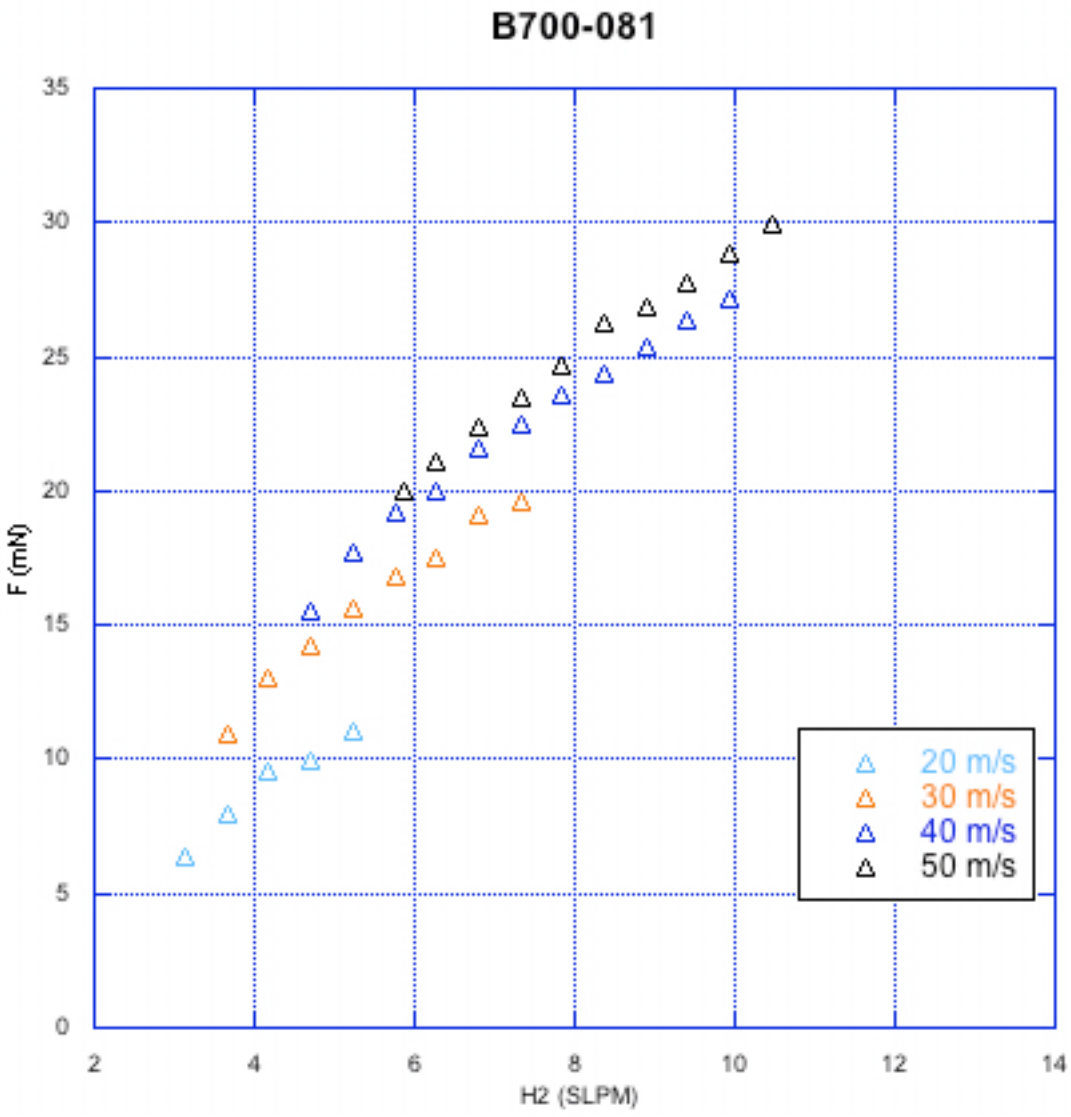

Figure 5-3: Thrust data for inlet 700-081 + 180 deg hybrid

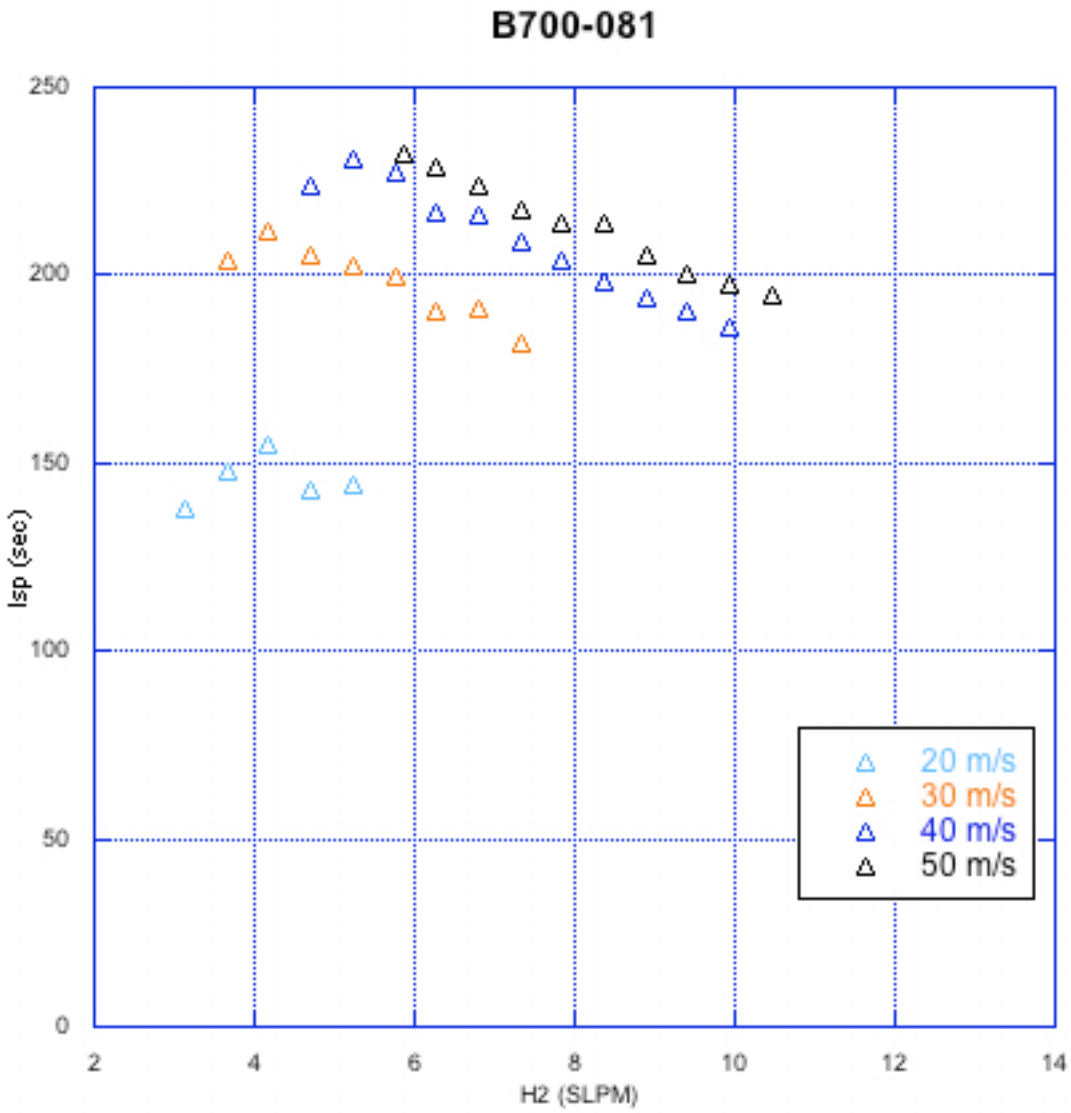

Figure 5-4: Specific impulse data for inlet 700-081 + 180 deg hybrid

This inlet was also tested in the modified hybrid configuration explained in section 2.1.3, which has two 125 degree inlets of the same size (shown in Figure 5-5). The data acquired from this configuration is given in Figure 5-6 and Figure 5-7. The interesting feature about the thrust profiles is how much difference the airspeed makes. This configuration is much bulkier than the other pulsejet bodies tested. This may have important

heat transfer implications. For instance, this configuration will run at static conditions for a short while, but eventually it cuts out. It essentially overheats, but the heating time is much longer because of the extra material. This could account for the far superior performance at higher speeds since the increased airflow around the pulsejet body would create extra convective cooling. This is also why the maximum fuel flow rates increase at higher speeds. The configuration could run at 40 m/s with 10 SLPM of fuel but it would eventually cease running, having overheated and switched to “torch” mode. This situation is shown in Figure 5-5 where the flames and the glowing red 125 degree inlets are both indicators of undesirable behavior. When this configuration is able to achieve steady state, the performance can be very good, reaching almost 30 mN of thrust and exceeding 220 seconds of specific impulse.

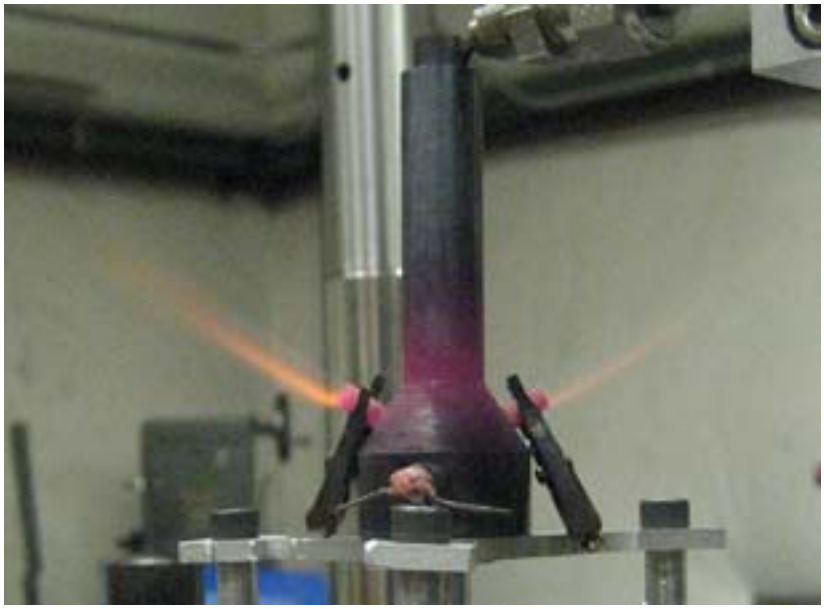

Figure 5-5: Hybrid configuration in "torch" mode

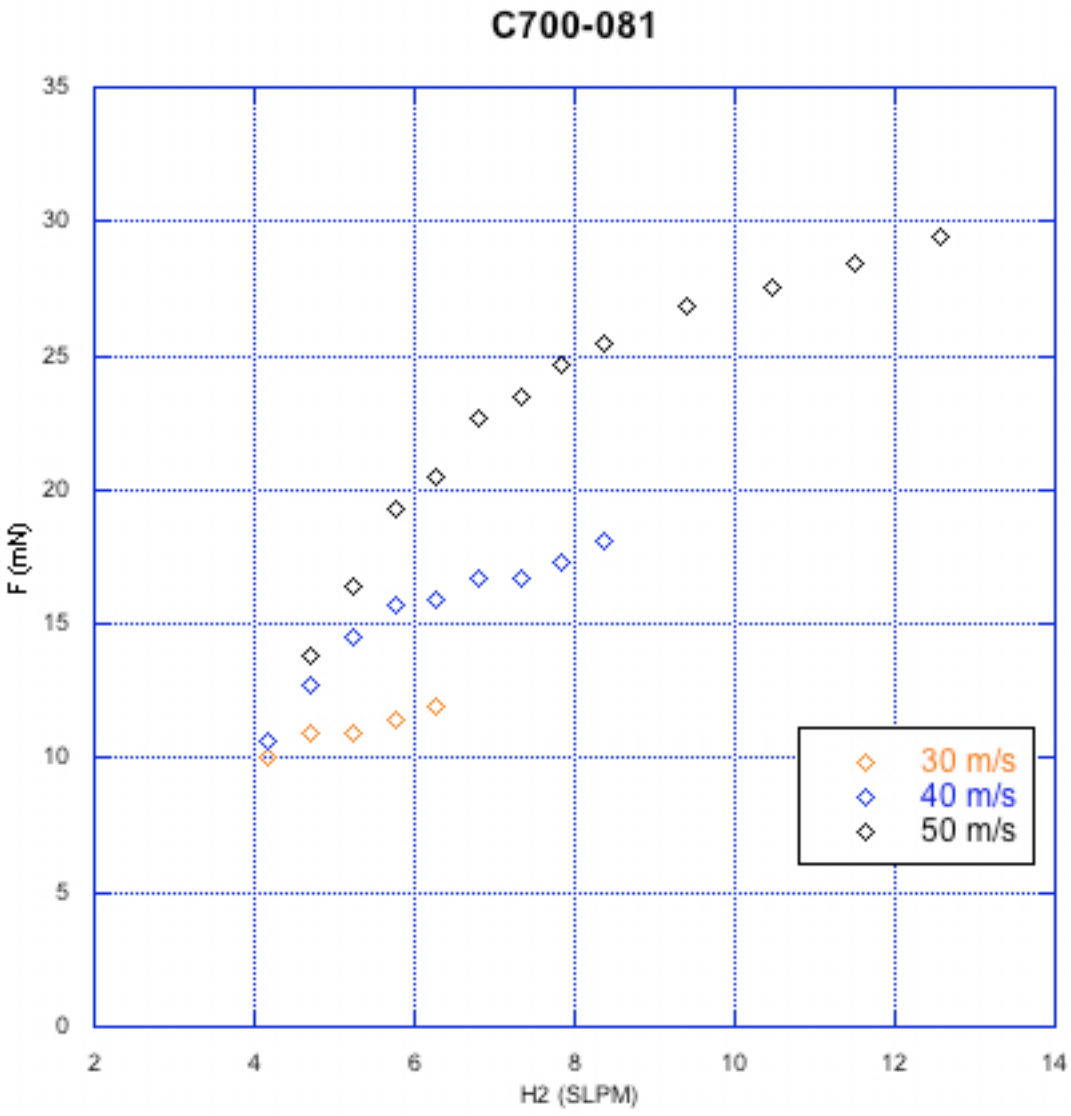

Figure 5-6: Thrust data for inlet 700-081 + 125 deg hybrid

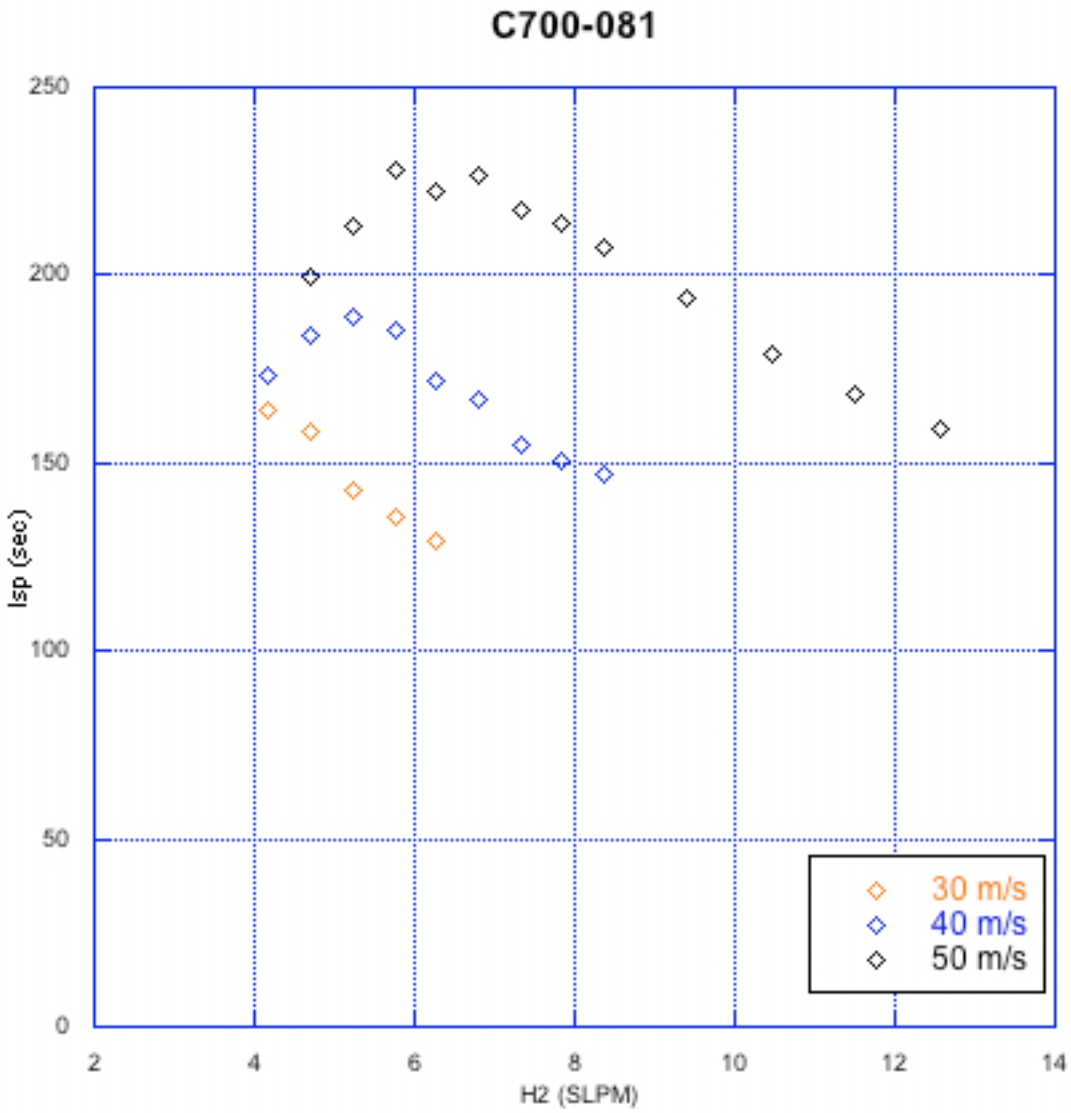

Figure 5-7: Specific impulse data for inlet 700-081 + 125 deg hybrid

Inlet 700-100 was then tested in the modified hybrid configuration. Its behavior was not unlike the other hybrid configurations tested. Thrust typically increased with both fuel flow rate and airspeed as shown in Figure 5-8. Thrust peaked at about 24 mN at almost 9 SLPM. Referring to Figure 5-9, specific impulse surpassed 200 seconds once. The most surprising characteristic of these results is the relatively short range of fuel flow rates.

Considering this is the largest inlet area tested so far, one would expect it to have a greater range. The issue here is not that it necessarily will not run above this point. In fact, it does operate but the thrust begins fluctuating wildly. It seems as if the pulsejet is oscillating back and forth between two modes; one is resonant, which is preferred, and the other is "torch" mode, which is not. The policy with other configurations has been to not record data during "torch" mode or any data during transitional stages where no single thrust value would be appropriate.

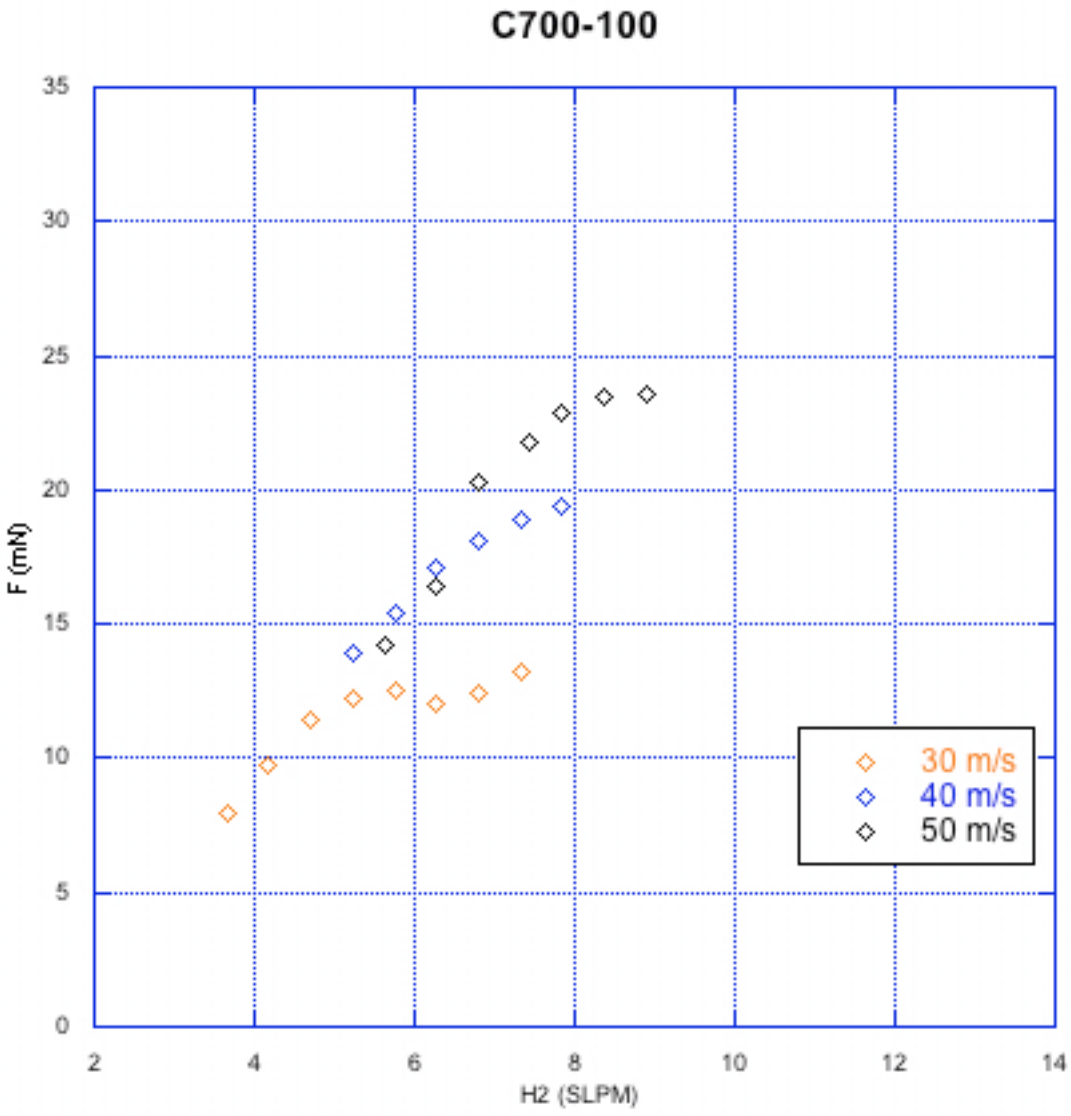

Figure 5-8: Thrust data for inlet 700-100 + 125 deg hybrid

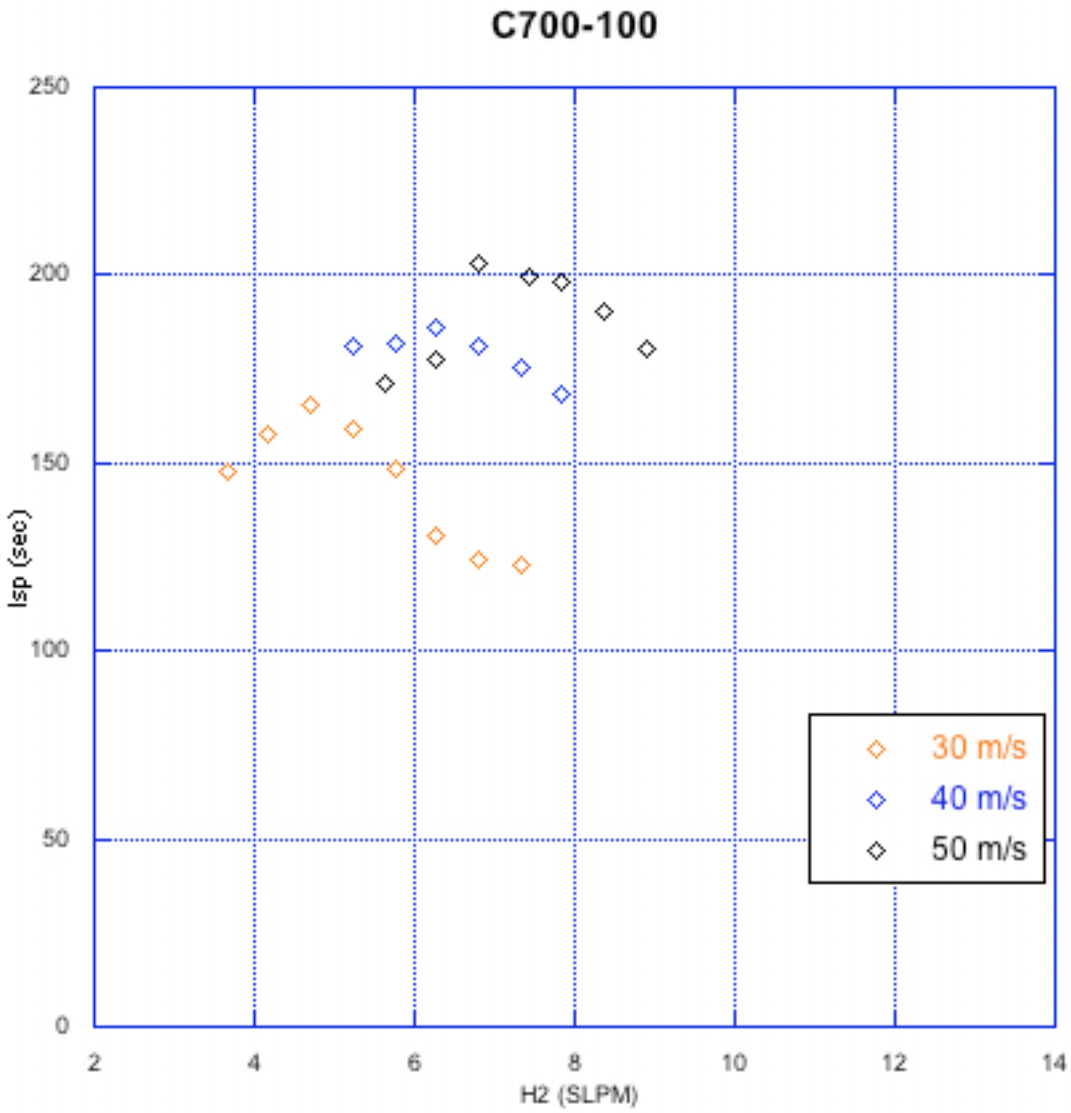

Figure 5-9: Specific impulse data for inlet 700-100 + 125 deg hybrid

The hybrid configuration with inlet 700-125 has the largest total inlet area of any configuration tested. It was also the most difficult to test. Figure 5-10 and Figure 5-11 show the thrust and specific impulse data, which could only be collected at 50 m/s. For most of these runs, the thrust would start out considerably higher than the results would indicate. However, the thrust continuously decreases as the jet heats. The results shown are the values

obtained once steady state was reached. Thrust does reach over 21 mN and Isp peaks at about 170 seconds. This configuration ran at static conditions for about 20 seconds before quitting. At 40 m/s, it could run for a couple of minutes but it eventually transitioned to "torch" mode without stabilizing. This case is similar to inlet 700-150 in that the large inlet area appears to approach the practical limit with this particular pulsejet body.

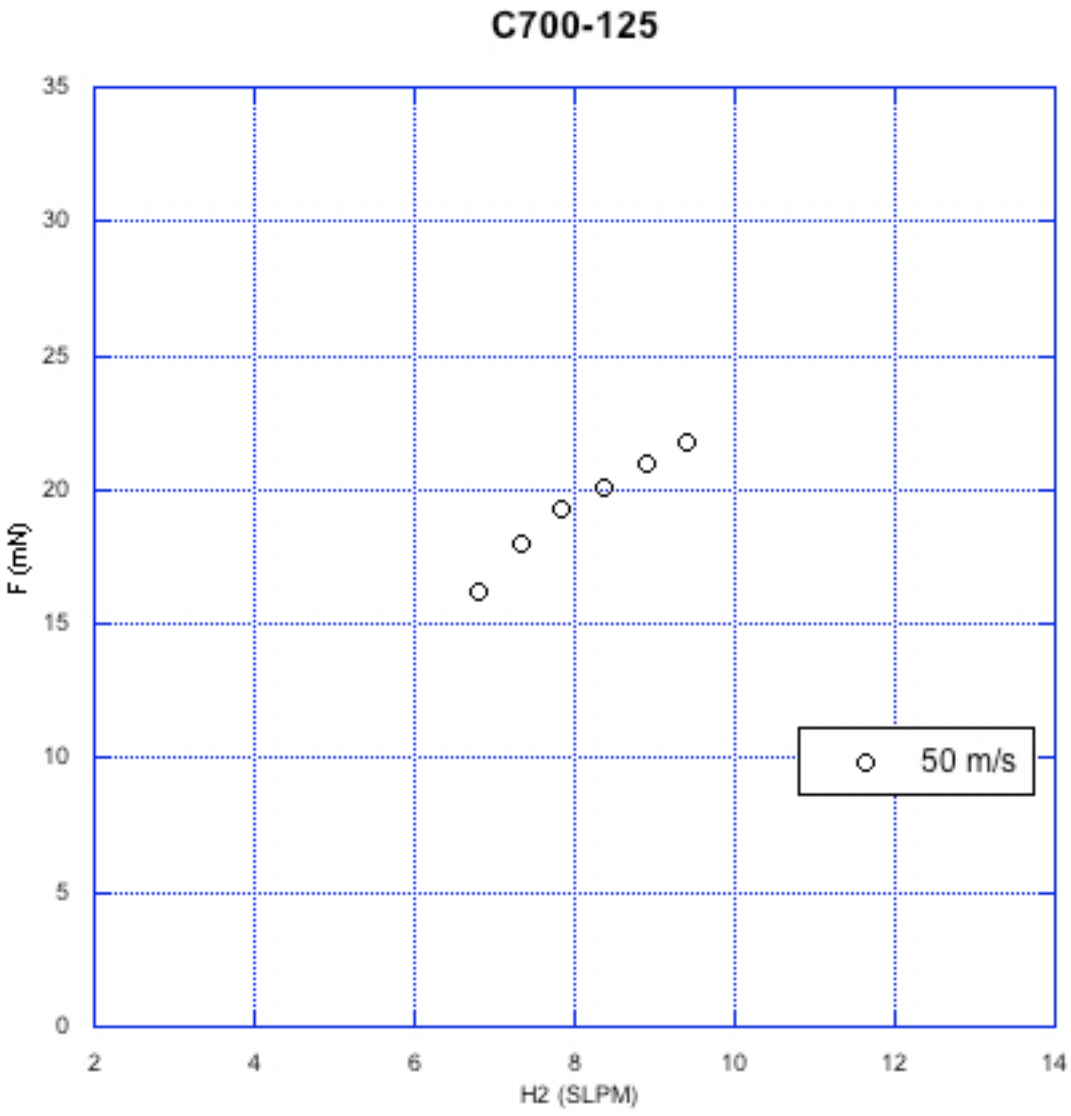

Figure 5-10: Thrust data for inlet 700-125 + 125 deg hybrid

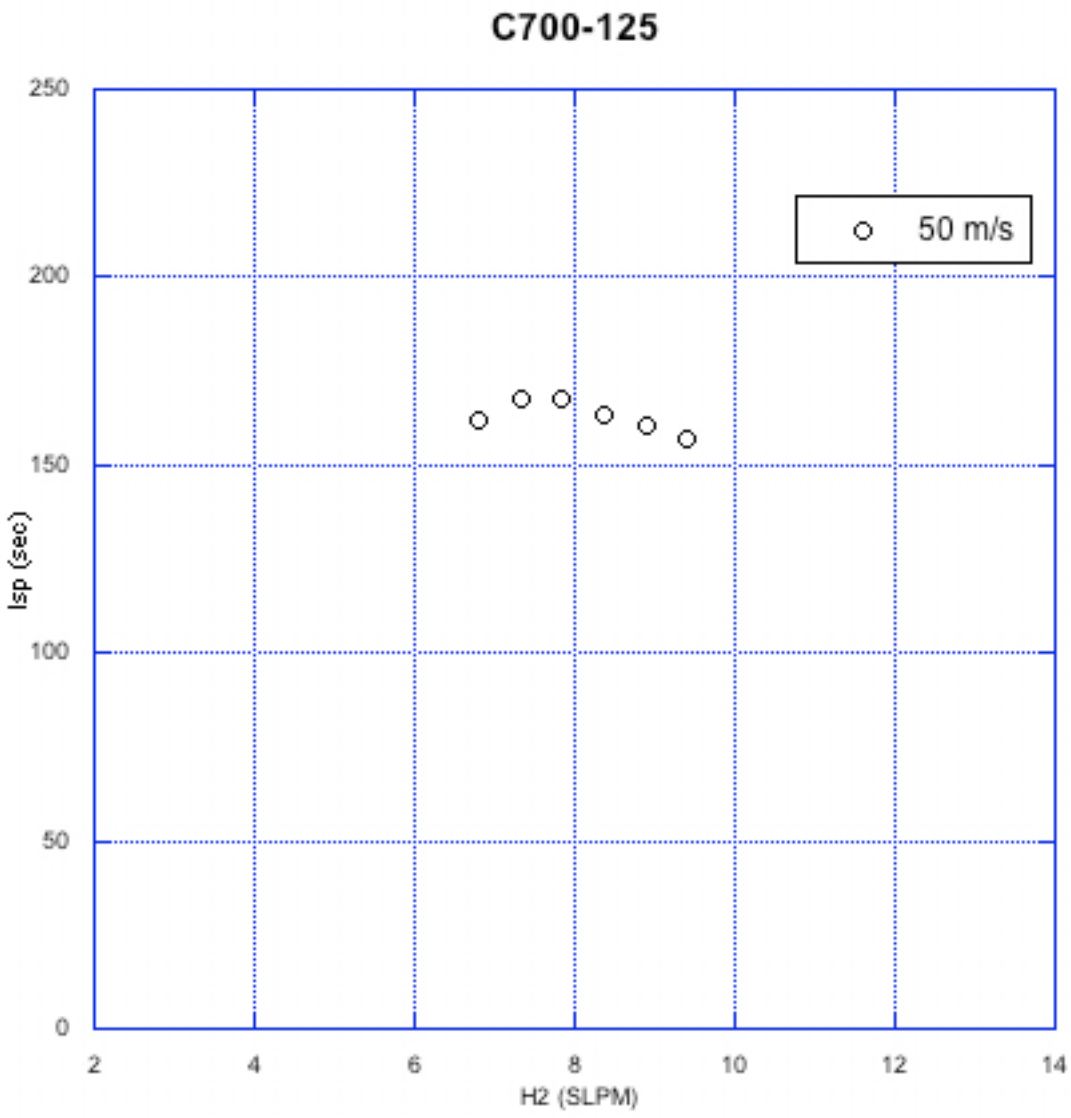

Figure 5-11: Specific impulse data for inlet 700-125 + 125 deg hybrid

5.2 Hybrid Configuration Trends

Some of the trends that are noticeable with the hybrid configurations and their similarities to forward facing configurations will be discussed here. Two trends are clear

from the plots associated with the results on hybrid configurations. Once again, the thrust increases monotonically with fuel flow rate. Also, the specific impulse tends to peak near the middle or beginning of the fuel flow range. The other trend is the increase in thrust as the airspeed increases. This effect is much more regular with the hybrid configurations than it was with forward facing configurations. Of all the cases reported above, there are only 3 occurrences of the thrust at one speed exceeding the thrust of a higher speed at the same fuel flow rate. With forward facing inlets, there can be many exceptions to associating higher speeds with higher thrust, but with the hybrid configurations, it is the rule. The same is true of specific impulse.

As for understanding the differences in performance among the hybrid configurations, one may refer to Table 5-1 which lists the peak thrust and its associated specific impulse as well as the peak specific impulse and its associated thrust. This table also gives the total area of all three inlets for each variant.

Table 5-1: Peak results for hybrid configurations

Configuration	Forward Inlet area (cm^2)	Total Inlet area (cm^2)	Peak Thrust (mN)	Isp at Peak Thrust (sec)	Peak Isp (sec)	Thrust at Peak Isp (mN)
500-088 + 180deg	0.039	0.117	31.2	203	218	25.1
700-081 + 180deg	0.033	0.111	29.9	194	232	20.0
700-081 + 125deg	0.033	0.111	29.4	159	228	19.3
700-100 + 125deg	0.051	0.129	23.6	181	203	20.3
700-125 + 125deg	0.079	0.157	21.8	157	168	18.3

One notable characteristic of this table is how dominant the 500-088 configuration is. The only category in which it does not lead is peak Isp, in which it is only marginally worse than the best two cases. This is a little surprising since it is the shortest inlet of all tested here. As was seen with the forward facing only inlets, the general rule is better performance with longer forward facing inlets. On the other hand, this inlet has the same area as, and a more comparable length to, the rearward facing inlets used in these configurations. Perhaps the symmetry is advantageous.

Another trend that can be seen with this information is that the peak Isp is a function of the total inlet area. In order of decreasing specific impulse, the variants go from smallest area to largest area. Since the only area that is actually changing is the forward facing inlet, this trend supports the idea that a smaller area on the forward facing inlet should result in higher efficiency.

When compared to forward facing only configurations, the advantages of hybrid configurations is mixed. With the increased overall inlet area, hybrids certainly can handle larger fuel flow rates. As a consequence, they also tend to have higher peak thrusts. The highest thrust obtained by forward facing inlets was about 24 mN, which is met or exceeded by four of five hybrid configurations. On the other hand, peak specific impulses were not as high as those seen with forward facing inlets. Inlet 700-125 alone outperforms all of the hybrids at 50 m/s and low fuel flow rates. Of course, the possibility remains that an inlet even narrower than those listed above could exceed any results obtained yet. Another difference is the very regular behavior of the hybrids, particularly with respect to airspeed.

This could be a big advantage for design purposes although it is a little dull for research applications.

These preliminary results indicate that hybrids may make good candidates for small propulsion devices. They had never been tried before and this small amount of research was performed mostly just to see if the idea could work and to get some idea of how the performance of a hybrid compares to the more conventional configurations. They do have superior thrust characteristics and they do respond positively to increases in forward flight speeds. The deficiencies in specific impulse are not great and may well be remedied by investigating smaller forward facing inlets. More work is needed to understand the superior performance of the 500-088 hybrid. The most troubling result was that none of the hybrids could run indefinitely at static conditions.

5.3 Case Study: Inlet 700-081

Inlet 700-081 presents an interesting case because it is the only inlet tested as a forward facing only inlet, a rearward hybrid with 180 degree inlets, and a modified rearward hybrid with 125 degree inlets. This offers a unique opportunity to compare the three configurations. The largest difference between the 3 configurations is that the forward facing one only allowed operation at 50 m/s. The hybrids both ran at lower speeds although neither allowed sustained operation at static conditions. The lesson here is that a minimum inlet area must be present in order for the pulsejet to operate well. This makes sense intuitively and this case study proves it.

Figure 5-12 displays the thrust results for all three at an airspeed of 50 m/s. As expected, the enlarged total inlet area on the hybrids allows for much higher fuel flow rates. As usual, higher fuel flow rates mean higher thrust values. The interesting comparison here is between the two hybrids. Below 8 SLPM, both configurations have virtually indistinguishable profiles. Above 8 SLPM, the configuration with 180 degree inlets proceeds to outperform the other hybrid. The advantage of the rearward inlets is that products that escape through the inlets have their momentum at least partially aligned with the exhaust, thus contributing to thrust. The 180 degree inlets are exactly aligned with the exhaust and would be expected to produce the maximum thrust possible, all else being equal. For this reason, the rearward hybrid is expected to have superior performance, and this is the case above 8 SLPM. The most likely reason for this is that the amount of material leaving through the rearward inlets simply isn't significant below the 8 SLPM point. As more fuel is dumped into the combustion chamber, more air is needed for the combustion and higher peak pressures result. This results in higher mass fluxes and, assuming the frequency is at least the same, higher momentum fluxes as well. As the momentum flux of material leaving the inlet increases, the differences in thrust should become noticeable because the component of momentum lost due to the angle of the inlets would become larger. The difference between these two profiles should continue to grow as the fuel flow rate is increased.

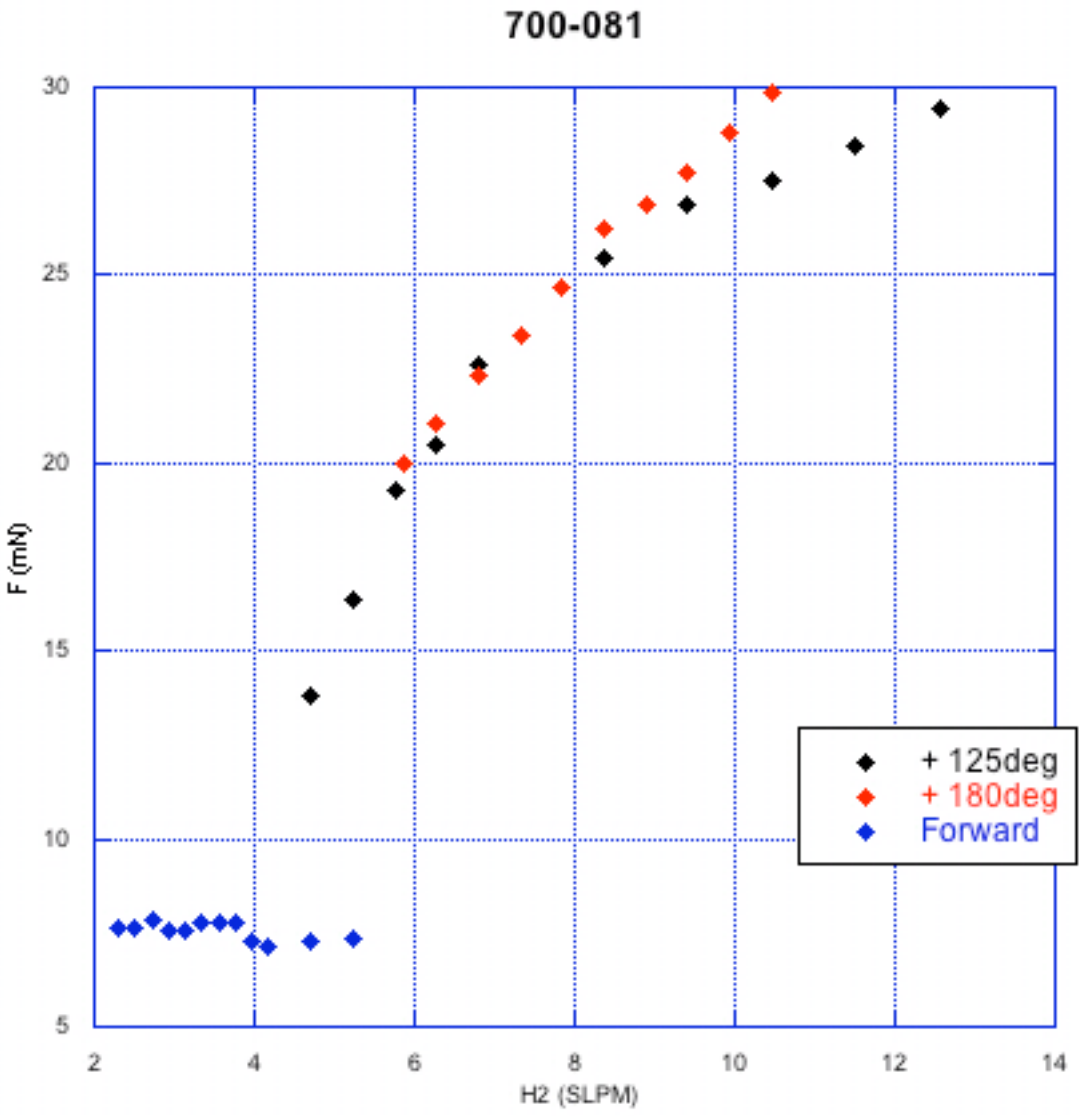

Figure 5-12: Thrust for all cases with inlet 700-081 at 50 m/s

The specific impulse profiles at 50 m/s are compared side by side in Figure 5-13. Two points should be made here. First, it is interesting that all three configurations have roughly the same peak Isp. Also, notice that due to the linear thrust profiles of the forward and the + 180 degree variants, both peak in specific impulse at the lowest fuel flow rate.

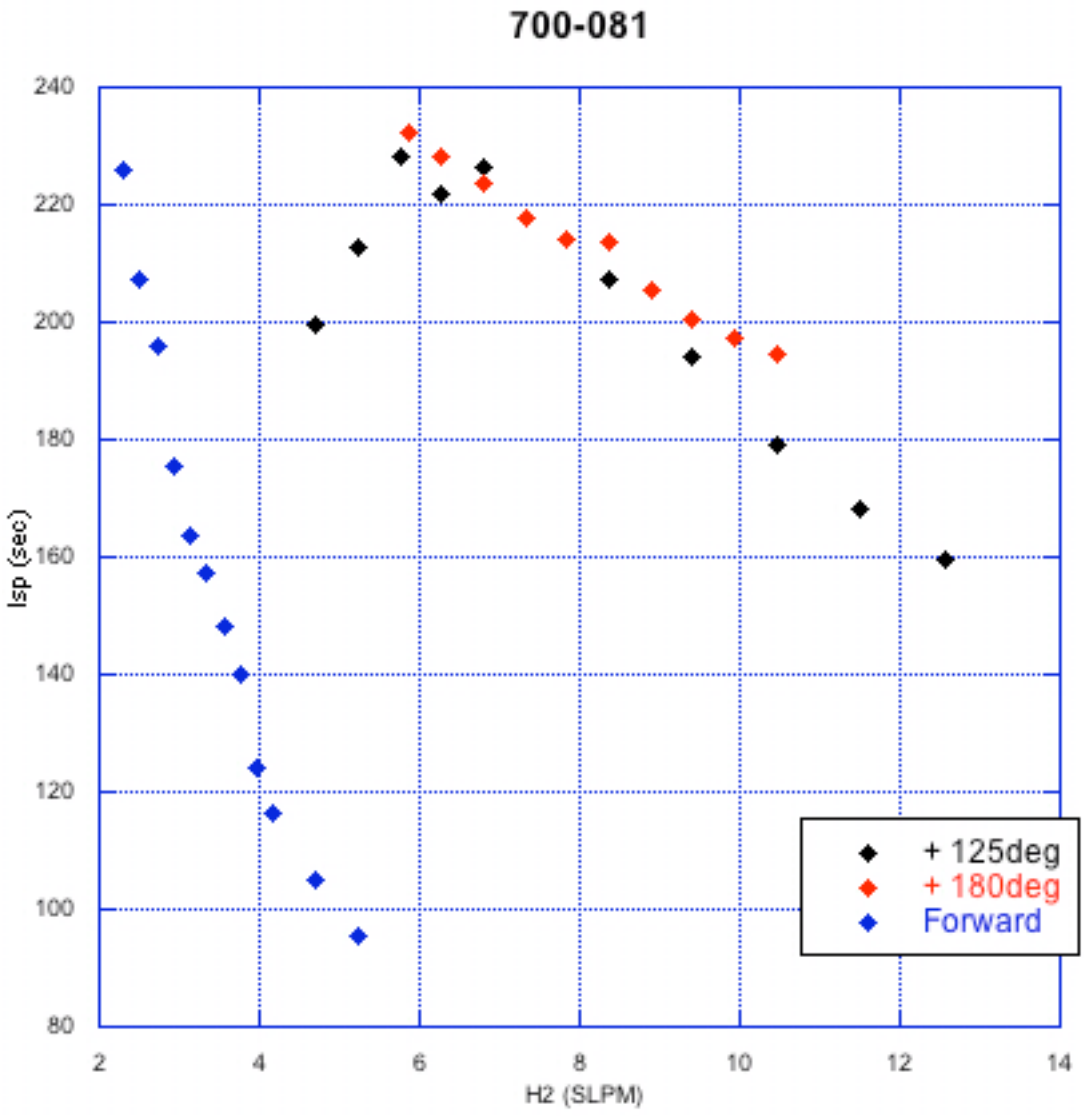

Figure 5-13: Specific impulse for all cases with inlet 700-081 at 50 m/s

6 Other Results

In addition to the primary results discussed above, a number of secondary results were obtained during this research. These results are briefly discussed below.

6.1 Operation on Hydrocarbon Fuels

From an early stage in the research, it was desirable to investigate the possibilities of operating the 8 cm pulsejets on fuels other than hydrogen. Hydrogen is a very energetic fuel, which is what allows it to operate at such high frequencies. Furthermore, the pulsejet also benefits from hydrogen's high rate of diffusion in air, which is an order of magnitude greater than that of hydrocarbons, as well as its wide flammability limits (Waitz, 1998). Unfortunately, hydrogen suffers from existing only at very low densities, which results in a relatively low energy density compared to some other common fuels (such as propane). To increase the density to a suitable level, hydrogen must be maintained at extremely low temperature or at very high pressure if not both. This poses a major structural obstacle, especially when considering vehicles with sizes on the scale that might find an 8 cm pulsejet useful.

As reviewed briefly in section 1.4, Schoen, Ordon, and McCauley had all done previous research on alternative fuels in valveless pulsejets. A couple of them had run on propane and McCauley even achieved successful operation on heavier hydrocarbons. However, none of these accomplishments occurred at the 8 cm level. And, theoretically, as the frequency increases, the fluid mechanical timescale approaches the chemical kinetic timescale, meaning the fuel needs to react more quickly.

Ultimately, propane was the goal, but a couple of intermediate fuels were also tested. The only true success was acetylene. Acetylene is known to be a very energetic fuel and was immediately successful both with and without forced air at the 8 cm level. Figure 2-4 shows a pulsejet in hybrid configuration operating on acetylene as revealed by the characteristic white flames. Unfortunately, for practical purposes, acetylene solves few of the problems posed by hydrogen. It becomes very unstable at pressures barely above atmospheric, making storage and transportation difficult. Little quantitative data was taken on acetylene but results showed that, by comparison with hydrogen, operation on acetylene was at lower sound pressure levels, with lower frequencies, higher exhaust temperatures, and producing much lower thrust levels.

Two modifications were made in an attempt to run the pulsejet on propane. Firstly, the pulsejet itself was modified with a catalytic coating. This was done through Artisan Microplating, who had previously worked with Adam Kiker. They were able to coat the interior surface of the pulsejet with a 1 micron palladium coating followed by a 3 micron platinum coating. Unfortunately, this trick did not speed up the propane reactions enough to allow operation, although there was some anecdotal evidence that the coating improved the pulsejet's ability to operate on acetylene. In order for a catalytic coating to make a big difference, a high rate of mass transport to the surface must exist. This would mean increasing the combustor surface area relative to the combustion chamber volume. Lengthening the combustion chamber, which would result in a longer engine, could do this. Creating "folds" or channels along the interior surface of the combustion chamber could also do this, but this would be a very difficult task at such small scales, and the catalytic coating

process would also be greatly complicated. Of course, by increasing the surface area relative to the volume, the rate of heat transfer from the fluid to the surface also increases, which will increase the chances of flame extinction.

The second modification was to run the propane through a heating apparatus before it arrived to the fuel injector as was described in section 2.8. This approach had been used by earlier researchers and was shown to be successful. In this case, however, it was never fully successful. The pulsejet could sustain operation with forced air and a combination of hydrogen and propane, but the hydrogen fuel flow rate could not go below 1 SLPM or the pulsejet would cease operation. Even so, it operated at much lower sound levels and often oscillated between a loud hydrogen mode and a soft propane mode (which could be distinguished by blue flames). McCauley found this same behavior when operating a larger pulsejet on both propane and gasoline. The modified pulsejet introduced in section 2.1.3 incorporates the fuel tube into the exhaust tube, allowing for regenerative heating of the fuel as it enters the combustion chamber, but this innovation also fell short of success.

True operation on propane alone was never achieved and this author remains skeptical that it is even possible at such length scales. MAPP gas, which is liquefied petroleum gas mixed with methylacetylene-propadiene, is used in welding because it has properties approaching those of acetylene but without the storage problems. A brief but unsuccessful attempt was made at running the pulsejet on this fuel.

6.2 Sound Pressure Level

Before any reasonable thrust results were obtained, it was theorized that sound pressure level was a good approximation to thrust output. In other words, higher sound pressure levels indicated higher thrust levels. In this way, certain inlets were characterized as better performers without the quantitative data as proof. Later test proved this not to be a good assumption.

Sound pressure level for the forward facing 8 cm pulsejets is typically in the range 95 dB to 110 dB. For any given inlet, sound pressure level increases somewhat with increasing fuel flow rate or with increasing forward flight speed. In this way, SPL may be good indicator of the trends in thrust. However, SPL does not vary much from inlet to inlet. So while inlet 300-125 and 700-125 may be operating at the same SPL but as shown above, they would probably be operating at much different thrust levels.

6.3 Comparisons with Computational Results

Equally important to the experimental research done at AERL is the computational work done by other advanced degree students at NCSU. The low cost and speed of computing makes it a very attractive supplement to research being done in the lab. Of course, it is important that results from both disciplines match. For this reason, it is appropriate here to compare four of the above cases with four computational cases at the same conditions. This is done in Table 6-1.

Table 6-1: Comparison of computational and experimental results

Condition	Computational	Experimental
Inlet 700-125, 0 m/s, H2 @ 9 mg/s	T = 13.8 mN f = 1610 Hz	n/a*
Inlet 700-125, 50 m/s, H2 @ 9 mg/s	T = 21.6 mN f = 1616 Hz	T = 23.7 mN f = 1368 Hz
Inlet 700-150, 0 m/s, H2 @ 9 mg/s	T = 0.74 mN	n/a
Inlet 700-150, 0 m/s, H2 @ 9 mg/s	T = 17.8 mN	T = 11.2 mN

For the first case in the table, inlet 700-125 at 0 m/s, no experimental data exists at that condition but at the nearest condition (7.1 mg/s fuel mass flow rate) the thrust has a value of 12.7 mN and a frequency of 1432 Hz. If one can further equate the very low thrust value of the third condition with the inability to operate experimentally (hence the n/a) then all four conditions may be seen to be almost equivalent, at least in terms of thrust. In a recent publication by Zheng et al, numerical simulations looked at the effects of a convective stream on pulsejet operation (2008). One of the important findings was that as the velocity increased, peak thrust occurred at smaller inlet diameters or longer inlet lengths. The results presented here show exactly that, namely that the maximum thrust for a shorter inlet occurs at a lower velocity than that of a longer inlet. The conclusion may be that the computer predicts thrust reasonably well.

However, it cannot be said that the computer predicts frequency very well. Furthermore, the computer simulations seem to be ill equipped even to determine whether or not a certain configuration will operate at all. This is exemplified by the third condition above but even more forcefully by the fact that computer simulations could not run the pulsejet using inlet 415-125, which was arguably the easiest configuration to operate in the laboratory. If, as it seems to this author, the acoustic characteristics of the pulsejet determine

its ability to operate, then one may conclude that the computational simulations do a poor job of dealing with the acoustics. On the other hand, the fluid mechanics may determine the performance of the pulsejet, assuming it will operate at all, and the computer appears to do a reasonable job of predicting thrust. It should also be noted here that the computer simulations also have no problem running the pulsejets on propane, although this difficulty may be unrelated to the problems described above. To further expound on the differences between computational and experimental results, the next section discusses the "optimized" geometry.

6.4 "Optimized" Geometry

The "optimized" geometry pulsejet was introduced in section 2.1.4 and was designed through a code written in MATLAB. This pulsejet was machined as specified by the program and attempts were made to operate it in the laboratory. The results of these experiments are given in Figure 6-1.

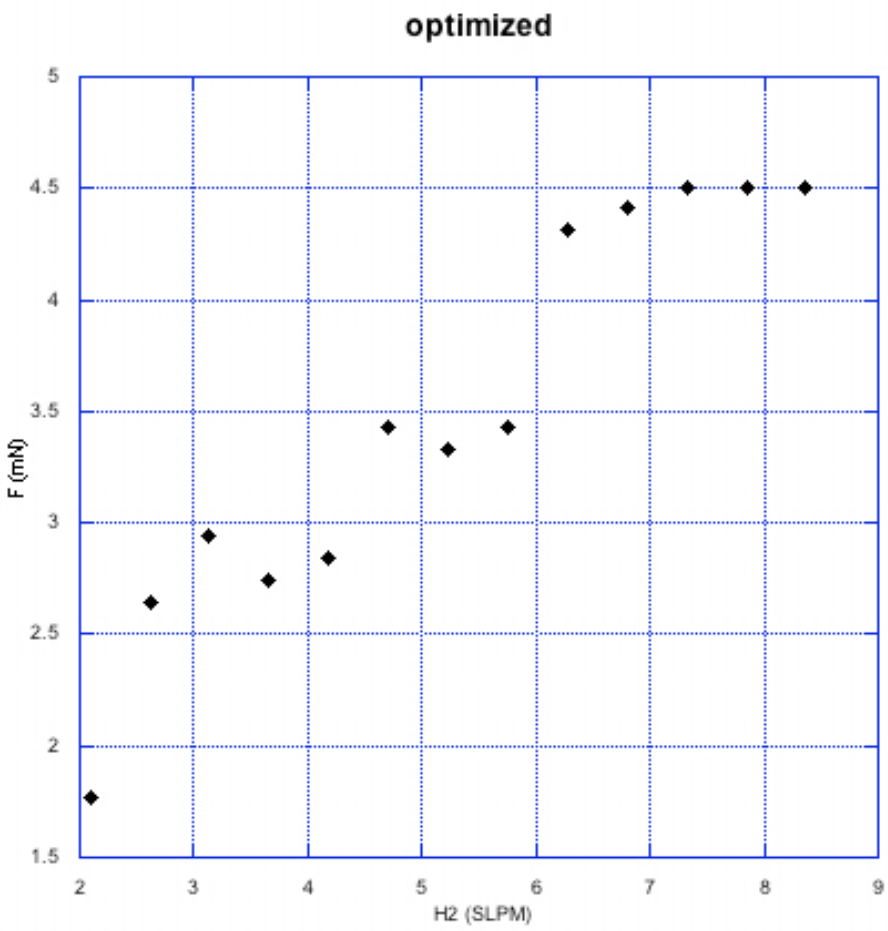

Figure 6-1: Thrust results for "Optimized" 8 cm pulsejet

The pulsejet would not operate at static conditions and the above results are given for tests with forced air at 50 m/s. The results of this experiment are quite dismal showing extremely low thrust measurements at any fuel flow rate. According to general operating standards, this pulsejet would probably be considered inoperable since forced air was crucial to getting any pulsing whatsoever. While the step of using computational results to drive physical experimentation is an important one, clearly there is still some disagreement between the numerical simulations and what happens in the lab.

6.5 Experiments on 4 Centimeter Valveless Pulsejet

In addition to running the 8 cm pulsejets, pulsejets were also designed with a length of 4 cm. The design process was discussed in section 2.1.5. While operation at this scale was not the focus of this research, operation was achieved with forced air using both hydrogen and acetylene. The frequency for one of the tests was measured at 2720 Hz, which is about double the frequencies seen at the 8 cm scale. From the analytical equations used in section 4.3, it can be shown that if all linear dimensions are halved (as was done here), the operating frequency should double. No thrust measurements were taken for this size because the apparatus was not appropriate for such small magnitudes.

7 Conclusions

The primary conclusions to be drawn from this discussion are as follows:

1. Accurate thrust measurements for small valveless pulsejets are difficult to obtain, but the procedure outlined above produces reliable and repeatable results. Of the forward facing configurations, the maximum thrust was measured to be 24.4 mN and the specific impulse peaked at 295 sec. For the hybrid configurations, the highest thrust measured was 31.2 mN and the best specific impulse was 232 sec.
2. Hybrid configurations may produce the highest thrust, but often at the expense of higher fuel flow rates. A well-designed forward facing inlet may be the way to go if fuel efficiency is the primary concern.
3. Higher fuel flow rates almost always lead to higher thrust values and higher frequencies, with most of the exceptions coming at the highest fuel flow rates. On the other hand, specific impulse tends to peak near the middle or low end of the fuel flow rate range.
4. Increasing the simulated airspeed generally has the effect of increasing the net thrust of forward facing configurations. This trend is more pronounced at longer inlet lengths. This trend is also more consistent with hybrid configurations. Higher simulated airspeed is also observed to decrease the operating frequency.
5. Increasing the inlet length has a number of consequences for pulsejets: 1) Reduced backflow of combustion products through the inlet resulting in lower inlet temperatures and higher mass flow rates through the exit; 2) Lower exit plane

temperatures due to higher velocities; 3) Higher net thrust due to both higher velocities and more mass flux through the exit, and; 4) Lower frequency because of inlet length's role in the Helmholtz model and the decreased speed of sound in the exhaust tube.

6. Decreasing the inlet area has beneficial effects on performance as long as the pulsejet receives an adequate amount of fresh air with each cycle. This conclusion is primarily supported by results with the hybrid configurations.
7. There is some evidence to support the intuitive notion that 180 degree, rearward facing inlets offer the best performance in a hybrid configuration.
8. The analytical model, which involves averaging the inlet frequency (modeling the inlet as a Helmholtz resonator) and the exhaust frequency (modeling the exhaust as a wave tube) still provides good predictions of operating frequency, but in this case, a $1/8^{th}$ wave tube model for the exhaust tube was a better predictor.
9. Computer generated results, using the commercial CFD package CFX, correlate fairly well with experimental performance data. However, numerical models are unable to adequately predict whether or not a given geometry will actually operate in the lab.
10. Acetylene was shown to work but hydrogen is still the fuel of choice in small pulsejets, due to the requirement for a very short chemical time.

8 Future Work

Much of the behavior of small valveless pulsejets has been elucidated through this research, but as should always be the case, as many questions were generated as answers. For this reason, future work in this field is necessary.

The thrust results, particularly as they relate to airspeed, need to be validated by true wind tunnel experiments. The method of aiming an air nozzle at the inlet face was only intended as an expeditious solution to an urgent problem. The results are believable but certainly some of the physics of an actual convective stream were lost, especially the possible effects of convective heat transfer from the pulsejet exterior to the air.

The effects of varying inlet length are, at this point, well understood but more should be done with inlet area. Potentially, decreasing inlet area should have effects similar to increasing the inlet length. The inlet area changes in this experiment were probably too drastic, pushing the acoustics beyond the operational zone of the pulsejet. For that matter, the same basic pulsejet body was used throughout this period of research. There is much more to learn about the effects of varying combustion chamber volume and shape as well as exhaust tube length and cross-sectional area.

Rearward facing inlets and hybrid configurations offer some promise of delivering better performance. Much more should be done to develop a sense of their limitations. It is believed that the “backwards” inlets will suffer from being immersed in a convective stream, but this has not been verified. In fact, this again calls for true wind tunnel testing.

9 References

Geng, Tao (2007), "Numerical Simulations of Pulsejet Engines," PhD. Dissertation, North Carolina State University, Raleigh.

Foa J. V., *Elements of Flight Propulsion*, John Wiley & Sons, New York, 1960.

Kiker, A.P. (2005), "Experimental Investigations of Mini-Pulsejet Engines," M.S. Thesis, North Carolina State University, Raleigh.

Kumar, A.K.R. (2007), "Experimental Investigation on Pulsejet Engines," M.S. Thesis, North Carolina State University, Raleigh.

McCauley, C.T. (2006), "Experimental Investigations of Liquid Fueled Pulsejet Engines," M.S. Thesis, North Carolina State University, Raleigh.

Ordon, R.L. (2006), "Experimental Investigations in to the Operational Parameters of a 50 Centimeter Class Pulsejet Engine," M.S. Thesis, North Carolina State University, Raleigh.

Putnam A.A., Belles F.E., and Kentfield J.A.C. "Pulse Combustion." Progress in Energy and Combustion Science. Vol.12, Issue 1. 1986.

Schoen, M.A. (2005), "Experimental Investigations in 15 Centimeter Class Pulsejet Engines," M.S. Thesis, North Carolina State University, Raleigh.

Spadaccini C.M., Peck J., and Waitz I.A. "Catayltic Combustion Systems for Microscale Gas Turbine Engines" Journal of Engineering for Gas Turbines and Power. Jan. 2007, Vol. 129.

Waitz I.A., Gauba G. and Yang-Sheng, Z. "Combustors for Micro-Gas Turbine Engines." Journal of Fluids Engineering. March 1998, Vol. 20.

Zheng F., Ordon R.L., Scharton T.D., Kuznetsov A.V., and Roberts W.L. "A New Acoustic Model for Valveless Pulsejets and Its Application to Optimization Thrust." Journal of Engineering for Gas Turbines and Power. July 2008, Vol. 130.